MONO- AND TRIMETALLIC COBALT(II) AND MONOMETALLIC COBALT(III) AMINE-BIS(PHENOLATE) COMPLEXES: SYNTHESIS AND STRUCTURAL PROPERTIES

UTTAM KUMAR DAS

Mono- and Trimetallic Cobalt(II) and Monometallic Cobalt(III) Amine-bis(phenolate) Complexes: Synthesis and Structural Properties

By

Uttam Kumar Das

A thesis submitted to the School of Graduate Studies

in partial fulfillment for the degree of

Master of Science

Department of Chemistry

Memorial University

July 2010

St. John's, Newfoundland and Labrador, Canada

Abstract

This thesis describes the syntheses and structures of a series of monometallic and two trimetallic cobalt(II) amine-bis(phenolate) complexes. The protonated tripodal tetradentate ligand precursors dimethylaminoethylamino-*N,N*-bis(2-methylene-4,6-di-*tert*-butylphenol), $H_2[O_2NN']^{BuBuNMe2}$ and diethylaminoethylamino-*N,N*-bis(2-methylene-4,6-di-*tert*-amylphenol), $H_2[O_2NN']^{AmAmNEt2}$ were reacted with cobaltous acetate tetrahydrate under varying conditions to afford both mono- and trimetallic species. X-ray crystallographic data of monometallic complexes $[LCo[O_2NN']^{BuBuNMe2}]$ (L = H_2O, CH_3OH, CH_3COCH_3, propylene oxide) showed that the Co^{II} ion adopts a distorted trigonal bipyramidal coordination environment. In the absence of base and in the presence of excess cobaltous acetate, trimetallic complexes were isolated containing a central Co^{II} in an octahedral environment coordinated to four CH_3OH and two bridging acetate ligands between two $Co[O_2NN']$ fragments with Co^{II} in a trigonal bipyramidal setting. The mono- and trimetallic Co^{II} complexes reported were also characterized by UV-vis spectroscopy, mass spectrometry, cyclic voltammetry and magnetic measurements. The Co^{II} ions in these complexes are all high-spin and the trimetallic species show very weak antiferromagnetic behaviour when modeled as a linear isotropic trimer. Electrochemical studies reveal that the redox processes are most likely ligand based but a metal centered redox process is also possible. These works have recently been published: U. K. Das, J. Bobak, C. Fowler, S. E. Hann, C. F. Petten, L. N. Dawe, A. Decken, F. M. Kerton* and C. M. Kozak*, *Dalton Trans.*, 2010, 39, 5462.

This thesis also describes several oxidation attempts and a successful synthesis of a monometallic Co^{III} amine-bis(phenolate) complex. The oxidation reactions were carried out using a variety of oxidizing agents under both aerobic and anaerobic conditions. However, only silver nitrate gave promising results in yielding a monometallic Co^{III} amine-bis(phenolate) complex under aerobic conditions. The monometallic species was characterized by ^1H NMR spectroscopy, mass spectrometry, and elemental analysis.

Acknowledgements

I would like to express my indebtedness and deepest sense of gratitude to my supervisors Dr. Chris Kozak and Dr. Fran Kerton, for giving me the opportunity to join their research group, "Centre for Green Chemistry and Catalysis", and for their encouragement, thoughtful suggestions, proper guidance and constructive supervision throughout the progress of my study and research work.

I express my sincere thanks to supervisory committee member Dr. Yuming Zhao for his valuable suggestion during the program and his cooperation during the progress of this thesis. I am greatly thankful to C-CART and GaP members for their help; Dr. Louise Dawe for solving X-ray structures, Dr. Celine Schneider for NMR, Linda Windsor and Lidan Tao for MALDI-TOF MS. I would like to thank Dr. Laurence Thompson and Dr. Konstantin Shuvaev for valuable discussions and acquisition of magnetic data. My thanks also goes to Rodney Smith, Reza B Moghaddam and Abdul Al-Betar in Dr. Peter Pickup's group, for their help in using their instruments to collect electrochemical data.

I would like to thank NSERC of Canada (Dr. Kozak and Dr. Kerton's Discovery Grants, Research tools and Instrument Grants), School of Graduate Studies and Department of Chemistry of Memorial University for their generous financial support. I would also like to acknowledge all of the faculty and staff of the Chemistry Department for their help and support.

I wish to thank my colleagues: Nduka, Kamrul, Rebecca, Hassan, Zhenzhong, Samantha, Khaled and Xin for their help and cooperation during the work in the lab. My appreciation also goes to undergraduate students: Candace, Julia, Sarah, Chad, Elliot, Amy and Stephanie.

I express my heartiest thanks to my wife for her encouragement, patience and love she has shown me. I also express my gratitude to my Grandmother, parents and brothers for their encouragement and prayers. I thank my God for blessing without which it is impossible to reach at this stage.

Dedicated to my Grandfather

Table of Contents

List of Tables

List of Figures

List of Schemes

List of Symbols and Abbreviations

δ	chemical shift (in NMR)
ε	molar absorption coefficient (in UV-vis)
μ_{eff}	effective magnetic moment
μ_B	Bohr magneton
λ_{max}	maximum wavelength
$AgBF_4$	silver tetrafluoroborate
$AgNO_3$	silver nitrate
AgOAc	silver acetate
AP-CI	atmospheric pressure chemical ionization
B3LYP	Becke three parameter nonlocal functional with the nonlocal correlation functional of Lee, Yang and Parr
br	broad (in IR)
Br^-	bromide ion
CaH_2	calcium hydride
$CDCl_3$	deuterated chloroform
$CHCl_3$	chloroform
CH_2Cl_2	dichloromethane
CH_3COCH_3	acetone
CH_3OH	methanol
C_3H_6O	propylene oxide
$CoCl_2$	cobalt(II) chloride

Cl^-	chloride ion
d	doublet (in NMR)
DFT	density functional theory
DMSO	dimethyl sulfoxide
ESI MS	electrospray ionization mass spectrometry
Et_4NBr	tetraethylammonium bromide
Et_4NCN	tetraethylammonium cyanide
FAB	fast atom bombardment
FTIR	fourier transform infrared
g	gram
h or hr	hour
HOMO	highest occupied molecular orbital
H_2O	water
HRMS (ESI)	high resolution mass spectrometry (electrospray ionization)
I^-	iodide ion
^{i}Pr	isopropyl
IR	infrared
K	Kelvin
KBr	potassium bromide
L	litre
m	medium (in IR)
mA	milliampere
mg	milligram

mL	millilitre
mV	millivolt
m/z	mass-to-charge ratio
M	molar
MALDI-TOF MS	matrix assisted laser desorption ionization time-of-flight mass spectrometry
MHz	megahertz
MS	mass spectrometry
nm	nanometre
$[(n\text{-Bu})_4N]PF_6$	tetrabutylammonium hexaflurophosphate
$NaBPh_4$	sodium tertraphenylborate
NMR	nuclear magnetic resonance
OH^-	hydroxyl ion
ORTEP	Oak Ridge thermal ellipsoid plot
$OBzF_5$	pentafluorobenzoate
r.t.	room temperature
s	singlet (in NMR) and strong (in IR)
SCE	saturated calomel electrode
SCN^-	thiocyanate ion
sh	shoulder (in UV-vis)
t	triplet (in NMR)
t-Am	tertiary pentyl or amyl
t-Bu	tertiary butyl

T	temperature
THF	tetrahydrofuran
TMS	tetramethylsilane
UV	ultraviolet
vs	very strong (in IR)
VT-SQUID	variable temperature superconducting quantum interference devices
w	weak (in IR)
ZFS	zero field splitting

Chapter 1

Introduction to Cobalt(II) Complexes

1.1 Brief History of Cobalt

Cobalt minerals were known to ancient peoples, as they were once used to colour glass and pottery. For example, a small deep blue coloured glass object containing cobalt was found in the tomb of Pharaoh Tutankhamen dated 1300 BC.[1] However, in China cobalt blue was used for pottery glazes long before 1300 BC. Swedish chemist Georg Brandt (1694-1768) first isolated elemental cobalt in 1735, while studying a dark blue ore obtained from a local copper mine. The name 'cobalt' derives from the German word 'Kobald,' or, 'Kobalt' meaning 'goblin,' i.e. evil spirit, which appears to have been given originally by silver miners in Saxony. In the sixteenth century, silver miners in Saxony tried to smelt silver ore, but they were disappointed to observe toxic fumes of arsenic instead of obtaining silver. They were actually dealing with a cobalt ore which is now known as smaltite, cobalt arsenide ($CoAs_2$). The miners therefore cursed the ore as it had been bewitched by goblins and named it by the German word 'Kobald'.[1]

1.2 Abundance and Uses of Cobalt

Cobalt ranks 33rd in abundance of the elements in the earth's crust and is a commercially important element. Significant amounts of cobalt are found in Canada, Russia, Zambia, and Congo, and approximately 65% of the total world supply comes from these countries.[2] A considerable percentage of total world production of cobalt is obtained as a by-product of nickel mining. Cobalt does not exist as a free metal in nature, but occurs in approximately 200 ores. The commercially useful cobalt ores are smaltite ($CoAs_2$), cobaltite (CoAsS), and linnaeite (Co_3S_4).[2] Biologically, cobalt is an essential metal and found in vitamin B_{12}, one of the rare examples of an organometallic compound found in nature. Cobalt is used in alloys for magnets and jet engines, in ceramics, in catalysis, and in paints. Cobalt blue, an important part of an artist's palette of colours, is

References begin on page 52

used in porcelain, pottery, stained glass, tiles and enamel jewellery.[1] ^{60}Co is a radioactive metal that is used in radiotherapy. Only one naturally occurring isotope, ^{59}Co is NMR active and therefore ^{59}Co NMR spectroscopy is now used for the characterization of cobalt compounds both in solution and in the solid state.[2]

1.3 Overview of Cobalt Coordination Chemistry

Cobalt has become arguably the most important transition metal in the development of modern coordination chemistry. Since the early 1980s, cobalt coordination chemistry has continued to grow apace from understanding its place in biological systems to finding its application in the areas of catalysis and biotechnology. The Swiss chemist Alfred Werner (1866-1919) was awarded the Nobel Prize in 1913 'in recognition of his work on the linkage of atoms in molecules by which he has thrown new light on earlier investigations and opened up new fields of research especially in inorganic chemistry' and he has often been termed 'the father of modern coordination chemistry.' Moreover, his studies of optically active Co^{III} complexes in particular were important to the development of modern structural coordination chemistry. In honour of his importance in chemistry, Co^{III} ammine complexes are often called Werner complexes.[2] Other prize-winning research involving the studies of cobalt coordination chemistry was the determination of ligand substitution and electron transfer mechanisms in coordination complexes by Henry Taube (1983 Nobel Laureate).[2] It is notable that earlier advancement of cobalt coordination chemistry was focused on studying Co^{III} complexes extensively rather than Co^{II} because Co^{III} complexes are generally inert and diamagnetic and thereby easier to handle and investigate. Since a comprehensive study of cobalt coordination chemistry is beyond the scope of this thesis, the following sections will provide a brief outline of the more interesting and important aspects of Co^{II} coordination chemistry relevant to this work.

References begin on page 52

1.3.1 Oxidation States

Cobalt complexes containing the metal ions in all oxidation states from −1 to +5 are known, with Co^{III} complexes being the most numerous. Chemistry of low oxidation states cobalt (Co^{-1}, Co^{0}, Co^{I}) is dominated by organometallic complexes containing C-donor ligands, and 'classical' coordination complexes containing cobalt lower than +2 oxidation states are comparatively rare. However, the +1 oxidation state is important in vitamin B_{12} chemistry, where the vitamin B_{12} contains five-coordinate Co^{I} in a square pyramidal N_5 coordination environment. Simple cobalt salts most commonly contain the metal in the +2 oxidation state.[2] The common oxidation states of cobalt are +2 and +3. Co^{II} is a key oxidation state, and the coordination chemistry of Co^{II} is being increasingly explored with a wide variety of ligands. Moreover, the Co^{II} oxidation state is unique in that it is the only commonly occurring example of a d^7 electron configuration. Higher oxidation states (+4 and +5) are rare, and are usually stabilized by the presence of fluorine or oxygen atoms.[2,3]

1.3.2 Synthesis of Cobalt(II) Complexes

Co^{II} coordination complexes can easily be synthesized by mixing solutions of a commercially available Co^{II} salt with the appropriate ligand under varying conditions. Co^{II} species of the formula $CoX_2{\cdot}4H_2O$ or $CoX_2{\cdot}6H_2O$ (X = Cl, Br, I) generally serve as commercially available starting materials for cobalt coordination complex syntheses. These hydrated Co^{II} salts may be prepared by reaction of the metal with the appropriate mineral acid, whereas the anhydrous salts, CoX_2 can be synthesized by direct treatment of the metal with Cl_2, Br_2, or I_2 at elevated temperatures. The final product, i.e. Co^{II} coordination complex, can be isolated by concentrating the reaction mixture followed by crystallization using the remaining or a different solvent. For cationic and anionic complexes, a suitable counterion is added to precipitate the product, and then complexes can be isolated by subsequent crystallization.[2]

References begin on page 52

1.3.3 Geometry and Coordination Numbers

Tetrahedral and high-spin octahedral species dominate Co^{II} coordination chemistry but five-coordinate trigonal bipyramidal and square pyramidal species are also known. Tetrahedral complexes of Co^{II} are more numerous than for any other transition metal ion because of the fact that the crystal field stabilization energy difference between the octahedral and tetrahedral geometries is small for a high-spin d^7 electron configuration.[4] The polarizibility of the ligand also appears to be important in determining the stereochemistry of the complex. For example, ligands containing soft donor atoms (P, S, As, aromatic N) often yield tetrahedral complexes, while O- and amine N-donor ligands usually give octahedral complexes.[2] Because of the small stability difference between octahedral and tetrahedral Co^{II} complexes, there are several cases in which the two types with the same ligand are both known and may be in the equilibrium. Examples of these are Co^{II} aquo complexes. There is always some $[Co(H_2O)_4]^{2+}$ in equilibrium with $[Co(H_2O)_6]^{2+}$ in aqueous solution.[4]

Tetrahedral Co^{II} complexes are generally formed with either monodentate anionic ligands such as Cl^-, Br^-, I^-, SCN^-, N_3^-, and OH^- or with a combination of such anionic ligands and other neutral ligands. Some square-planar Co^{II} complexes containing phthalocyanine, porphyrin and macrocyclic ligands are also known. Octahedral complexes are common with a variety of ligands such as halides, pseudohalides, N- and O-donors. There are also a number of bimetallic carboxylate complexes of Co^{II} which show interesting magnetic behaviour and contain the $[Co_2(\mu\text{-}OH_2)(RCO_2)_2]^{2+}$ or $[Co_2(\mu\text{-}X)(\mu\text{-}RCO_2)_2]^+$ core (X = OH, Cl, Br), stabilized by chelating nitrogen ligands to complete the octahedral coordination.[4]

Both trigonal bipyramidal and square pyramidal geometries have been found in five-coordinate Co^{II} species with phosphine and polydentate ligands respectively. Three, seven and eight-coordinate Co^{II} complexes are also reported; however, their formation is usually based on ligand topology. Traditionally, Co^{II} complexes are reactive as these d^7 paramagnetic ions are considered to be labile and therefore ligand exchange will be

References begin on page 52

facile.[3] Distribution of oxidation states and geometry in cobalt complexes is summarized in Table 1.1.

Table 1.1 Oxidation states and geometry of cobalt in a range of coordination compounds [4]

Oxidation state	Coordination number	Geometry	Examples
Co^{-I}, d^{10}	4	Tetrahedral	$[Co(CO)_4]^-$, $Co(CO)_3NO$
Co^0, d^9	4	Tetrahedral	$K_4[Co(CN)_4]$, $Co(PMe_3)_4$
Co^I, d^8	3	Trigonal planar	$(tempo)Co(CO)_2$
	4	Tetrahedral	$CoBr(PR_3)_3$
	5[a]	Trigonal bipyramidal	$[Co(CO)_3(PR_3)_2]^+$, $HCo(PR_3)_4$
	5	Square pyramidal	$[Co(NCPh)_5]ClO_4$
	6	Octahedral	$[Co(bipy)_3]^+$
Co^{II}, d^7	3	Trigonal planar	$\{Co(OCBu_3)_2[N(SiMe_3)_2]\}^-$, $Co_2(NPh_2)_4$
	4[a]	Tetrahedral	$[CoCl_4]^{2-}$, $CoBr_2(PR_3)_2$
	4	Square planar	$[(Ph_3P)_2N]_2[Co(CN)_4]$, $[Co(py)_4](Cl)(PF_6)$
	5	Trigonal bipyramidal	$CoH(BH_4)(PCy_3)_2$
	5	Square pyramidal	$[Co(ClO_4)(MePh_2AsO)_4]^+$, $[Co(CN)_5]^{3-}$
	6[a]	Octahedral	$[Co(NH_3)_6]^{2+}$
	8	Dodecahedral	$(Ph_4As)_2[Co(NO_3)_4]$
Co^{III}, d^6	4	Tetrahedral	$K_5Co^{III}W_{12}O_{40}\cdot 20H_2O$
	4	Square planar	$[Co(SR)_4]^-$
	5	Trigonal bipyramidal	$CoCl(TC\text{-}4,4)$[b]
	5	Square pyramidal	RCo(saloph)
	6[a]	Octahedral	$[Co(en)_2Cl_2]^+$, $[CoF_6]^{3-}$, CoF_3
Co^{IV}, d^5	4	Tetrahedral	$Co(1\text{-norbornyl})_4$
	6	Octahedral	$[CoF_6]^{2-}$
Co^V, d^4	4	Tetrahedral	$[Co(1\text{-norbornyl})_4]^+$

[a] Most common states

[b] TC-4,4 =

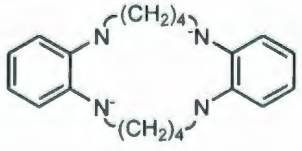

References begin on page 52

1.4 Cobalt(II) Complexes Containing Nitrogen and Oxygen Donor Ligands

All known types of N- and O-donor ligands are found in complexes with Co^{II}. The reason for the large number of Co^{II} complexes containing these two donor ligands is that nitrogen is 'moderately hard' and basic in nature and in combination with anionic 'hard' oxygen, multidentate ligands are able to stabilize the cobalt center. In polyamines either acyclic or macrocyclic but invariably multidentate, the π-accepting ability of imine donors results in the stabilization of lower oxidation states of cobalt, and many air-stable Co^{II} complexes are reported containing imine ligands.[3] Thus the coordination chemistry of Schiff base ligands, particularly salen-type ligands with cobalt, has been intensively studied and well documented, yielding both mono- and multimetallic Co^{II} species.[3] Co^{II} forms a variety of N-donor complexes of all electronic ground states (high and low-spin) depending on the ligand field strength and symmetry. Recently, chelating tetradentate amine-bis(phenolate) ligands bearing N- and O-donor atoms have emerged as an another important class of ligand which can also stabilize bimetallic Co^{II} complexes by appropriate tuning of steric and/or electronic demands. The following section (section 1.4.1) will provide a detailed discussion of recent reports of Co^{II} complexes bearing these ligands.

1.4.1 Cobalt(II) Complexes with Amine-bis(phenolate) Ligands

Co^{II} complexes of chelating tetradentate amine-bis(phenolate) ligands have attracted significant interest in recent years. The reasons for this include (i) their similarity to several redox and hydrolytic enzymes active-sites,[5-7] and (ii) the possibility of gaining a better understanding of the magnetic properties and redox behaviour of structurally characterized Co^{II} complexes.[8] In this field, a small group of dianionic tetradentate amine-bis(phenolate) ligands have been used for preparing Co^{II} complexes and they are shown in Figure 1.1.

References begin on page 52

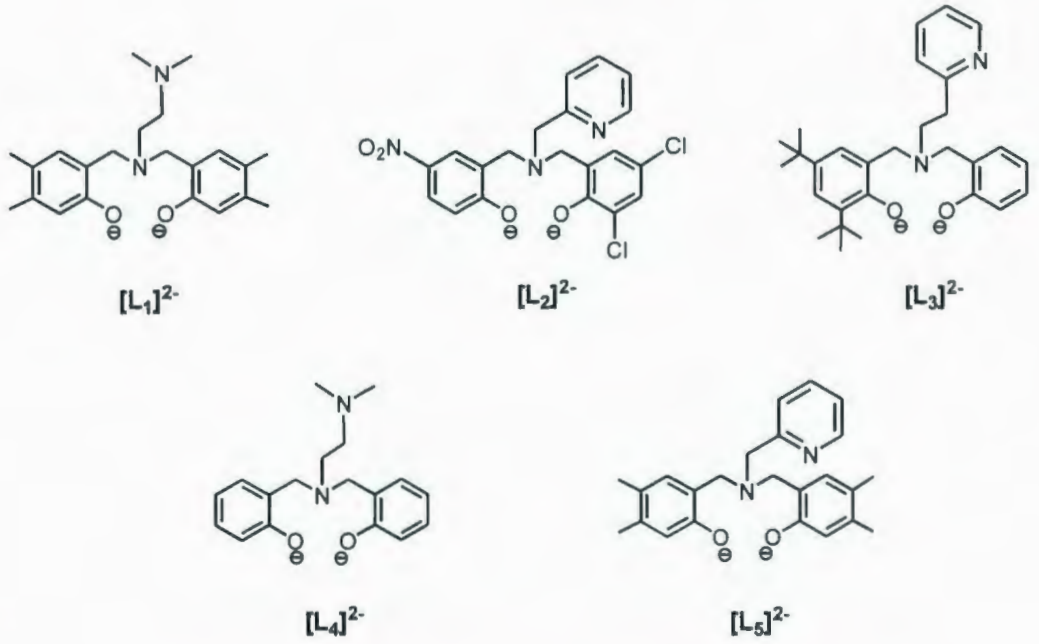

Figure 1.1 Examples of various amine-bis(phenolate) ligands.

Amine-bis(phenolate) ligands depicted in Figure 1.1 consist of two phenolate groups bearing no substituent (**L_4**) or different electron donating (**L_1**, **L_3**, **L_5**) and withdrawing groups (**L_2**), and a pendant unit (either an amine in both **L_1** and **L_4** or a pyridyl group in **L_2**, **L_3**, **L_5**) to afford an N_2O_2 donor set. It should be noted that few of the ligands studied to-date with cobalt possess sterically demanding groups on the phenolate donors. This contrasts strongly with their use in early transition metal chemistry where *ortho* positions on both of the phenolate donors are often *tert*-butyl groups.[9-11] A one-pot Mannich condensation reaction has been used to synthesize the symmetric ligands H_2**[L_1]**, H_2**[L_4]** and H_2**[L_5]** in moderate to good yields. The asymmetric ligands, H_2**[L_2]** and H_2**[L_3]** were synthesized in moderate yields by reacting 2-hydroxy-5-nitrobenzyl bromide and (3,5-dichloro-2-hydroxybenzyl)(2-pyridylmethyl)amine in THF under refluxing conditions[12] and by stirring a mixture of 2-((2-(2-pyridyl)ethylamino)-methyl)phenol and triethylamine in 1,4-dioxane with a solution of 2,4-di-*tert*-butyl-6-(chloromethyl)phenol,[8] respectively. An excess of triethylamine was used in synthesizing

References begin on page 52

both of these asymmetric ligands. All ligands used in the preparation of this thesis were synthesized by Mannich condensations in water.[13]

Regarding metal nuclearity, all Co^{II} amine-bis(phenolate) complexes published to-date possess bimetallic structures,[5-8,14] and each Co^{II} ion preferentially adopts a distorted trigonal bipyramidal coordination environment except one bimetallic Co^{II} complex in which one of the two Co^{II} ions is in an octahedral coordination environment.[7] To the best of our knowledge, no structurally characterized monometallic Co^{II} amine-bis(phenolate) complexes have been reported in the literature.

Phenolate ligands may facilitate the magnetic coupling between two paramagnetic metal ions, and the nature of magnetic interactions in phenolate-bridged metal systems is primarily influenced by the M-O-M angle and the M···M separation. Sousa and co-workers reported a structurally characterized bimetallic Co^{II} complex, $[(Co^{II}\mathbf{L_1})_2]$ **(1.1)** containing a tripodal amine-bis(phenolate) ligand, *N,N*-bis(3,4-dimethyl-2-hydroxybenzyl)-*N',N'*-dimethylethylenediamine $H_2[\mathbf{L_1}]$ (Figure 1.2).[5] The complex was prepared in high purity and yield using an electrochemical synthetic procedure. An acetonitrile solution of the ligand, containing 10 mg of tetramethylammonium perchlorate electrolyte, was electrolyzed using a platinum wire as the cathode and a cobalt plate as the sacrificial anode over a 1 h reaction period. The applied voltages and the current were 10 – 20 V and 5 mA respectively.

References begin on page 52

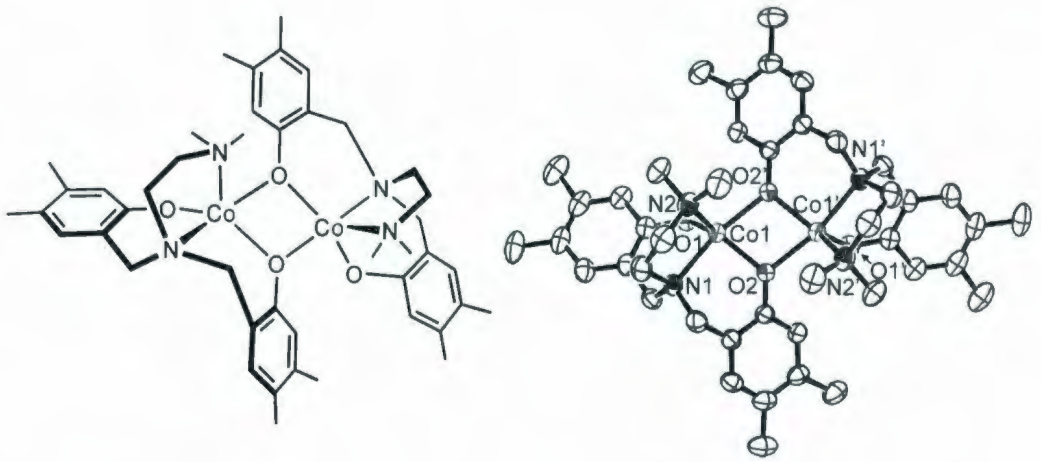

1.1

Figure 1.2 Bimetallic Co^{II} complex of amine-bis(phenolate) ligand, $[(Co^{II}L_1)_2]$ and ORTEP diagram of the molecular structure of **1.1** with 50% thermal ellipsoid probability.[5]

Crystallographic data for **1.1** reveals that both Co^{II} ions adopt distorted trigonal bipyramidal coordination environments. An angular structural parameter, τ [$\tau = (\beta-\alpha)/60$, where β = the largest angle obtained between apical donors and the metal, and α = the largest donor-metal-donor triangle in the equatorial plane giving $\tau = 1$ for a perfect trigonal bipyramid and $\tau = 0$ for a perfect square pyramid][15] is used as a trigonality index for this five-coordinate environment which gives the value of 0.63 for **1.1**, indicating a distorted trigonal bipyramidal geometry. Both equatorial planes are occupied by the two phenolate O-donors and the pendant nitrogen donors of the tetradentate ligand. The central nitrogen donor and one phenolate O-donor of the alternate ligand (in each case, the apical oxygen belongs to the other ligand in the bimetallic pair) are in the apical positions. However, although the four-membered ring formed by two of the Co^{II} ions and two bridging phenolate O-donors is essentially planar, the Co^{II}-O-Co^{II} bridge is slightly asymmetric with respect to the bond distances of bridging phenolate O-donors to Co^{II} ions as shown in Table 1.2. The bond distances between the Co^{II} ion and the terminally coordinated phenolate O-donors, and the Co^{II} ion and the nitrogen donors are comparable to the average Co-$O_{phenolate}$ and Co-N_{amine} bond distances observed in other five-

References begin on page 52

coordinate Co^{II} complexes; [1.891(6)–2.099(4) Å] for Co-$O_{phenolate}$ and [2.092(4)–2.197(5) Å] for Co-N_{amine} bond distances. Although two acetonitrile solvent molecules are present in the crystal lattice, these solvent molecules do not interact with the complex in any significant manner. **1.1** was also characterized by IR, EI-MS and UV-vis spectroscopy authenticating a high-spin bimetallic Co^{II} species with the Co^{II} ions in distorted trigonal bipyramidal coordination environments.

The magnetic data of **1.1** support the existence of two high-spin Co^{II} ions exhibiting strong orbital contributions. The experimental data were modelled using the Heisenberg dimer model considering $S_A = S_B = 3/2$. The best fit data corresponds to $g = 2.29$, weak antiferromagnetic coupling between the two Co^{II} ions with $J = -7.5$ cm^{-1}. The presence of temperature independent paramagnetism (TIP) was also included in the model, TIP = 113×10^{-6} cm^3 mol^{-1}.[5]

In recent enzymatic modelling studies, Krebs *et al.* reported a bimetallic Co^{II} complex, $[(Co^{II}\mathbf{L_2})_2(CH_3OH)]$ (**1.2**) using the tetradentate tripodal amine-bis(phenolate) ligand, (3,5-dichloro-2-hydroxybenzyl)(2-hydroxy-5-nitrobenzyl)(2-pyridyl)methylamine $H_2[\mathbf{L_2}]$ (Figure 1.3).[7] The Co^{II} complex **1.2** was obtained in moderate yield by stirring a 1:1 equimolar mixture of cobalt(II) perchlorate hexahydrate and ligand, $H_2[\mathbf{L_2}]$, for half an hour in acetone (5 mL) and methanol (5 mL) under basic conditions. The most interesting feature of the crystal structure of **1.2** is the difference in the coordination number and thereby geometry between the two Co^{II} ions. One Co^{II} ion is in a distorted trigonal bipyramidal ($\tau = 0.81$) coordination environment whereas the other Co^{II} ion shows an octahedral coordination geometry. The octahedral coordination environment at one Co^{II} ion is due to the presence of a methanol molecule in the coordination sphere. The bond distances of the bridging phenolate O-donors to the pentacoordinate Co^{II} ion are significantly shorter than the distances to the hexacoordinate Co^{II} ion which are depicted in Table 1.2.

References begin on page 52

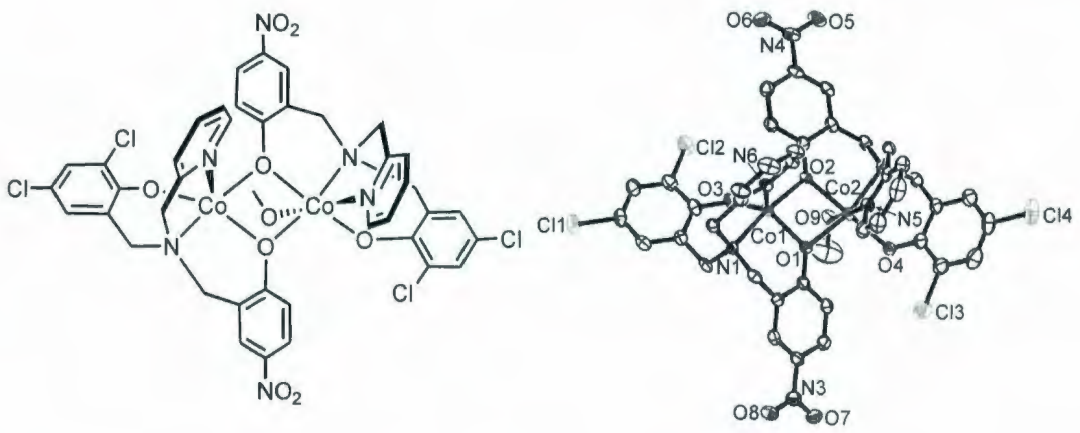

1.2

Figure 1.3 Bimetallic Co^{II} complex of amine-bis(phenolate) ligand, $[(Co^{II}\mathbf{L_2})_2(CH_3OH)]$ and ORTEP diagram of the molecular structure of **1.2** with 50% thermal ellipsoid probability.[7]

The electronic absorption spectrum of **1.2** shows an intense band at 395 nm (ε = 41600 L mol^{-1} cm^{-1}) and a weaker band at 567 nm (ε = 390 L mol^{-1} cm^{-1}) which are assigned to $\pi \rightarrow \pi^*$ transitions of the nitrophenolate group within the ligand and d-d transitions at the Co centers, respectively. The band at 567 nm is in good agreement with typical spin-allowed electronic transitions observed for high-spin Co^{II} in a trigonal bipyramidal ligand field. However, the ε value of this band is slightly high due to lowering of symmetry by the trigonal bipyramidal coordination at Co^{II} compared to a pure octahedral system, thereby easing the Laporte selection rule. The group also studied the magnetic behaviour of **1.2** which shows an average magnetic moment of 4.75 μ_B per Co^{II} ion at 300 K with a corresponding *g*-value of 2.45, indicating the presence of two Co^{II} ions in high-spin ground states. At lower temperatures a decrease in the effective magnetic moment is observed suggesting the presence of antiferromagnetic interactions between the metal centers as a result of a first order orbital contribution and spin-orbit coupling for the octahedral Co^{II} center. However, the value of *J* was not obtained for **1.2** which may be due to the complicated asymmetric coordination geometries at both Co^{II}

References begin on page 52

ions (one Co^{II} ion is in a distorted trigonal bipyramidal environment and the other is in an octahedral coordination environment).[7]

In 2008, Mukherjee and co-workers reported a structurally characterized bimetallic diphenolate-bridged Co^{II} complex, $[(Co^{II}\mathbf{L_3})_2]$ (**1.3**) containing an asymmetric tripodal tetradentate amine-bis(phenolate) ligand, 2,4-di-*tert*-butyl-6-{[(2-pyridyl)ethyl](2-hydroxybenzyl)amino-methyl}-phenol $H_2[\mathbf{L_3}]$ (Figure 1.4).[8] **1.3** was successfully synthesized by refluxing the appropriate metal salt and ligand $H_2[\mathbf{L_3}]$ with or without the use of triethylamine. Crystallographic analysis of **1.3** reveals that both Co^{II} ions are in similar five-coordinate environments bridged by two unsubstituted phenolate O-donors from the two $[\mathbf{L_3}]^{2-}$ ligands. Thus, the geometry around the two Co^{II} ions is distorted trigonal bipyramidal ($\tau = 0.66$). The Co_2O_2 core is almost planar but asymmetric in nature owing to the difference in bond distances of the bridging phenolate O-donors to the Co^{II} ions as mentioned in Table 1.2. The two Co^{II} centers are separated by 3.200(7) Å, an expected distance for phenolate-bridged bimetallic Co^{II} complex.[5] Between the two $Co\text{-}O_{phenolate}$ bond distances in each equatorial planes, the substituted phenolate O-donor coordinates more effectively to the metal [Co(1)–O(2) = 1.935(3) Å and Co(2)–O(4) = 1.927(3) Å] than the unsubstituted bridging phenolate O-donor [Co(1)–O(1) = 1.991(2) Å and Co(2)–O(3) = 1.969(3) Å].

References begin on page 52

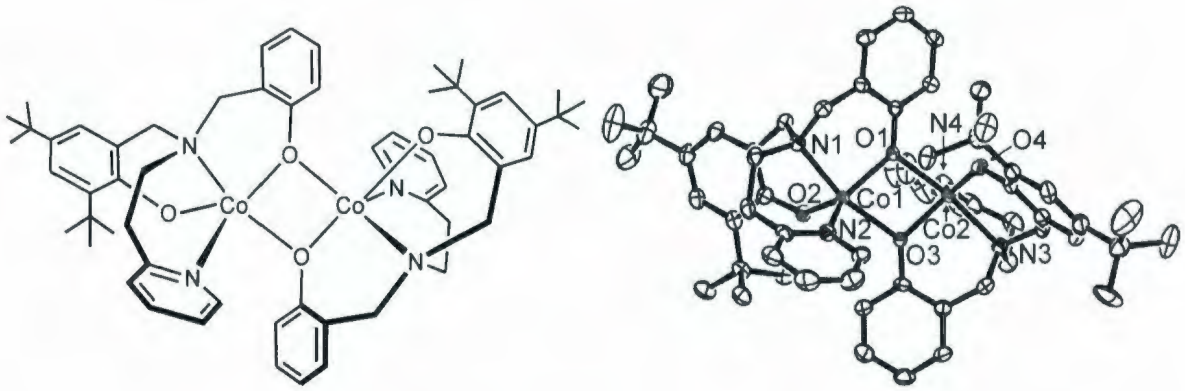

1.3

Figure 1.4 Bimetallic Co^{II} complex of amine-bis(phenolate) ligand, $[(Co^{II}\mathbf{L_3})_2]$ and ORTEP diagram of the molecular structure of **1.3** with 50% thermal ellipsoid probability.[8]

The absorption spectrum of **1.3** exhibits an intraligand transition, a charge-transfer transition and d-d transition bands. The d-d transitions at 570, and 740 nm with ε = 200 and 30 L mol^{-1} cm^{-1}, respectively support the presence of high-spin five-coordinate Co^{II} ions as these transitions are typical for high-spin Co^{II} ion in trigonal bipyramidal coordination environment, and are also observed in other bimetallic complexes such as **1.1** and **1.2**.

The temperature dependent (2-300 K) magnetic susceptibility measurements on powdered samples of **1.3** indicate both Co^{II} ions are weakly antiferromagnetically coupled. The experimental data were modeled using a Hamiltonian term, with $S_A = S_B$ = 3/2 resulting in *g*-value of 2.27 and J = -6.1 cm^{-1}. However, the most fascinating investigation of **1.3** was the study of its redox behaviour. The cyclic voltammograms (CV) of this complex were recorded at a scan rate of 100 mVs^{-1} in CH_2Cl_2, using a platinum working electrode. **1.3** shows two quasireversible one-electron oxidative responses, suggesting a successive oxidation of coordinated 2,4-di-*tert*-butyl-phenolate rings into phenoxyl radicals i.e. ligand-centered oxidations. The group also examined the nature of a two-electron oxidized species and the site of oxidation in **1.3** using coulometry and single-point DFT calculations at the B3LYP level of theory, respectively, which

References begin on page 52

conclude that between the two phenolate groups present in the ligand, only the one with the 2,4-di-*tert*-butyl substituent is oxidized.[8]

In related studies, Rajak *et al.* described the synthesis and characterization of a bimetallic Co^{II} complex, $[(Co^{II}\mathbf{L_4})_2]$ **(1.4)** using a N_2O_2 coordinating tetradentate ligand, *N,N*-bis(2-hydroxybenzyl)-*N',N'*-dimethylethylenediamine $H_2[\mathbf{L_4}]$ (Figure 1.5).[14] **1.4** was isolated in excellent yield by a stoichiometric reaction of cobaltous acetate tetrahydrate with the ligand $H_2[\mathbf{L_4}]$ in acetonitrile solution.

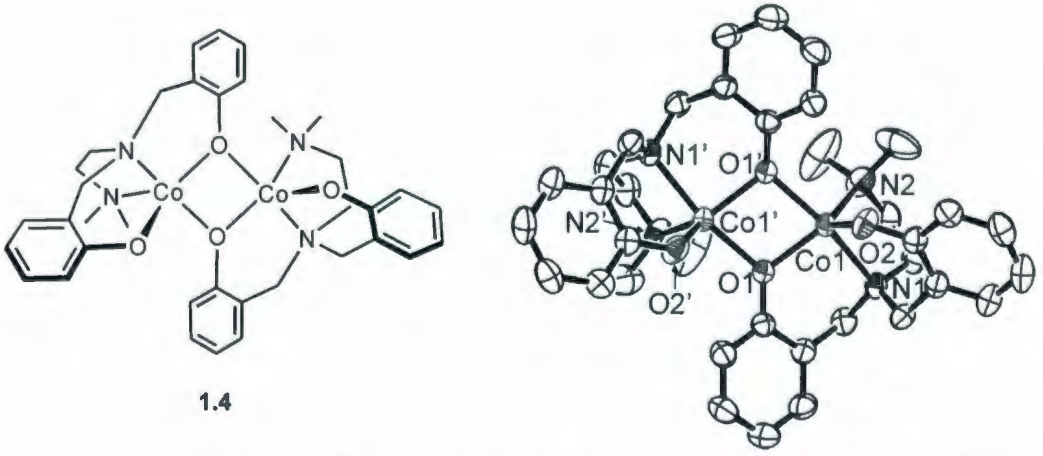

Figure 1.5 Bimetallic Co^{II} complex of amine-bis(phenolate) ligand, $[(Co^{II}\mathbf{L_4})_2]$ and ORTEP diagram of the molecular structure of **1.4** with 50% thermal ellipsoid probability.[14]

The crystal structure of **1.4** reveals that this complex is a centrosymmetric bimetallic species, where the two Co^{II} centers are connected by two bridging phenolate O-donors. Each Co^{II} ion is in a distorted trigonal bipyramidal (τ = 0.80) coordination environment. The equatorial planes are occupied by one nitrogen donor, one phenolate O-donor and one of the two bridging phenolate O-donors, whereas the apical positions are taken up by a nitrogen donor and the remaining bridging phenolate O-donor. Variable temperature magnetic moment measurements indicate that **1.4** exhibits antiferromagnetic interaction between the Co^{II} ions along with zero field splitting. The experimental magnetic data were modeled using Curie-Weiss law where **1.4** obeys the Curie-Weiss equation [$\chi = C/(T-\theta)$] over the whole temperature range giving the value of C = 5.29

References begin on page 52

cm^3 mol^{-1} K and $\theta = -11.23$ K signature of weak antiferromagnetic exchange between the two Co^{II} ions.[14] The redox behavior of **1.4** was also studied using cyclic voltammetry and differential pulse voltammetry. The results of these studies indicate that **1.4** shows a cathodic wave at 1.40 V, which is assigned to a $Co^{II}Co^{II} \rightarrow Co^{II}Co^{III}$ oxidation couple. Their conclusion contrasts with Mukherjee *et al.*[8] who reported phenolate complexes of this type, where the redox chemistry was proposed to be ligand based.

Exploring the catalytic activity of the transition metal complexes containing chelating alkoxide and aryl-oxide ligands, Garcia-Vazquez *et al.* most recently synthesized a structurally characterized bimetallic Co^{II} species, $[(Co^{II}\mathbf{L_5})_2]$ **(1.5)** of a tripodal ligand *N,N*-bis(4,5-dimethyl-2-hydroxybenzyl)-*N*-(2-pyridylmethyl)amine $H_2[\mathbf{L_5}]$ (Figure 1.6).[6] They used the same electrochemical oxidation procedure through which the bimetallic Co^{II} complex **1.1** was previously synthesized. Thus, the effectiveness of this synthetic procedure is once again established for producing neutral metal complexes in very good yields with high purity.

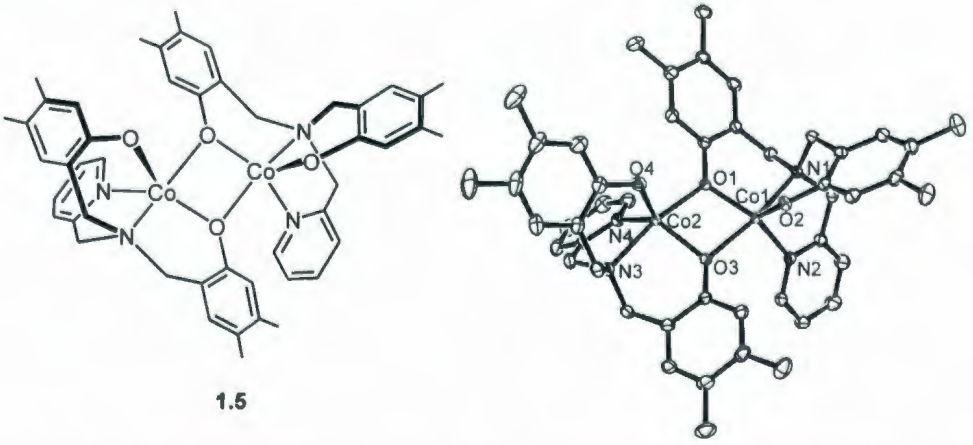

1.5

Figure 1.6 Bimetallic Co^{II} complex of amine-bis(phenolate) ligand, $[(Co^{II}\mathbf{L_5})_2]$ and ORTEP diagram of the molecular structure of **1.5** with 50% thermal ellipsoid probability.[6]

Crystallographic data for **1.5** reveal a bimetallic species containing two pentacoordinate Co^{II} ions. Using the previously defined structural parameter τ, the geometry around two Co^{II} centers is distorted trigonal bipyramidal ($\tau = 0.65$ and 0.71 for

References begin on page 52

the two Co^{II} ions). The four-membered ring formed by the two Co^{II} ions and the two bridging phenolate O-donors is nearly planar (r.m.s. deviation of 0.0882) though it is slightly asymmetric with two shorter bond distances [Co(1)–O(1) = 1.9744(12) and Co(2)–O(3) = 1.9965(12) Å] and two longer distances [Co(1)–O(3) = 2.0820(12) and Co(2)–O(1) = 2.0427(12) Å]. The two Co^{II} centers are separated by 3.1192(8) Å, a distance which is comparable with previously reported phenolate-bridged bimetallic Co^{II} complexes.[5,7,8,14] One water molecule is found in the crystal lattice which is hydrogen bonded to the non-bridging phenolate O-donors and not coordinated to a metal center. The magnetic behaviour of **1.5** is indicative of intramolecular antiferromagnetic interactions between the two Co^{II} ions. The experimental data were analyzed using the isotropic Hamiltonian $H = -JS_AS_B$ with $S_A = S_B = 3/2$. The best fit for calculated and experimental data afforded the value of $J = -4.2$ cm^{-1} and $g = 2.26$.[6]

Exploring catalytic activity using **1.5**, the catalytic decomposition of H_2O_2 was studied as a model reaction for catalase mimicry and **1.5** showed catalase-like activity.[6]

From the above discussion of amine-bis(phenolate) bimetallic Co^{II} complexes, the following aspects can be summarized: (i) three of the five amine-bis(phenolate) ligands are symmetric while two are asymmetric, (ii) two ligands contain amine donors whereas three have pyridyl groups as their pendant units, (iii) three ligands have electron donating small to moderately sterically demanding substituents, and one ligand ($\mathbf{L_2}$) contains electron withdrawing small substituents, and (iv) one ligand ($\mathbf{L_4}$) has no substituents on the phenol ring. These factors, therefore, affect the symmetry and stereochemistry of the bimetallic Co^{II} species; for example, complexes **1.1** and **1.4** are centrosymmetric while **1.2**, **1.3** and **1.5** are not. Each Co^{II} ion among five bimetallic complexes possesses distorted trigonal bipyramidal coordination environment except **1.2** in which one of the two Co^{II} ions is in an octahedral coordination environment. However, with respect to the geometrical parameter τ, **1.2** (the five-coordinate Co^{II} ion) and **1.4** are comparatively close to a perfect trigonal bipyramid and this may be due to both containing either small substituents or no substituents on the phenolate group. **1.2** is important to mention here because it is the only bimetallic complex which bears electron withdrawing substituents,

References begin on page 52

and the difference in geometry around two Co^{II} ions (one Co^{II} ion is coordinated to one methanol molecule in the coordination sphere) is likely due to the influence of these substituents. Indeed, electron withdrawing substituents attached to the phenolate rings in **1.2** tend to pull electron density toward them and subsequently these phenolate rings cause one of the two Co^{II} ions to be less electronically rich. This Co^{II} ion can, therefore, easily interact with other donor ligands such as methanol. This occurrence can be manifested by taking into consideration the other bimetallic Co^{II} complexes containing electron donating substituents. In those cases no significant interactions of Co^{II} ions with other donor ligands (solvent molecules in their crystal lattice) are observed and hence they do not deviate from a trigonal bipyramidal coordination environment. The two Co^{II} centers in each bimetallic species are separated by a comparable distance to that found in other phenolate-bridged bimetallic Co^{II} complexes except **1.3** which has a longer Co···Co distance of 3.200(7) Å. The antiferromagnetic behaviour observed for these bimetallic species is consistent with their structural characteristics. For instance, **1.1**, **1.3**, and **1.5** show weak antiferromagnetic interactions between the two Co^{II} ions as they display J values of -7.5 cm^{-1}, -6.1 cm^{-1} and -4.2 cm^{-1}, respectively. The reasons for the small experimental J values are (i) the geometry around the Co^{II} ion is more distorted and hence less appropriate for magnetic exchange, and (ii) the smaller Co–O–Co bond angles and hence the Co···Co separation which do not allow significant magnetic orbital overlap by the two Co^{II} ions through the bridges. On the basis of electronic spectra, **1.3** and **1.4** exhibit clear intraligand, charge-transfer and d-d transitions and **1.1** shows few characteristic transitions in the visible and near-IR region, indicative of the presence of a high-spin five-coordinate Co^{II} ion. This is because the UV-vis spectra were investigated in CH_2Cl_2 which is a non-coordinating solvent; hence, the Co^{II} ion can maintain its trigonal bipyramidal coordination environment in solution. **1.2** exhibits a strong absorption band which is due to the intraligand transition and for this strong absorption the d-d bands are obscured; only one weak d-d transition is observed at 567 nm. A clear comparison of all bimetallic structures in terms of selected bond distances and angles are listed in Table 1.2.

References begin on page 52

Table 1.2 Selected Bond Lengths [Å] and Angles [°] of bimetallic amine-bis(phenolate) Co^{II} complexes

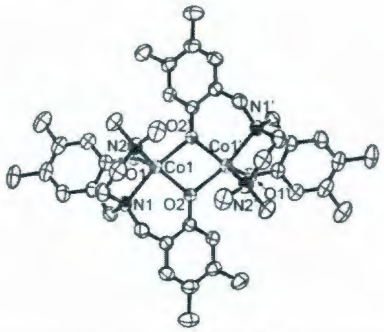

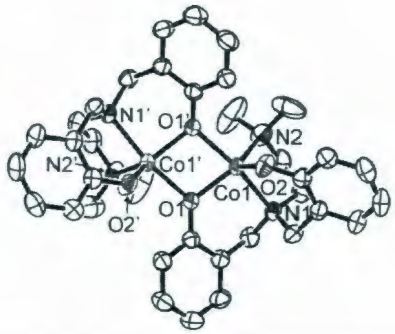

$[(Co^{II}L_1)_2]$				$[(Co^{II}L_4)_2]$			
Co(1)–O(1)	1.9289(16)	O(2)–Co(1)–N(2)	126. 34(7)	Co(1)–O(1)	2.0027(16)	O(2)–Co(1)–N(2)	125.97(8)
Co(1)–O(2)	1.9900(15)	O(1)–Co(1)–O(2)	122.03(7)	Co(1)–O(2)	1.9273(16)	O(1)–Co(1)–O(2)	118.76(6)
Co(1)–O(2')	2.0678(16)	O(1)–Co(1)–N(2)	111.31(7)	Co(1)–O(1')	2.0817(17)	O(2)–Co(1)–N(2)	114.92(9)
Co(1)–N(1)	2.1885(19)	O(1)–Co(1)–O(2')	104.21(7)	Co(1)–N(1)	2.1858(18)	O(1)–Co(1)–O(1')	79.70(6)
Co(1)–N(2)	2.156(2)	Co(1)–O(2)–Co(1')	102.04(7)	Co(1)–N(2)	2.145(2)	Co(1)–O(1)–Co(1')	100.19(6)
Co(1)···Co(1')	3.1547(8)	O(1)–Co(1)–N(1)	91.08(7)	Co(1)···Co(1')	3.134(4)	O(1')–Co(1)–O(2)	101.36(5)
		O(2)–Co(1)–N(1)	90.75(7)			O(1)–Co(1)–N(1)	90.72(7)
		O(2)–Co(1)–O(2')	77.70(7)			O(1')–Co(1)–N(2)	95.80(6)
		O(2')–Co(1)–N(2)	95.55(7)			N(2)–Co(1)–N(1)	81.94(7)
		N(2)–Co(1)–N(1)	82.47(8)			O(2)–Co(1)–N(1)	91.71(6)
		O(2')–Co(1)– N(1)	164.15(7)			O(1')–Co(1)–N(1)	166.38(6)

References begin on page 52

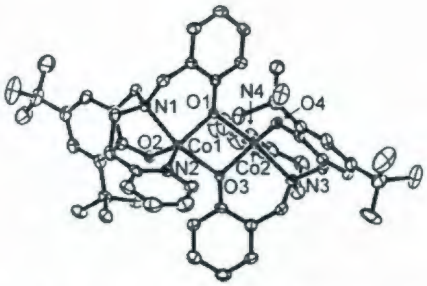

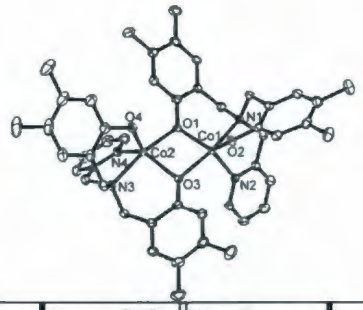

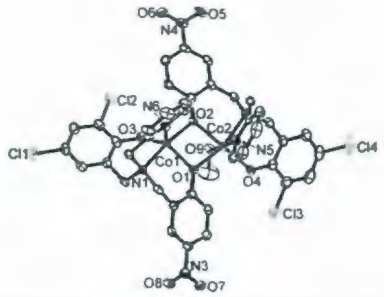

$[(Co^{II}L_3)_2]$		$[(Co^{II}L_5)_2]$	$[(Co^{II}L_2)_2]$			
Co(1)–O(1)	1.991(2)	1.9744(12)	Co(1)–O(1)	1.995(3)	O(1)–Co(1)–O(3)	123.4(2)
Co(1)–O(2)	1.935(3)	1.9341(12)	Co(1)–O(2)	2.046(3)	O(1)–Co(1)–N(6)	114.0(2)
Co(1)–O(3)	2.125(3)	2.0820(12)	Co(1)–O(3)	1.935(3)	O(1)–Co(1)–O(2)	82.0(2)
Co(1)–N(1)	2.183(3)	2.1982(14)	Co(1)–N(1)	2.156(3)	O(1)–Co(1)–N(1)	91.9(2)
Co(1)–N(2)	2.067(3)	2.0865(14)	Co(1)–N(6)	2.066(4)	O(1)–Co(1)–O(3)	97.7(2)
Co(2)–O(1)	2.112(3)	2.0427(12)	Co(2)–O(1)	2.133(3)	O(2)–Co(1)–N(6)	98.6(2)
Co(2)–O(3)	1.969(3)	1.9965(12)	Co(2)–O(2)	2.093(3)	O(2)–Co(1)–N(1)	171.8(2)
Co(2)–O(4)	1.927(3)	1.9222(12)	Co(2)–O(4)	2.010(3)	O(3)–Co(1)–N(6)	121.9(2)
Co(2)–N(3)	2.166(3)	2.1699(14)	Co(2)–O(9)	2.162(3)	O(3)–Co(1)–N(1)	90.3(2)
Co(2)–N(4)	2.118(4)	2.0710(15)	Co(2)–N(2)	2.159(3)	N(1)–Co(1)–N(6)	78.9(2)
Co(1)···Co(2)	3.200(7)	3.1192(8)	Co(2)–N(5)	2.119(4)	O(1)–Co(2)–O(2)	77.7(2)
			Co(1)···Co(2)	3.163(1)	O(1)–Co(2)–O(9)	92.7(2)
Co(1)–O(1)–Co(2)	102.46(11)	101.86(5)			O(1)–Co(2)–N(2)	159.2(2)
Co(1)–O(3)–Co(2)	102.75(11)	99.75(5)			O(1)–Co(2)–N(5)	89.8(2)
O(1)–Co(1)–O(2)	122.03(11)	117.83(5)			O(2)–Co(2)–O(4)	172.2(2)

References begin on page 52

O(1)–Co(1)–O(3)	76.99(10)	78.10(5)			O(2)–Co(2)–O(9)	81.6(2)
O(1)–Co(1)–N(1)	89.14(11)	89.75(5)			O(2)–Co(2)–N(2)	85.6(2)
O(1)–Co(1)–N(2)	124.30(12)	125.17(5)			O(2)–Co(2)–N(5)	96.1(2)
O(2)–Co(1)–O(3)	103.56(11)	103.79(5)			O(4)–Co(2)–O(9)	90.9(2)
O(2)–Co(1)–N(1)	90.18(12)	91.02(5)			O(4)–Co(2)–N(2)	93.6(2)
O(2)–Co(1)–N(2)	113.66(12)	115.89(5)			O(4)–Co(2)–N(5)	91.4(2)
O(3)–Co(1)–N(1)	164.18(11)	164.01(5)			O(9)–Co(2)–N(2)	97.1(2)
O(3)–Co(1)–N(2)	91.98(12)	99.28(5)			O(9)–Co(2)–N(5)	176.1(2)
N(1)–Co(1)–N(2)	89.58(13)	79.14(5)			N(2)–Co(2)–N(5)	79.6(2)
O(1)–Co(2)–O(3)	77.77(10)	78.54(4)				
O(1)–Co(2)–O(4)	88.13(11)	101.70(5)				
O(1)–Co(2)–N(3)	169.99(11)	166.80(5)				
O(1)–Co(2)–N(4)	95.31(13)	96.99(6)				
O(3)–Co(2)–O(4)	120.59(12)	116.10(5)				
O(3)–Co(2)–N(3)	93.11(11)	92.78(5)				
O(3)–Co(2)–N(4)	101.29(13)	124.21(5)				
O(4)–Co(2)–N(3)	91.33(12)	91.02(5)				
O(4)–Co(2)–N(4)	137.65(13)	119.18(6)				
N(3)–Co(2)–N(4)	92.50(14)	79.57(5)				

References begin on page 52

1.4.2 Cobalt(II) Complexes with Tripodal Ligands

"Capping" ligands in which a central donor atom bears three pendant arms possessing identical or different donor groups are generally termed as tripodal or tripod ligands. They can be symmetrical or unsymmetrical with respect to their pendant donor groups and substituents. In terms of the pendant arms or linkers they can also be divided into aliphatic and aromatic tripodal ligands. Over the past few decades metal complexes of tripodal ligands have gained considerable interest because of their chemical and biological significance. They have served as model compounds for biological systems and have shown utility in catalysis.[16-21] As a result, since the discovery of tris(pyrazolyl)borate (Tp) ligands or "scorpionates" by Trofimenko in 1966,[22] a wide variety of multidentate tripodal ligands have been developed and numerous transition metal complexes bearing these ligands have been prepared and their structures and properties investigated. The coordination chemistry of cobalt complexes supported by these ligands has also been well studied due to their ability to model metalloenzyme active sites.[7,8,14,23-26] Moreover, different chemical and structural properties such as molecular recognition, magnetism and redox studies of these complexes have been reported.[24,27,28] It appears that among previously reported tripodal cobalt complexes, typically inert Co^{III} complexes have been investigated widely.[18,26-32] Nevertheless, many tripodal ligands have also been designed in recent years for stabilizing Co^{II} ions in a range of structural variation.[5-8,14,23-25,33-38] A few previously reported ligands of this class used with Co^{II} are depicted in Figure 1.7.

References begin on page 52

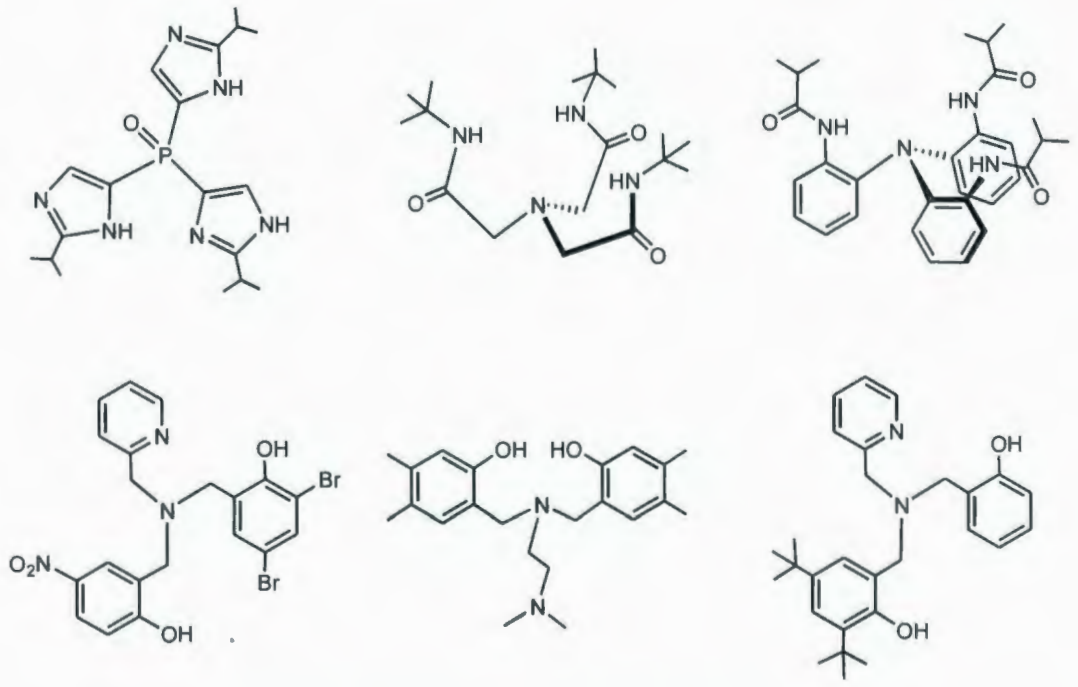

Figure 1.7 Examples of previously reported tripodal ligands used with Co^{II}.

It is appropriate to mention here that recently structurally characterized bimetallic Co^{II} complexes containing tripodal amine-bis(phenolate) ligands, bottom in Figure 1.7, were synthesized and their important structural properties and applications were thoroughly investigated.[5-8,14] A comprehensive discussion of these species is given in the previous section (section **1.4.1**). This section will therefore provide a brief study of the few previously reported Co^{II} complexes bearing other types of ligands of this class and their special structural properties.

In an effort to develop the chemistry of cobalt complexes using unsymmetrical tripodal ligands, Sakiyama *et al.* reported a structurally characterized monometallic cationic Co^{II} complex, (**1.7**) with bis[2-(3,5-dimethylpyrazol-1-yl)ethyl][pyrazol-1-yl]amine (bppa) (Figure 1.8).[34] **1.7** was synthesized by the reaction of the tripodal ligand, bppa, with Co^{II} chloride hexahydrate in the presence of $Na[B(C_6H_5)_4]$ using ethanol as the solvent. In the solid state, **1.7** contains two crystallographically independent molecules in the form of complex cations, $[Co(bppa)Cl]^+$, of which the molecular structures are

References begin on page 52

similar. X-ray analysis demonstrated that the Co^{II} is in a distorted trigonal bipyramidal coordination environment. The three N-donors of the pyrazolyl arms of the ligand occupy the equatorial positions whereas the axial sites are taken up by the remaining amino N-donor and the chloride ion, respectively.[34]

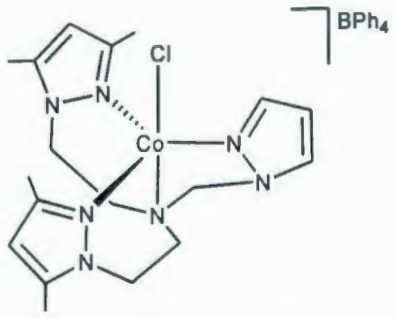

1.7

Figure 1.8 Monometallic cationic Co^{II} species using unsymmetrical tripodal ligand.

Temperature dependent magnetic data of **1.7** were indicative of the existence of a high-spin (S = 3/2) Co^{II} ion yielding a magnetic moment of 4.50 μ_B at 300 K. The experimental data were processed using the Curie-Weiss law, $\chi_A = 5Ng^2\beta^2/[4k(T-\theta)] + N\alpha$ and the best fit parameters were obtained as $\theta = -0.82$ K, $g = 2.26$, and $N\alpha = 600 \times 10^{-6}$ $cm^3\ mol^{-1}$. These results suggested that the magnetic interaction between the two Co^{II} ions is very weak and the observed long distance for the closest Co···Co separation [7.699(3) Å] in the crystal was consistent with this. The diffuse reflectance spectrum of this complex displayed several absorption bands (572, 1080, 1350, and 1690 nm) in the visible and near-IR region. These bands were assigned to characteristic d-d transitions for a high-spin Co^{II} ion in a trigonal bipyramidal geometry irrespective of the distortion.[34]

Gou and co-workers have reported a structurally characterized heptacoordinate monometallic cationic Co^{II} species, **(1.8)** using a tripodal ligand as a unique study for polycoordinate complex synthesis (Figure 1.9).[17] The group synthesized **1.8** by an *in situ* reaction where an aqueous solution of 2,2′,2″-triaminoethyl amine and 2-pyridinecarboxaldehyde N-oxide was mixed with an aqueous solution of hydrated Co^{II} chloride followed by the addition of the potassium salt, KPF_6.

References begin on page 52

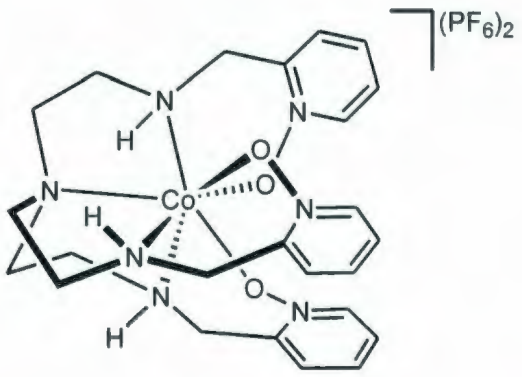

1.8

Figure 1.9 Monometallic cationic Co^{II} species of a polydentate tripodal ligand.

The crystal structure of **1.8** revealed that the coordination geometry around the Co^{II} ion as mono-capped antitrigonal prismatic with a N_4O_3 donor set, in which the central N-donor of the ligand bonded to the metal creates a crystallographic C_3 axis. Two ideal equilateral triangles, parallel to each other, are formed by the three N-donors and the three O-donors of the ligand. The group also compared the related bond distances between the metal center and the N- and O-donors with previous literature. Magnetic susceptibility data of **1.8** indicated the existence of a high-spin Co^{II} ion.[17]

By means of a constrained tripodal ligand which supports the formation of trigonal monopyramidal complexes, the Borovik group reported an anionic structurally characterized monometallic Co^{II} complex, (**1.9**) of a deprotonated ligand, tris((*N-tert*-butylcarbamoyl)methyl)amine, $[(^{tBu}NC(O)CH_2)_3N]^{3-}$ (Figure 1.10).[33] They designed the ligand by substituting a tertiary amine with three pendant amido moieties which can stabilize coordinatively unsaturated metal ions. Sterically demanding *tert*-butyl substituents attached to the amido donors also prevent the vacant coordination site being occupied by other ligands. The ligand was synthesized by a reaction of *tert*-butylamine with nitrilotriacetic acid in pyridine in the presence of triphenyl phosphite as a dehydrating agent. The deprotonation of the ligand was achieved by using potassium hydride in dimethyl formamide which then reacts with the cobalt salt, $[Co(DMSO)_6](ClO_4)_2$ to afford the monomeric Co^{II} species.

References begin on page 52

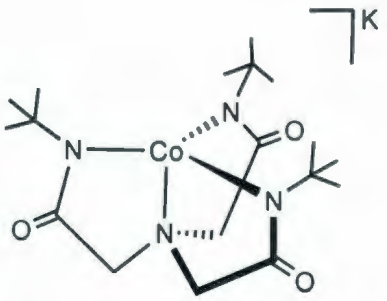

1.9

Figure 1.10 Monometallic anionic Co^{II} species of a constrained tripodal ligand.

X-ray crystallographic data of **1.9** revealed that the Co^{II} ion adopts a trigonal monopyramidal coordination environment. The three amido N-donors are coordinated to the metal center in a trigonal plane and the tertiary amine N-donor is bonded apically. The trigonal monopyramidal geometry was also confirmed by the identical bond distances and the similar angles between the Co^{II} ion and the three amido N-donors [the three Co-N_{amido} bond distances are 1.972(2), 1.970(2), and 1.974(2) Å and the average N_{amido}-M-N_{amido} angle is 119.05(6)°]. The apical amine N-donor lies perpendicular to the trigonal plane which ultimately gives **1.9** nearly C_3 symmetry where the axis of the symmetry coincides with the Co-N_{amine} bond. The effective magnetic moment of **1.9** in the solid state is 4.30 μ_B, which is consistent with the presence of a high-spin (S = 3/2) Co^{II} ion. The visible electronic absorption spectrum exhibited a symmetrical band at 414 nm, an unsymmetrical band centered at 590 nm, and a broad shoulder at 700 nm which were similar to a previously reported trigonal monopyramidal Co^{II} complex. Redox behaviour was also studied for this complex and the cyclic voltammagram showed a quasi-reversible redox process at 0.77 V *vs* SCE which was assigned to the Co^{II}/Co^{III} couple. However, at lower scan rates this redox process became irreversible, and further investigation directed at obtaining stable oxidized products of **1.9** was unsuccessful. The group reasoned that this tripodal ligand does not have the ability to stabilize high-valent metal ions. They proposed that the chelating ring strain upon metal complexation is likely responsible for this inability. It was also observed that the five membered metal-chelate rings are significantly distorted in the Co^{II} species and this distortion would be more pronounced in

References begin on page 52

the case of the Co^{III} analogue.[33] Hence it is clear that the unusual rigidity of this ligand limits not only the binding of additional ligands but also the redox chemistry of **1.9**.

In similar studies, MacBeth *et al.* reported two phenylamine-based tripodal ligands and their structurally characterized monometallic Co^{II} complexes.[38] The two tripodal ligands were tris(2-aminophenyl)amine, [N(*o*-$PhNH_2)_3$], and its triamidoamine derivative, 2,2′,2″-tris(isobutylamido)triphenylamine, [N(*o*-$PhNHC(O)^{iPr})_3$]. A cationic Co^{II} complex, $[Co^{II}(N(o\text{-}PhNH_2)_3)Br]^+$ **(1.10)** was prepared by metalation of the tetraamine ligand, [N(*o*-$PhNH_2)_3$], with Co^{II} bromide in a methanol/tetrahydrofuran mixture followed by an *in situ* salt metathesis reaction using $NaBPh_4$. In order to obtain the anionic Co^{II} complex, $[Co^{II}(N(o\text{-}PhNC(O)^{iPr})_3]^-$ **(1.11)**, the ligand was treated with potassium hydride and then transmetalated with Co^{II} bromide. Finally a salt metathesis reaction using Et_4NBr afforded **1.11**. The schematic representations of **1.10** and **1.11** are depicted in Figure 1.11.

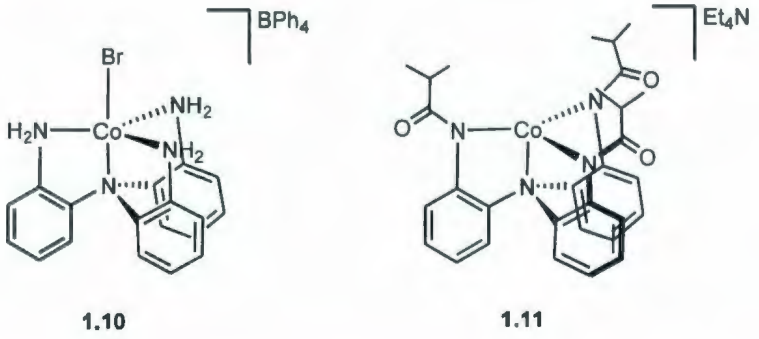

Figure 1.11 Monometallic ionic Co^{II} complexes, $[Co(N(o\text{-}PhNH_2)_3)Br]^+$ (left) and $[Co(N(o\text{-}PhNC(O)^{iPr})_3]^-$ (right).

Crystallographic analysis of **1.10** revealed that the Co^{II} is in a perfect trigonal bipyramidal coordination environment with a τ value of 1.0 (Figure 1.11). The equatorial trigonal coordination plane is comprised of the three primary amine N-donors and the apical sites are occupied by a Br^- ligand and the tertiary amine N-donor lying within the backbone of the ligand. A slight distortion of the trigonal plane is present and this is due to the metal ion lying out of the plane toward the axial ligand Br^-. The room temperature

References begin on page 52

magnetic data of **1.10** confirmed the formation of a high-spin (S = 3/2) Co^{II} ion (μ_{eff} = 4.37 μ_B).[38]

On the other hand the solid state structure of **1.11** contains two crystallographically independent but geometrically identical molecules in the unit cell. X-ray data showed that the Co^{II} ion adopts a trigonal monopyramidal coordination geometry where the three anionic amido N-donors are bonded to the metal center in the trigonal plane and the axial site is occupied by the tertiary amine N-donor. The average Co-N_{amido} bond distance is 1.959(9) Å and the position of the Co^{II} ion is slightly above that of the trigonal plane toward the vacant coordination site. The three isopropyl groups attached to the amido donors are oriented in a way that they make a flexible cavity above the Co^{II} ion which does not limit the binding of an additional ligand through the vacant coordination site. This contrasts with the Co^{II} complex, **1.9** reported by Borovik and co-workers.[33] MacBeth and Jones showed that a five-coordinate Co^{II} species can be prepared by dissolving **1.11** in dimethyl formamide and treating it with excess Et_4NCN. The formation of the five-coordinate species was confirmed by FTIR, UV-vis, and electrochemical studies. The room temperature magnetic data of **1.11** certified the existence of a high-spin Co^{II} ion with μ_{eff} of 4.69 μ_B.[38]

Most recently in biomimetic studies to model metalloenzyme active sites, Kunz and co-workers developed a water soluble neutral tripodal ligand and prepared a structurally characterized cationic Co^{II} species, (**1.12**) using this ligand.[25] The group synthesized the ligand, tris[2-organylimidazol-4(5)-yl]phosphine oxides (4-TIPO^{iPr}) by oxidizing one of their previously designed ligands, tris[2-organylimidazol-4(5)-yl]phosphines (4-TIP^{iPr}) with hydrogen peroxide. They designed their tripodal ligand in such a way that the incorporation of a polar bond P=O enhances its water solubility and also prevents the P-donor from binding to the metal. The complex **1.12** was synthesized by stirring the ligand with Co^{II} nitrate hexahydrate in methanol at room temperature (Figure 1.12). **1.12** was characterized by elemental analysis, FAB MS, $^{31}P\{^1H\}$ NMR, and single crystal X-ray diffraction.[25]

References begin on page 52

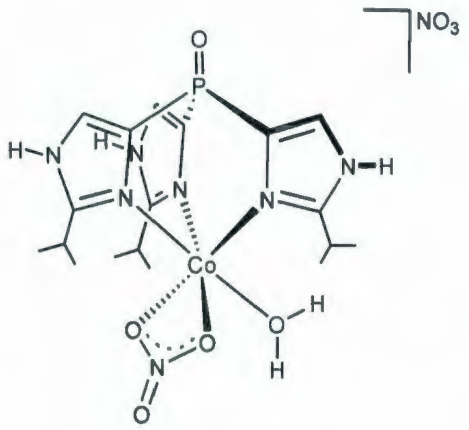

1.12

Figure 1.12 Monometallic cationic Co^{II} species prepared by a water soluble neutral tripodal ligand.

The crystal structure data of **1.12** revealed that the Co^{II} ion adopts a distorted octahedral coordination environment in which the two N-donors of the ligand and the two O-donors of the nitrato ligand occupy the basal plane and the remaining N-donor of the ligand and an aquo ligand occupy the axial sites. It was also observed that the tripodal ligand is coordinated to the Co^{II} ion facially. The axial Co-N bond *trans* to the aquo ligand is slightly longer than the Co-N bond *trans* to the nitrato ligand. The differences in the Co-O bond lengths and dihedral angles of the nitrato ligand confirmed its bidendate coordination mode. The authors noted that the structural motif of this species is strikingly similar to the structure of a Co^{II}-substituted carbonic anhydrase in which the Co^{II} ion is coordinated to the three histidyl ligands of the enzyme, one water molecule and two O-donors of a bicarbonate ligand. Thus, the group established a water soluble and perfectly hydrolytically stable model complex which could mimic the tris(histidine) motif and by introducing hydrophobic pockets, it could potentially be very useful in catalysis and polymer chemistry.[25]

It is evident that the above discussed tripodal ligands were designed by altering both pendant arms and substituents i.e. tuning sterics and electronics to afford monometallic Co^{II} species with a range of structural properties and potential applications.

References begin on page 52

It should also be noted that the used synthetic procedure plays a crucial role in the formation of these species. In addition, subtle differences in the steric bulkiness as well as the position of the substituents into the tripodal amine-bis(phenolate) ligands can afford both monometallic (Chapter 2) and bimetallic Co^{II} complexes (section 1.4.1) with different coordination geometries. On the other hand, simple modification in the tetradentate amine-based tripodal ligands can give monometallic ionic species with uncommon structural geometries (complexes **1.9**, **1.10**, and **1.11**).

1.4.3 Cobalt(II) Complexes with Schiff Base Ligands

A Schiff base (or azomethine), named after German chemist Hugo Schiff (1834-1915), is a functional group which contains a secondary imine i.e. a carbon-nitrogen double bond with the nitrogen atom connected to an aryl or alkyl group but not hydrogen. The general formula of the Schiff bases is therefore $R_1R_2C=N-R_3$, where R_3 is an aryl or alkyl group that makes the Schiff base a stable imine.[39] Schiff bases are some of the most extensively studied ligands and have been used to stabilize numerous metal complexes since the early days of coordination chemistry. The reason for their rich coordination chemistry of these ligands is their ease of preparation, their structural variety and varied denticities. Moreover, the π-accepting ability of imine nitrogen donors helps to stabilize metal ions in lower oxidation states.

In terms of cobalt chemistry, particularly with Co^{II}, a wide range of complexes containing Schiff base ligands have been intensively studied over the decades.[40-62] This field began when Tsumaki reported that square planar Co^{II} Schiff base complexes possess the ability to activate molecular oxygen when it is coordinated in the axial positions of such species.[63] Since then, many complexes have been reported to be capable of reversibly binding molecular oxygen and consequently employed as models in the study of reversible fixation of molecular oxygen.[41,43,46,64,65] Also, some are able to catalyze the oxidation of phenols, alcohols, flavonoids, nitroalkanes, hydrazines or olefins using molecular oxygen as the oxidant and therefore can serve as models for oxygenases, peroxidases, or mono- and dioxygenases.[57,66-69] The Co^{II} complexes based on tetradentate

References begin on page 52

Schiff base ligands have received significant interest because of their relevance to vitamin B_{12} models,[70-73] and biomimetic catalysis.[74] Moreover, multimetallic Co^{II} complexes using phenol based Schiff base ligands along with other appropriate co-ligands are known to display interesting magnetic behaviour.[51,75,76]

Surveying scientific literatures related to Co^{II} Schiff base coordination compounds, it can be seen that a huge number of these compounds are phenol-based Schiff base complexes, i.e. salen type ligands, another versatile and well-documented class of ligand in coordination chemistry. Therefore, a study on cobalt salen complexes is essential and the following section (section 1.4.4) will provide a detailed discussion of these complexes. Herein, the cobalt Schiff base complexes not strictly bearing salen type ligands but containing other types of Schiff base ligands are briefly described.

Whilst investigating the influence of the ligand moiety on dioxygen affinities and the performance of catalytic oxidation reactions as mimics of mono-oxygenases, Zeng and co-workers reported novel monometallic Co^{II} complexes using mono-Schiff base ligands containing various crown ether rings (Figure 1.13).[77] They prepared these ligands by the reaction of aromatic amines with crown ether-functionalized salicylaldehyde. Only one Co^{II} species, (**1.13**) was structurally characterized. X-ray structure determination of **1.13** displayed that the geometry around the Co^{II} ion is pseudo-tetrahedral, and the shape of this complex was compared with a flying bird where two aza-crown ether rings resemble the wings extending from the coordination center.

References begin on page 52

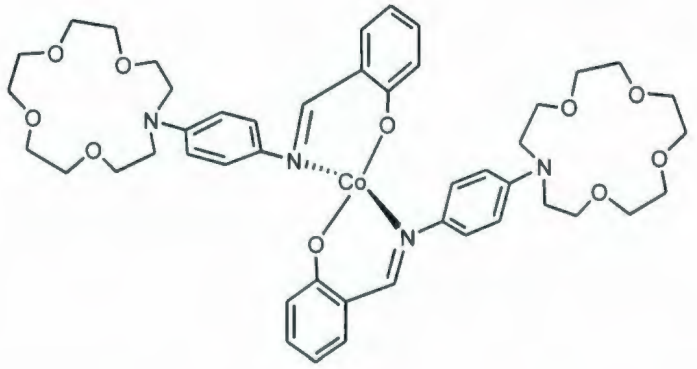

1.13

Figure 1.13 Monometallic Co^{II} complex with crown ether-containing Schiff base ligand.

The group studied the dioxygen affinities of all Co^{II} complexes. The study showed that the crown ether rings and temperature influence the dioxygen binding to the Co^{II} species. The oxygenation equilibrium constants (K_{O2}) and thermodynamic parameters ($\Delta H°$ and $\Delta S°$) showed that the dioxygen affinities were greatly affected by temperature; higher temperatures gave lower oxygenation constants presumably due to poor solubility of O_2. The structure of the Schiff base influenced the oxygen binding in such a way that when more crown ether rings were linked to the Co^{II} species, the dioxygen affinity was higher (larger oxygenation constants, K_{O2}) than those with fewer crown ether rings or uncrowned analogs. It was proposed that the macrocycle effect of the crown ether ring may play an important role in facilitating the binding of the oxygen molecule with the Co^{II} ion. The same group also investigated the catalytic oxidation performance of these species and observed that the crowned Schiff base Co^{II} complexes efficiently converted styrene to benzaldehyde with 100 % selectivity at 25 °C under an atmospheric pressure of O_2.[77]

In an enzymatic modelling attempt, Demir *et al.* reported a Co^{II} complex, (**1.14**) using a novel iminooxime Schiff base ligand, 3-hydroxyphenylamino-isonitroso-3,4-dimethoxyacetophenone (Figure 1.14).[59] They prepared this ligand, by heating a reaction mixture of isonitroso-3,4-dimethoxyacetophenone and 3-aminophenol in methanol. **1.14** was synthesized by the reaction of the ligand with the corresponding metal salts.

References begin on page 52

However, although they characterized **1.14** by elemental analysis, FT-IR, UV-vis, and room temperature magnetic susceptibility which are in good agreement with the formation of this species, no X-ray structure was obtained to better understand the geometry of the metal center along with other structural phenomena.

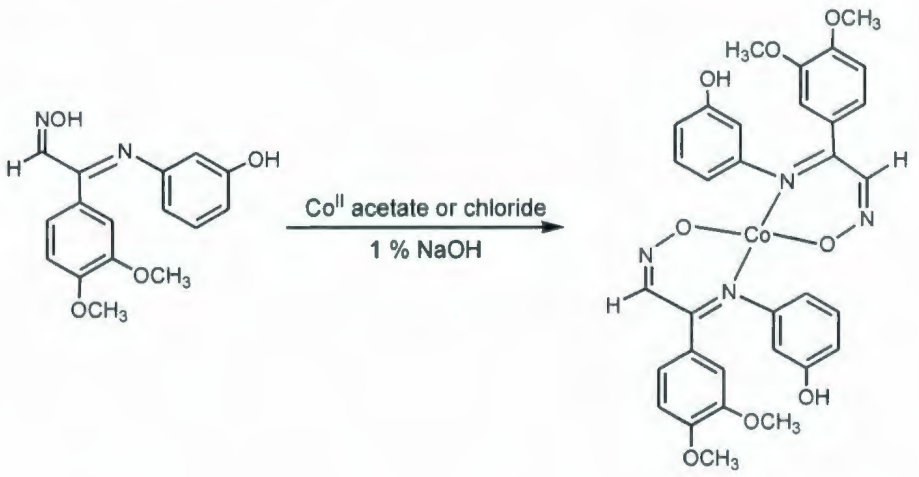

1.14

Figure 1.14 Schiff base iminoxime ligand and its Co^{II} complex.[59]

Formation of stable metal complexes through substitution of the N-H amide proton on a particular ligand is often difficult. However, incorporation of additional donor atoms in that ligand frame can lead to a stable chelating ligand which results in the formation of such metal complexes.[62] Recently, Sousa-Pedrares and co-workers reported a structurally characterized monometallic Co^{II} complex, (**1.15**) which contains a new Schiff base ligand derived from hydrazones bearing a secondary amide group (Figure 1.15).[62] They synthesized their ligand by condensation of a 1:1 mixture of 2-pyridinecarbaldehyde and a premade amine precursor (2-(aminosulfonyl)benzoic hydrazide) in methanol using *p*-toluenesulfonic acid as a catalyst. The group developed an electrochemical synthetic procedure to synthesize **1.15** by anodic oxidation of the metal and deprotonation of the ligand at the cathode.

References begin on page 52

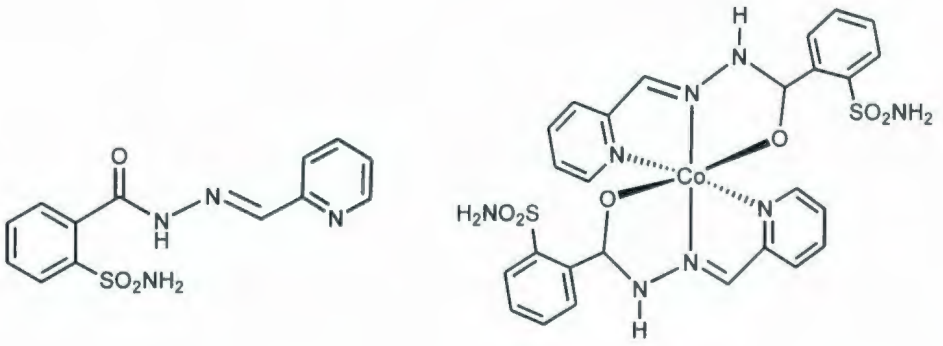

1.15

Figure 1.15 Hydrazonic Schiff base ligand and its monometallic Co^{II} complex.

Crystallographic analysis of **1.15** showed that the Co^{II} ion adopts a distorted octahedral coordination environment where the metal center is bonded to two monoanionic tridentate ligands by two nitrogen atoms (an imine nitrogen and a pyridine nitrogen) and oxygen atom from each of the two ligands. These ligands are oriented in such a way that a meridional isomer is obtained possibly due to the rigidity of the tridentate ligands. Three different types of bond distances [Co-O, Co-N_{imine}, and Co-$N_{pyridine}$] are observed in **1.15**. It is worth noting that the IR spectra of **1.15** exhibited a medium intensity band at *ca.* 1260 cm^{-1} assignable to ν(C-O) which is indicative of the amide proton loss during the complexation, and the anionic ligand is predominantly in the enolate resonance form in the complex. The slightly longer C-$O_{enolate}$ and shorter C-N_{amide} bond distances [1.276(5) Å for C-$O_{enolate}$ and 1.320(5) Å for C-N_{amide}] in comparison to those found in the free ligand [C=O and C-N_{amide} bond distances are in the range of 1.230 – 1.219 Å and 1.373 – 1.347 Å, respectively] are also consistent with the increased conjugation by the ligand in its deprotonated form.[62]

It is therefore certain that plenty of work has been reported on a range of monometallic Co^{II} complexes containing different types of Schiff base ligand and their uncommon structural features have also been investigated. However, although such complexes (including salen derivatives) have been known for long time, new examples with interesting structures and reactivities are still being developed.

References begin on page 52

1.4.4 Cobalt(II) Complexes with Salen type Ligands

Ligand design through the incorporation of specific donors and stereochemically rigid or flexible backbones plays a vital role in the stabilization of metal ions in a range of oxidation states. In this regard, salen type ligands can be designed with specific functions. These Schiff base ligands are prepared *via* the condensation of salicylaldehydes and diamines. They are tetratendate, and contain two imine N- and two phenolate O-donors that preferentially adopt a square planar geometry with the four donor atoms nearly coplanar (Figure 1.16).

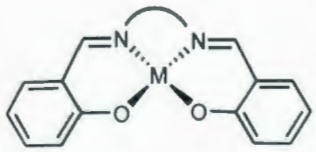

Figure 1.16 Metal complex with salen-type ligand.

The key features of these ligands are (i) the π-accepting ability of imine donors, (ii) facile introduction of various sterically demanding and/or electron donating/withdrawing substituents to the ligand periphery, (iii) the ability to incorporate both chiral and achiral modules into the backbone of the ligand, and (iv) the possibility of phenolate O-donors to bind more than one metal ion. All of these inherent features consequently have made salen type ligands excellent candidates for stabilizing a variety of transition metals. A few recently reported ligands of this class used with Co^{II} are shown in Figure 1.17. It is observed that these ligands distinguish themselves by the variation of electron donating and withdrawing substituents attached to the phenolate rings as well as both chiral and achiral groups connected to the imine donors i.e. backbone of the ligands. Some of these ligands are therefore symmetric on the basis of peripheral groups except $[L_1]^{2-}$ type ligand which can be both symmetric and asymmetric.

References begin on page 52

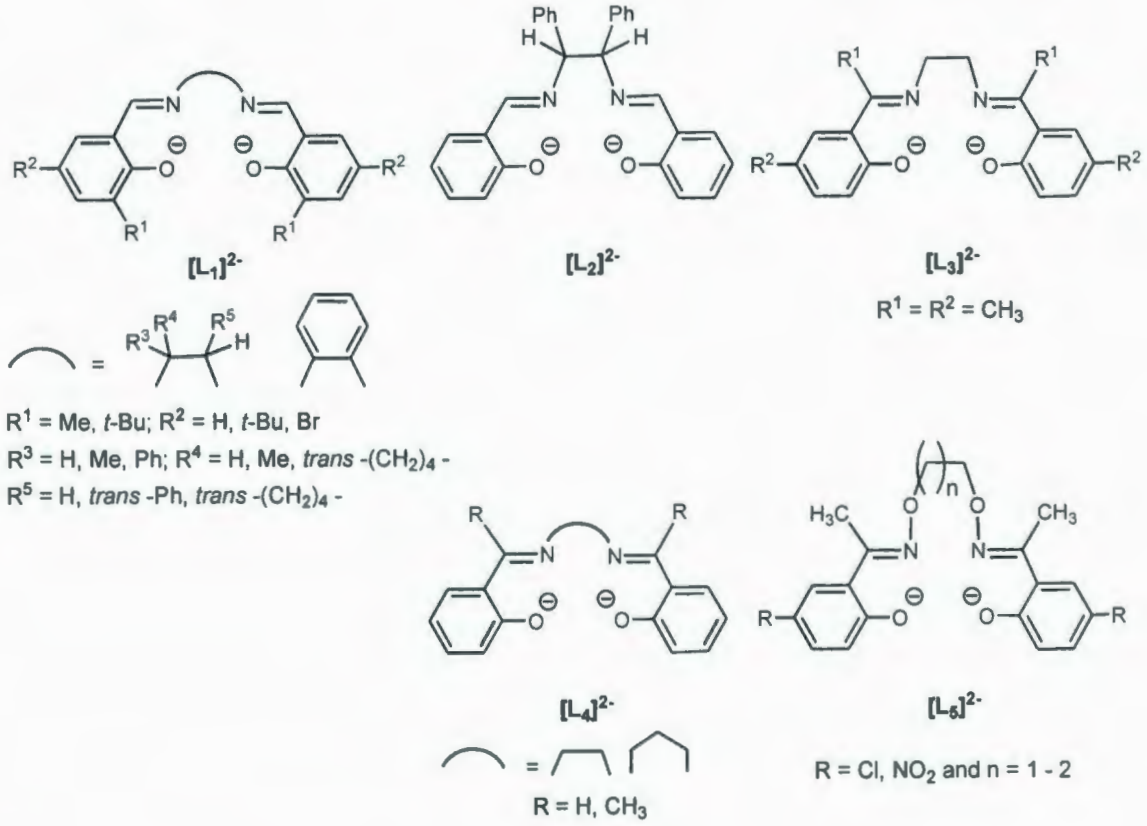

Figure 1.17 Examples of recently reported salen type ligands.

After being discovered in the 19th century, the synthesis and chemistry of salen type ligands and their numerous metal complexes have been extensively studied for decades.[78-94] Amongst various metal salen complexes, cobalt variants are some of the most well-studied coordination compounds. There has also been widespread and continuing interest in these complexes because they have found utility in a broad range of applications. Notable examples are their use (i) as oxygen carriers as Co^{II} salen complexes can reversibly bind O_2,[78] and consequently act as catalysts for oxidation of different organic substrates,[95,96] (ii) as antiviral agents, due to their ability to interact with proteins and nucleic acids,[87] (iii) as mimicks for biological cofactors, such as cobalamin owing to their similarity to several metalloenzymes,[87] and (iv) as efficient catalysts for homopolymerization of epoxides,[88,97,98] and alternating copolymerization of CO_2 with epoxides.[99-102]

References begin on page 52

During the development of efficient cobalt catalysts for homopolymerization of epoxides and alternating copoplymerization of CO_2 with epoxides, Geoffrey Coates and co-workers prepared a series of monometallic Co^{II} salen complexes along with their structurally characterized Co^{III} analogs. The Co^{II} salen complexes were synthesized by reactions in a 1:1 toluene/methanol mixture of cobaltous acetate tetrahydrate with the salen type ligand $H_2[\mathbf{L_1}]$ under N_2, while these ligands were prepared by condensation of chiral/achiral diamines with appropriate salicylaldehydes.[100] Subsequently these complexes were characterized by IR and HRMS (ESI). It is notable that, none of the Co^{II} salen complexes reported by Coates group were structurally characterized except one square planar complex, [Co^{II}(salph)] where salph = *N,N'*-bis(3,5-di-*tert*-butylsalicylidine-1,2-benzenediamine) (**1.16**) (Figure 1.18).[97] The reason given for not structurally characterizing other Co^{II} salen complexes was their facile synthesis and their ability to be characterized by other spectroscopic methods, e.g. IR and mass spectrometry. Moreover, one of the reported Co^{II} salen complexes is commercially available.[100]

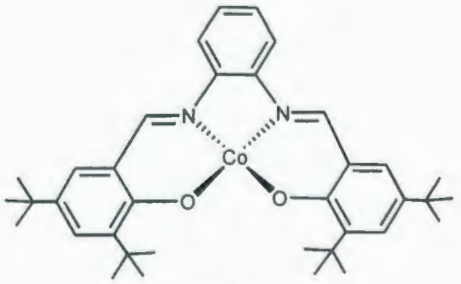

1.16

Figure 1.18 Monometallic Co^{II} salen complex, [Co^{II}(salph)].[97]

In an earlier investigation of chiral metal Schiff base complexes for a better understanding of their redox and structural features, Leung *et al.* reported a structurally characterized monometallic Co^{II} salen complex, (**1.17**) using Jacobsen's Schiff base ligand, (*R,R*)-(–)-*N,N'*-bis(3,5-di-*tert*-butylsalicylidene)cyclohexane-1,2-diamine (Figure 1.19).[82] The group prepared **1.17** by heating a 1:1 molar ratio of the ligand in toluene and cobaltous acetate in aqueous ethanol at 100 °C in the presence of triethylamine, followed by washing with ethanol and recrystallizing in a chloroform/hexane mixture. X-ray data

References begin on page 52

revealed that the Co^{II} ion possesses a pseudo-square planar coordination geometry with two *cis* phenolate O- and two *cis* imine N-donors. The bond distances between the Co^{II} center and the phenolate O- and the imine N-donors are *ca.* 1.84 and 1.88 Å respectively, which are similar to a previously reported Co^{II} complex, [Co^{II}(bsalen)] [bsalen = *N,N'*-(3-*tert*-butylsalicylidene)tetramethylethane-1,2-diamine]. The redox behaviour of **1.17** was also studied and the cyclic voltammogram showed two reversible oxidation waves at 0.0 and 0.6 V *vs* ferrocene-ferrocenium, which were assigned to the metal-centered (Co^{III}-Co^{II}) and ligand-centered oxidations, respectively. These reduction potentials were comparable to previously reported Co^{II} salen complexes.[82]

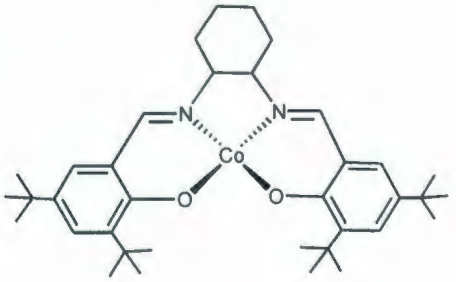

1.17

Figure 1.19 Monometallic Co^{II} complex using Jacobsen salen type ligand.

Recently Tyler and co-workers developed a chiral salen type ligand, H_2[$\mathbf{L_2}$] introducing phenyl rings in the ethylene linker and reported a structurally characterized monometallic Co^{II} salen complex, [$Co^{II}\mathbf{L_2}$] (**1.18**) (Figure 1.20).[92] This complex was synthesized by stirring a 1:1 equivalent mixture of the salen ligand and cobaltous acetate tetrahydrate in methanol for 3 hrs. The solid was collected by gravity filtration and dried under high vacuum. X-ray quality crystals were obtained by slow diffusion of diethyl ether into the dichloromethane solution of this species. Crystallographic analysis of **1.18** revealed that one salen ligand is coordinated to the Co^{II} ion with two phenolate O-donors and two imine N-donors. The Co^{II} ion adopts a slightly distorted square planar geometry. The two bond angles formed by the two imine N-donors and the two phenolate O-donors with the Co^{II} center are identical [i.e. N-Co-O = 94.47(6)°] and nearly 10° larger than the other two bond angles between the imine N-donors and the Co^{II} center [N-Co-N =

References begin on page 52

86.39(6)°], and phenolate O-donors and the Co^{II} ion [O-Co-O = 85.91(5)], respectively. It can also be seen that the ligand binds the Co^{II} ion in a nearly symmetric fashion which is evidenced by almost equivalent $Co\text{-}N_{imine}$ and $Co\text{-}O_{phenolate}$ bonds [the average $Co\text{-}N_{imine}$ and $Co\text{-}O_{phenolate}$ bond distances are 1.862(6) and 1.843(4) Å, respectively]. These bond distances are similar to previously reported Co^{II} complexes. Elemental analysis and the IR spectrum were found to be in good agreement with the formation of **1.18**. The electronic absorption spectrum of this species displayed several intense absorption bands in the high energy region assignable to ligand field transitions and one weak band in the low energy range assigned to most likely d-d transition.[92]

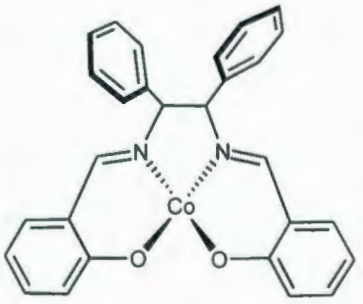

1.18

Figure 1.20 Monometallic Co^{II} complex with salen type ligand, $[Co^{II}\mathbf{L_2}]$.

It has been reported that monometallic Co^{II} salen complexes can act as bidentate chelating ligands for both transition and non-transition metals to afford multimetallic species. In an attempt to obtain such a multimetallic species, Randaccio and co-workers reported a structurally characterized trimetallic mixed-valent $Co^{III}\text{-}Co^{II}\text{-}Co^{III}$ salen complex, (**1.19**) (Figure 1.21).[91] **1.19** was synthesized by mixing previously characterized bimetallic organocobalt derivatives[84] containing salen type ligand, $H_2[\mathbf{L_3}]$ with a stoichimetric amount of $CoCl_2$ in a dichloromethane/isopropyl alcohol mixture. Crystallographic data revealed that **1.19** comprised of a central $Co^{II}Cl_2$ unit connected by two $[RCo^{III}\mathbf{L_3}]$ where (R can be either CH_2Cl or CF_3CH_2) fragments with two bridging chloro ligands and four bridging phenolate O-donors. Each metal ion is in octahedral coordination environment. The solid state structure also confirmed that **1.19** can be

References begin on page 52

isolated as *cis* (when R = CH_2Cl, C_2 symmetry) and *trans* isomers (when R = CF_3CH_2, C_{2h} symmetry) with respect to the positions of the chloro ligands around the central Co^{II} ion. The room temperature magnetic moment of **1.19** indicated the existence of one high-spin Co^{II} and two low-spin Co^{III} ions. However, despite the presence of a paramagnetic metal center in **1.19**, the group successfully characterized this species using ^1H NMR spectroscopy which showed well resolved resonances and slow interconversion of the *cis* and *trans* isomers on the NMR time-scale in solution.[91]

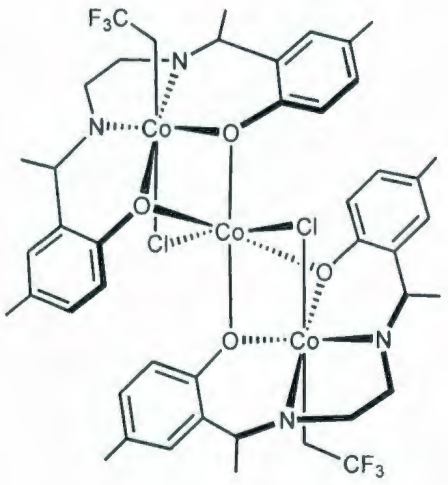

1.19

Figure 1.21 Trimetallic Co^{III}-Co^{II}-Co^{III} salen complex (*trans* isomer, C_{2h} symmetry).

In related studies, Ghosh *et al.* reported a similar type of structurally characterized mixed-valent Co^{III}-Co^{II}-Co^{III} complex using the salen type ligand, H_2**[L$_4$]**.[87] They synthesized the trimetallic species by a reaction in a methanol solution of cobaltous acetate tetrahydrate and the salen ligand in a 3:2 molar ratio in the presence of air. Crystallographic analysis of this complex revealed that the central Co^{II} ion is coordinated to six O-donors (four bridging phenolate and two bridging acetato O-donors) whereas each terminal Co^{III} ion is coordinated to a salen ligand and two acetate ligands of which one acetate ligand binds terminally and the other one is bridging. Each cobalt ion is in a distorted octahedral coordination environment.[87] The room temperature magnetic moment

References begin on page 52

indicated the presence of a high-spin Co^{II} ion similar to the previous mixed-valent trimetallic species depicted in Figure 1.21.[91]

During the course of investigating analytically pure multimetallic Co^{II} complexes using a salen type ligand incorporating a propylene linker to the diimines, Marzilli and co-workers reported a structurally characterized linear, trimetallic Co^{II} complex, (Co^{II}-Co^{II}-Co^{II}) (**1.20**) (Figure 1.22).[79] X-ray structural analysis revealed that **1.20** is centrosymmetric and the central Co^{II} ion is bonded to four bridging phenolate O-donors and two acetato O-donors from each of the two acetate bridges. The terminal Co^{II} ions are in distorted octahedral coordination geometries where the salen ligand occupies four equatorial positions, and two apical positions are taken up by two O-donors (one from the bridging acetate and the other from a dimethyl formamide molecule). The room temperature magnetic moment of **1.20** confirmed the existence of high-spin Co^{II} ions (S = 3/2).[79]

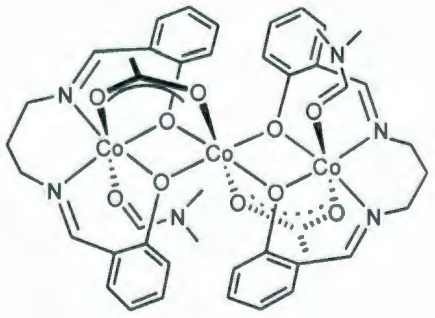

1.20

Figure 1.22 Trimetallic Co^{II}-Co^{II}-Co^{II} salen complex.

It is worth noting that although the room temperature magnetic data were obtained for all of the above mentioned trimetallic species, no temperature dependent magnetic measurements were reported which would have been more effective in confirming the spin state of the metal ions. It is also observed from the synthetic procedures for trimetallic species that the mixed-valent cobalt salen complexes (Co^{III}-Co^{II}-Co^{III}) were prepared in the presence of air whereas for the uniformly Co^{II} trimer an inert atmosphere

References begin on page 52

was required. Indeed, two new structurally characterized trimetallic Co^{II} species containing amine-bis(phenolate) ligands were synthesized and are described in this thesis (Chapter 2) for which an inert N_2 atmosphere was needed. However, once isolated, these complexes are air stable.

The most recent example of a structurally characterized trimetallic Co^{II} salen complex, (**1.21**) was reported by Dong and co-workers using a salen-type bisoxime ligand, H_2**[L$_5$]** (Figure 1.23).[89] **1.21** contains electron withdrawing substituents on the phenolate rings and a trimethylene group in the backbone of the ligand. Crystallographic data showed that **1.21** is centrosymmetric containing an inversion center at the central Co^{II} ion. The coordination sphere of each of the two terminal Co^{II} ions was completed by the N_2O_2 donor set of the ligand, one O-donor of a bridging acetate ligand and one O-donor of a methanol molecule. The environment of the central Co^{II} ion contains four bridging phenolate O-donors and two bridging acetate O-donors. Thus, the three Co^{II} ions were all in octahedral coordination environments.[89]

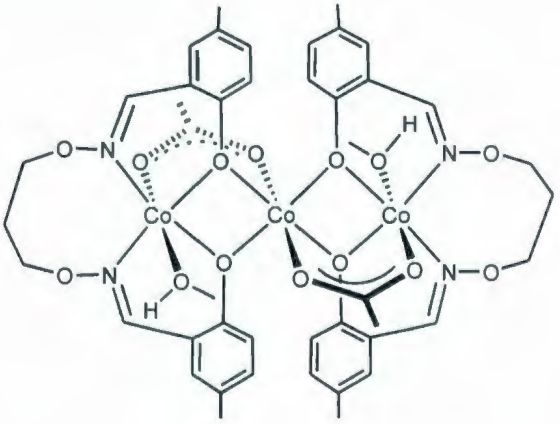

1.21

Figure 1.23 Trimetallic Co^{II}-Co^{II}-Co^{II} salen complex.

From the above examples of mono- and trimetallic cobalt salen complexes it is clear that salen type ligands can stabilize both mono- and trimetallic cobalt complexes. This arises from their ability to form μ^2-phenolate bridges thus affording multimetallic

References begin on page 52

species. Bimetallic cobalt salen complexes also exist and the most recent example of a structurally characterized species of this type was reported by Tyler *et al.* along with the previously described monometallic Co^{II} salen complex.[92] The bimetallic species (**1.22**) has two oxidized cobalt ions i.e. Co^{III} which are in octahedral coordination environments. Each Co^{III} ion is coordinated to a salen ligand, one chloride ligand, and bridging phenolate O-donors. One structurally characterized neutral trimetallic species (Co^{III}-Co^{II}-Co^{III}) was also investigated by the same group which contains two salen ligands and four acetate ligands. In this case the two terminal Co^{III} ions are equivalent giving the molecule C_2 symmetry. The central Co^{II} ion is coordinated to six O-donors (four from the bridging phenolates and two from the bridging acetate ligands). These bridging acetate ligands occupy two sites that are *cis* to each other on the Co^{II} center.[92] The schematic representation of **1.22** is shown in Figure 1.24.

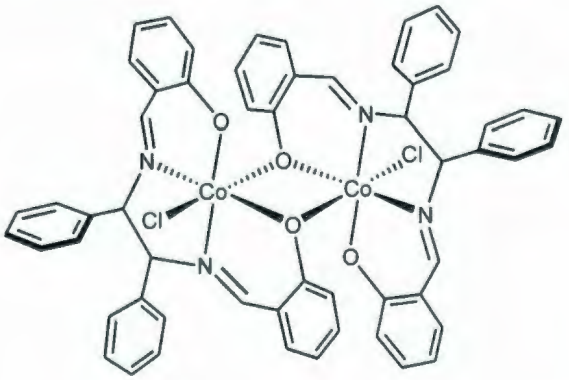

1.22

Figure 1.24 Bimetallic Co^{III} salen complex.

On the basis of above discussions of mono-, bi- and trimetallic cobalt salen complexes it can be concluded that two types of trimers, Co^{II}-Co^{II}-Co^{II} and Co^{III}-Co^{II}-Co^{III} have been reported previously. It was rationalized in the literature[87] that the ligand field strength controls the formation of these trimers; the weak field salen type ligands tend to stabilize Co^{II} ions whereas strong field ligands usually stabilize Co^{III} ions. This phenomenon can be seen when polymethylene spacers or attached bulky groups connect the imines then the ligand acts as weak field ligand ($\mathbf{L_2}$ and $\mathbf{L_5}$). On the other hand if there

References begin on page 52

is only an ethylene linker connecting the imines, the ligand behaves as a strong field ligand ($\mathbf{L_3}$ and $\mathbf{L_4}$). However, in addition to the ligand field strength, other factors such as the flexibility of the Schiff base (modifying the linker connecting the imines), the role of the co-ligands, and the synthetic procedure are all equally important in the formation of such multimetallic species. In comparison to the examples of the previously reported mono- and trimetallic cobalt salen complexes, bimetallic Co^{II} salen complexes are rarer. All of the trimetallic cobalt salen complexes described above have both multiple acetate and phenolate bridges between the metal centers along with other co-ligands.

1.5 Electronic Structures of Cobalt(II) Complexes

Co^{II} complexes show a great variety of structural environments and therefore the electronic structures, i.e. the optical and magnetic properties, of the Co^{II} ion are extremely diverse.[4] However, since the Co^{II} complexes described in this thesis possess five coordinate coordination environments, this section will provide useful information about electronic structures of five coordinate Co^{II} complexes along with a general description of electronic structures for six coordinate Co^{II} species. Theoretically, the d^7 electron configuration of the Co^{II} ion gives rise to different free ion terms such as ^4F, ^4P, ^2G and several other doublet terms which can be described by Russell-Saunders coupling. Among these free ion terms, ^4F lies lower in energy than the ^4P and forms the ground state of the ion, according to Hund's rule. In the octahedral crystal field, ^4F splits into $^4T_{1g}$, $^4T_{2g}$ and $^4A_{2g}$ states of which $^4T_{1g}$ forms the ground state. Since ^4P term does not split in the octahedral field, ^4P transforms as $^4T_{1g}$. The doublet term ^2G splits into $^2A_{2g}$, $^2T_{1g}$, $^2T_{2g}$ and ^2E_g states. Of these, the $^2E_g(G)$ state corresponds to the strong field configuration $t_{2g}^6e_g^1$, the $^4T_{1g}(F)$ state corresponds to the $t_{2g}^5e_g^2$ configuration, the $^4T_{2g}(F)$, $^4T_{1g}(P)$ and $^2A_{1g}(G)$ states correspond to the $t_{2g}^4e_g^3$ configuration and $^4A_{2g}(F)$ state corresponds to the $t_{2g}^3e_g^4$ configuration.[103] For high-spin octahedral complexes there is a quartet ground state and three spin-allowed electronic transitions to the excited quartet states. However, $^4A_{2g}(F)$ state is usually close to the $^4T_{1g}(P)$ and the transitions to these two states are close together. The visible spectrum for octahedral complexes is thus

References begin on page 52

dominated by the highest energy transition $^4T_{1g}(F) \rightarrow {}^4T_{1g}(P)$ and show absorbance maxima around 500 nm. The other two lower-energy transitions $^4T_{1g}(F) \rightarrow {}^4A_{2g}(F)$ and $^4T_{1g}(F) \rightarrow {}^4T_{2g}(F)$ can also be observed; however, the former transition is essentially a two-electron process and it is therefore weaker by about a factor of 10^{-2} than the other transitions resulting in a shoulder on the main visible band. The latter one generally occurs in the near-IR region (1000 – 2000 nm).[2,4]

In low-spin octahedral complexes a sufficiently strong ligand field ($\Delta_o \geq 15000$ cm^{-1}) can cause $^2E_g(G)$ to be the ground state. The electron configuration for the $^2E_g(G)$ state is $t_{2g}^6e_g^1$, and a Jahn-Teller distortion typically occurs in low-spin octahedral systems to remove the orbital degeneracy and to achieve lower energy. Consequently octahedral low-spin Co^{II} complexes are rare, tending to dissociate ligands to form low-spin four- or five-coordinate species. An authentic example of a low-spin Co^{II} complex investigated by Nishida *et al.*, showing a Jahn-Teller distortion to form a complex of axial symmetry, is the Salcomine-type Co^{II} complex, $[Co^{II}(sals)]$ where sals = Bis(salicylaldehyde)-meso-stilbenediimine. The group measured the optical and magnetic properties of this square-planar species, and established the presence of a low-spin Co^{II} ion in good agreement with its experimental value.[104] Another example of Jahn-Teller distortion occurring in Co^{II} coordination chemistry is $[Co(CNPh)_6]^{2+}$, which is axially distorted.[4] The Tanabe-Sugano diagrams for octahedral complexes with d^7 electron configuration is given in Figure 1.25 where the term energies E are expressed as the ratio E/B (B is the Racah parameter), and the ligand-field splitting Δ_o is expressed as Δ_o/B.

References begin on page 52

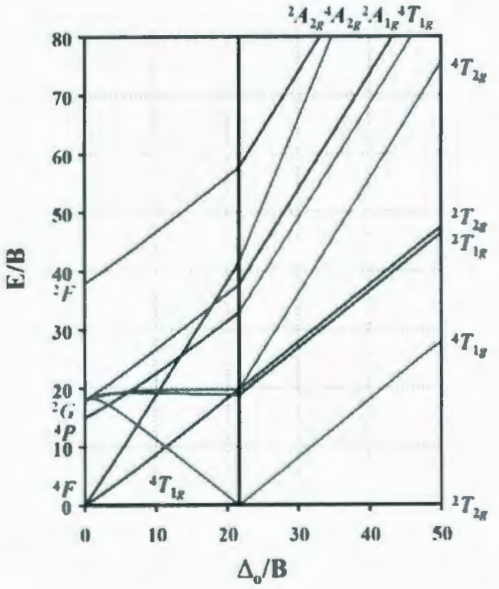

Figure 1.25 Tanabe-Sugano diagrams for octahedral complexes with d^7 electron configuration.

Five-coordinate Co^{II} complexes possess both trigonal bipyramidal and square pyramidal structural environments with D_{3h} and C_{4v} symmetry respectively, in high-spin (three unpaired electrons) and low-spin (one unpaired electron) configurations as well as intermediate configurations with C_{2v} symmetry.[4] A wide variety of such species containing weak and/or strong field ligands leading to high and low-spin species have been reported.[105, 106] For a regular high-spin trigonal bipyramidal system, the ^4F term splits, in D_{3h} symmetry, into $^4A_2' < {}^4A_2''$, $^4A_1'' < {}^4E'' < {}^4E'$ while ^4P gives $^4A_2' < {}^4E''$. However, this sequence may be modified if the Co^{II} complex is either irregular (e.g. CoL_4L' or CoL_3L_2') or there is some angular distortion. For example, if the axial-equatorial ligand angle in a CoL_5 species deviates from 90° then the degeneracy of the $^4A_2''$, $^4A_1''$ is lost. The electronic transitions in trigonal bipyramidal Co^{II} complexes generally occur both in the visible and near-IR region starting from the $^4A_2'$ ground state.[107] Indeed, for a high-spin Co^{II} ion in a trigonal bipyramidal field, there are six spin-allowed electronic transitions are possible starting from $^4A_2'(F)$ ground state.[106]

References begin on page 52

For distorted high-spin trigonal bipyramidal systems, the electronic structure can be best described in terms of lower group symmetry such as C_{3v} and the terms are arranged in ascending order of energy as $^4A_2$, $^4A_1$ and $^4A_2$, ^4E, ^4E originates from ^4F while $^4A_2$ and ^4E yielding from ^4P, respectively. In addition, there are also trigonal bipyramidal Co^{II} complexes whose electronic structure can only be described in terms of C_{2v} symmetry with a two-fold axis bisecting the equatorial plane. For example, the electronic spectrum of $[Co(PyNO)_5]^{2+}$ ion can only be analyzed by means of C_{2v} symmetry.[107] It is established that a very extensive mixing between the orbitals of the ligands and the metal ion has occurred which is indicated by their intense absorption bands in the visible region. In such cases the ^4F and ^4P terms are generally intermixed without counting the effect of spin-orbit coupling, and form several new states. The splitting of ^4F and ^4P terms into several states for a high-spin d^7 ion both in strong and weak field environments in D_{3h} symmetry is shown in Figure 1.26.

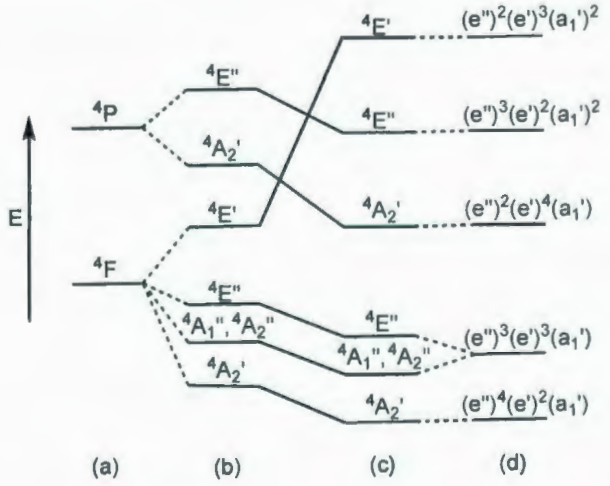

Figure 1.26 Correlation diagram for a d^7 ion ($S = 3/2$) in a high-spin trigonal bipyramidal (D_{3h}) environment. (a) Free ion terms, (b) weak field terms, (c) strong field configurations neglecting interelectronic repulsion, and (d) including interelectronic repulsion.[107]

The electronic structure of low-spin trigonal bipyramidal Co^{II} complexes were reported by Venanzi and coworkers who also calculated the d^7 energy levels.[105] In this case the ground configuration, $(e'')^4(e')^3$ derives from ^2G state. One low energy transition

References begin on page 52

occurs probably in the near-IR and a grouping of closely spaced high energy transitions are observed in the visible region. However, the same group later revealed a different interpretation which says that the ground state is $^2E'$ and it is subject to Jahn-Teller distortion. The lower energy visible band is observed due to the transition from a component of e′ to a_1' and the higher energy visible band is from the transition between the split components of e″ and e′.[107]

1.6 Application of Cobalt(II) Complexes in Catalysis

The synthesis and chemistry of Co^{II} coordination complexes has been extensively studied for decades.[2-4] There has also been widespread and increasing effort given to these complexes owing to their remarkable applications in many areas. Catalysis is such an area where many Co^{II} complexes have been developed to act as catalysts. As mentioned earlier, these type of complexes have been employed in enzymatic modelling and catalysis,[6,57,59,66-69] biomimetic catalysis,[25,74] catalytic oxidation of different organic substrates.[95,96] In recent years these complexes have also been applied to the polymer chemistry as efficient catalysts. Noteworthy examples are (i) cobalt-mediated radical polymerization, (ii) homopolymerization of epoxides, and (iii) copolymerization of carbon dioxide and epoxides. The following section will provide a discussion on the first example (cobalt-mediated radical polymerization) and the other two examples are discussed briefly in Chapter 4.

1.6.1 Cobalt-Mediated Radical Polymerization

Recently cobalt-mediated radical polymerization (CMRP) has become a popular technique in polymer chemistry.[108-116] Among several controlled radical polymerization (CRP) techniques, CMRP has the ability to properly control and design polymer chains as well as to regulate their physical and chemical properties. The first CMRP was reported by Wayland and Harwood groups simultaneously in the mid-nineties to polymerize acrylic monomers.[117,118] Ten years later Jerome *et al.* successfully employed this technique for the polymerization of vinyl acetate, a non-acrylic monomer, which had long

References begin on page 52

been a challenge for CRP because of the high reactivity of the propagating radical. The group used Co^{II}(bis(acetylacetonato)) complex which showed high efficiency in controlling the radical polymerization of vinyl acetate.[109]

Prior to the recent development of CMRP, significant efforts were made to deeply understand the principle and mechanism of CRP in the light of cobalt chemistry. In this respect two important features were investigated and studied in detail. First, the observation of a "Persistent Radical Effect" was shown by Co^{II} complexes resulting from the facile homolytic Co-C bond cleavage of Co^{III}-alkyl complexes. This was identified by Fischer in 1986[119] and has been discussed in detail.[120-125] Upon "Thermal/Photolytic" treatment of the Co^{III}-alkyl species, persistent Co^{II} and transient carbon-centered radicals are generated. The carbon-centered radical then reacts with an alkenyl monomer to form a new radical. The persistent Co^{II} species can reversibly trap the newly formed radical with the release of an unsaturated product (carbon-carbon bond formation) upon dehydrocobaltation as depicted in Scheme 1.1.

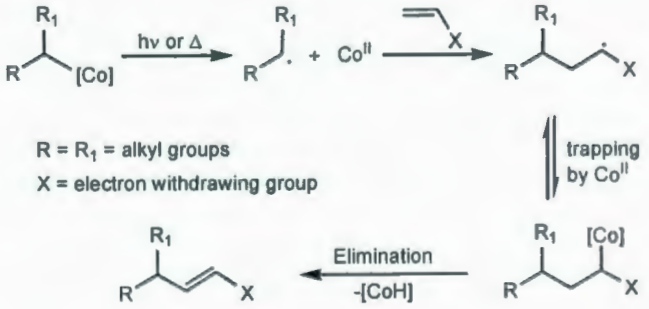

Scheme 1.1 General mechanism of carbon-carbon bond formation using Co^{III}-alkyl complexes.[116]

The second feature is catalytic chain transfer polymerization (CCTP). It was noted that some Co^{II} complexes e.g. cobaloximes and Co^{II} porphyrins (Figure 1.27) are effective chain transfer catalysts in producing poly(alkyl methacrylate)s (PMMAs).[126-128] In the proposed mechanism,[126] a polymeric radical can react with the Co^{II} species to either form an Co^{III}-alkyl complex or an unsaturated polymeric chain *via* hydrogen atom abstraction and Co^{III}-H. The catalytic cycle is closed when a monomer reacts with the

References begin on page 52

Co^{III}-H and generates a primary radical by hydrogen atom transfer from the cobalt hydride. However, all growing radicals as well as the primary radical can be reversibly trapped by the Co^{II} species. It therefore seemed that there were two pathways by which CMRP can occur; generation of persistent Co^{II} radical through reversible Co-C bond cleavage and dehydrocobaltation.

In CRP systems, a controlling agent is required to minimize the termination step through temporary deactivation of a propagating chain and its instantaneous concentration. Furthermore, in order to obtain well-defined polymers chain breaking and chain transfer reactions must also be negligible. In CMRP, the cobalt complex, notably Co^{II}, acts as a controlling agent which can deactivate the growing chains and prevent chain breaking/transfer reactions. Thus, an ideal CMRP mechanism can be represented by a schematic diagram (Scheme 1.2) as proposed by Rinaldo Poli and co-workers.[116]

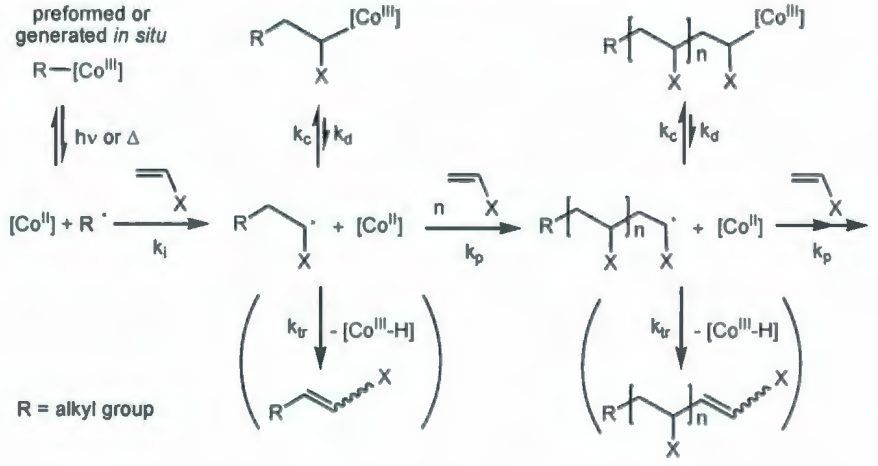

Scheme 1.2 General mechanism of the cobalt-mediated radical polymerization.[116]

It is seen from this mechanism that a preformed or *in situ* generated Co^{III}-alkyl complex undergoes reversible Co-C homolytic cleavage under "Thermal/Photolytic" conditions and releases a persistent Co^{II} radical and a transient alkyl radical. It is worthwhile noting that the Co^{II} species is not necessarily a classical radical because its electronic configuration may possess one or three unpaired electrons (high-spin $S = 1/2$ or 3/2) depending on the ligand field strength. Computational calculations for predicting the

References begin on page 52

strength of Co-C bond addressed the difference in spin state of the Co^{II} species during the homolytic cleavage.[116] Nevertheless, the Co^{II} species plays an important role of a reversible radical trap like a classical persistent radical. The polymerization is started when the transient alkyl radical adds a monomer to form a radical chain. At this stage temporary deactivation by the Co^{II} radical (k_c) or dehydrohydrocobaltation (k_{tr}) event can be occurred depending on the choice of the Co^{II} complex as well as the monomer (absence of hydrogen atoms sensitive to abstraction by the Co^{II} species) and. The radical chain can be regenerated because of the low Co-C bond strength (k_d). The CMRP process can thus be seen as a sequence of subsequent carbometallations of vinyl monomers. It was also observed that particular monomers not containing α-methyl groups that may be prone to hydrogen atom abstraction are the better choice for CMRP.[116]

Four types of monomers and three main classes of cobalt complexes have successfully been used to date in CMRP process. The monomers are acrylic esters, acrylic acid, vinyl esters and acrylonitrile and the CMRP active cobalt complexes are cobaloximes, cobalt porphyrins and β-diketonato derivatives of Co^{II} (Figure 1.27).

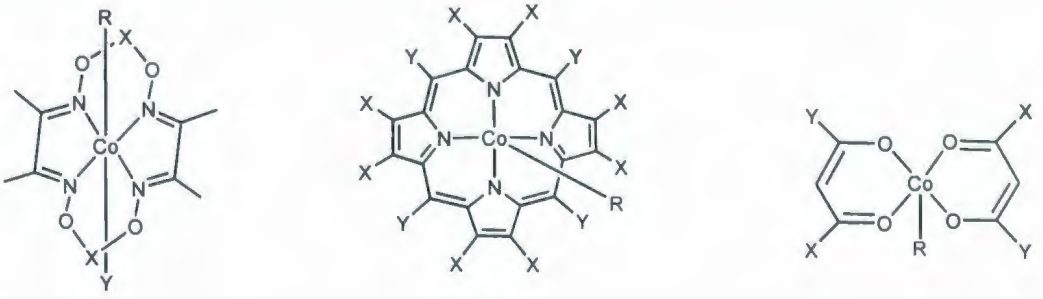

1.23 **1.24** **1.25**

X = H, CH_3, CF_3, $C(CH_3)_3$, $CH(CH_3)OMe$, Br Y = H, Ph, Py, $^{subst.}$Ph, CH_3, CF_3, $C(CH_3)_3$

R = $CH(CH_3)_2$, $CH_2C(CH_3)_3$, $CH(CO_2CH_3)CH_3$, $CH(CH_3)(OCOCH_3)$, $(CH_2)_2CO_2Me$, $CH(OAc)CH_3$

Figure 1.27 Examples of CMRP active cobalt complexes, cobaloximes (**1.23**), cobalt porphyrins (**1.24**), and bis (β-diketonato) cobalt complexes (**1.25**).[116]

References begin on page 52

The advantages provided by this technique are (i) it can be conducted at low temperatures ranging from 0 to 60 °C, (ii) it can give polymers with high molar masses (M_n > 200000 g/mol), (iii) it has been successfully applied in aqueous dispersed media e.g. suspensions and miniemulsions.[116] It is therefore certain that the cobalt-mediated radical polymerization process has opened a new window towards the further improvement of polymer chemistry.

The work described in the following chapters involves the syntheses and characterizations of both mono- and trimetallic Co^{II} complexes. These were achieved by reacting cobaltous acetate salt with sterically hindered tripodal amine-bis(phenolate) ligands under varying conditions and characterizing by X-ray crystallography, UV-vis spectroscopy, and mass spectrometry. Electrochemistry and magnetic properties were also studied for these complexes. The oxidative synthesis of a monometallic Co^{III} amine-bis(phenolate) complex was also performed and its preliminary characterizations are discussed.

References begin on page 52

1.7 References

1. J. Emsley, *Nature's building blocks: An A-Z Guide to the Elements*, Oxford University Press, Oxford and New York, 2001, 115.

2. A. G. Blackman, *Cobalt: Inorganic & Coordination Chemistry in "Encyclopedia of Inorganic Chemistry" online resource*, John Wiley & Sons Inc., Hoboken, NJ, 2006, 1-25.

3. P. V. Bernhardt, and G. A. Lawrance, *in "Comprehensive Coordination Chemistry II"*, Ed. J. A. McCleverty and T. J. Meyer, Elsevier Pergamon, Amsterdam, 2004, vol. 6, 1-122.

4. F. A. Cotton, G. Wilkinson, C. A. Murillo and M. Bochmann, *Advanced Inorganic Chemistry*, John Wiley & Sons Inc., New York, 1999, Chapter 17, 814.

5. L. Rodriguez, E. Labisbal, A. Sousa-Pedrares, J. A. Garcia-Vazquez, J. Romero, M. Luz Duran, J. A. Real and A. Sousa, *Inorg. Chem.*, 2006, **45**, 7903.

6. E. Labisbal, L. Rodriguez, O. Souto, A. Sousa-Pedrares, J. A. Garcia-Vazquez, J. Romero, A. Sousa, M. Yanez, F. Orallo and J. A. Real, *Dalton Trans.*, 2009, 8644.

7. D. Schnieders, A. Hammerschmidt, M. Merkel, F. Schweppe and B. Krebs, *Z. Anorg. Allg. Chem.*, 2008, **634**, 2933.

8. A. Mukherjee, F. Lloret and R. Mukherjee, *Inorg. Chem.*, 2008, **47**, 4471.

9. S. Groysman, I. Goldberg, M. Kol, E. Genizi and Z. Goldschmidt, *Organometallics*, 2003, **22**, 3013.

10. E. Y. Tshuva, S. Groysman, I. Goldberg, M. Kol and Z. Goldschmidt, *Organometallics*, 2002, **21**, 662.

References begin on page 52

11. E. Y. Tshuva, I. Goldberg, M. Kol and Z. Goldschmidt, *Organometallics,* 2001, **20**, 3017.

12. M. Merkel, F. K. Muller and B. Krebs, *Inorg. Chim. Acta,* 2002, **337**, 308.

13. F. M. Kerton, S. Holloway, A. Power, R. G. Soper, K. Sheridan, J. M. Lynam, A. C. Whitwood and C. E. Willans, *Can. J. Chem.,* 2008, **86**, 435.

14. R. Singh, A. Banerjee, Y. Gordon and K. K. Rajak, *Transition Met. Chem.,* 2009, **34**, 689.

15. A. W. Addison, T. N. Rao, J. Reedijk, J. Van Rijn and G. C. Verschoor, *J. Chem. Soc., Dalton Trans.,* 1984, 1349.

16. S. Trofimenko, *Prog. Inorg. Chem.,* 1986, **34**, 115.

17. S. Gou, X. You, K. Yu and J. Lu, *Inorg. Chem.,* 1993, **32**, 1883.

18. G. A. McLachlan, S. J. Brudenell, G. D. Fallon, R. L. Martin, L. Spiccia and E. R. T. Tiekink, *J. Chem. Soc., Dalton Trans.,* 1995, 439.

19. A. Deroche, I. Morgenstern-Badarau, M. Cesario, J. Guilhem, B. Keita, L. Nadjo and C. Houee-Levin, *J. Am. Chem. Soc.,* 1996, **118**, 4567.

20. M. P. Suh, J. Lee, M. Y. Han and T. S. Yoon, *Inorg. Chem.,* 1997, **36**, 5651.

21. R. G. M. Moreno, M. V. Alipazaga, M. H. G. Medeiros and N. Coichev, *Dalton Trans.,* 2005, 1101.

22. S. Trofimenko, *Scorpionates-The Coordination Chemistry of Polypyrazolylborate Ligands,* Imperial College Press, London, 1999.

23. D. M. Jenkins, A. J. Di Bilio, M. J. Allen, T. A. Betley and J. C. Peters, *J. Am. Chem. Soc.,* 2002, **124**, 15336.

References begin on page 52

24. G. Wu, Z. Zhang, T. Okamura, W. Sun and N. Ueyama, *Z. Anorg. Allg. Chem.*, 2006, **632**, 1560.

25. P. C. Kunz, A. Zribi, W. Frank and W. Klaeui, *Z. Anorg. Allg. Chem.*, 2007, **633**, 955.

26. A. Mohamadou, C. Gerard and J. Marrot, *Polyhedron*, 2008, **27**, 3036.

27. H. Nakamura, Y. Sunatsuki, M. Kojima and N. Matsumoto, *Inorg. Chem.*, 2007, **46**, 8170.

28. H. Nakamura, M. Fujii, Y. Sunatsuki, M. Kojima and N. Matsumoto, *Eur. J. Inorg. Chem.*, 2008, 1258.

29. S. Djebbar-Sid, O. Benali-Baitich and J. P. Deloume, *J. Mol. Struct.*, 2001, **569**, 121.

30. P. M. Jaffray, L. F. McClintock, K. E. Baxter and A. G. Blackman, *Inorg. Chem.*, 2005, **44**, 4215.

31. H. Y. Fu, J. M. Dou, D. C. Li and D. Q. Wang, *Acta Crystallogr., Sect. E: Struct. Rep. Online*, 2006, **E62**, m2213.

32. P. V. Bernhardt, Y. Kim and Sujandi, *Aust. J. Chem.*, 2006, **59**, 783.

33. M. Ray, B. Hammes, G. P. A. Yap, A. L. Rheingold and A. S. Borovik, *Inorg. Chem.*, 1998, **37**, 1527.

34. J. Lim, M. Mikuriya and H. Sakiyama, *Bull. Chem. Soc. Jpn.*, 2001, **74**, 2131.

35. C. A. Dodds, M. Lehmann, J. F. Ojo, J. Reglinski and M. D. Spicer, *Inorg. Chem.*, 2004, **43**, 4927.

36. M. T. Whited, E. Rivard and J. C. Peters, *Chem. Commun.*, 2006, 1613.

References begin on page 52

37. R. L. Lucas, M. K. Zart, J. Murkerjee, T. N. Sorrell, D. R. Powell and A. S. Borovik, *J. Am. Chem. Soc.*, 2006, **128**, 15476.

38. M. B. Jones and C. E. MacBeth, *Inorg. Chem.*, 2007, **46**, 8117.

39. A. D. McNaught, *IUPAC Compendium of Chemical Terminology-Online version*, Royal Society of Chemistry, Cambridge, England, 2000.

40. L. Sacconi, M. Ciampolini and G. P. Speroni, *Inorg. Chem.*, 1965, **4**, 1116.

41. D. Chen and A. E. Martell, *Inorg. Chem.*, 1987, **26**, 1026.

42. T. K. Chondhekar, *Acta Cienc. Indica, Chem.*, 1988, **14**, 297.

43. D. Chen, A. E. Martell and Y. Sun, *Inorg. Chem.*, 1989, **28**, 2647.

44. A. Kotocova and J. Sima, *Chem. Pap.*, 1994, **48**, 175.

45. M. Hirotsu, M. Kojima, K. Nakajima, S. Kashino and Y. Yoshikawa, *Bull. Chem. Soc. Jpn.*, 1996, **69**, 2549.

46. E. V. Rybak-Akimova, W. Otto, P. Deardorf, R. Roesner and D. H. Busch, *Inorg. Chem.*, 1997, **36**, 2746.

47. N. Rath, S. Jena, V. Chakravortty and K. C. Dash, *J. Indian Chem. Soc.*, 1998, **75**, 160.

48. S. Sailaja, M. R. Reddy, K. M. Raju and K. H. Reddy, *Indian J. Chem. , Sect. A: Inorg., Bio-inorg., Phys., Theor. Anal. Chem.*, 1999, **38A**, 156.

49. S. M. E. Khalil and H. F. O. El-Shafiy, *Synth. React. Inorg. Met. Org. Chem.*, 2000, **30**, 1817.

References begin on page 52

50. E. Szlyk, A. Surdykowski, M. Barwiolek and E. Larsen, *Transition Met. Chem.*, 2000, **25**, 670.

51. B. Chiari, A. Cinti, O. Crispu, F. Demartin, A. Pasini and O. Piovesana, *J. Chem. Soc., Dalton Trans.*, 2001, 3611.

52. S. Marjadi, C. M. Desai and B. J. M. Desai, *Acta Cienc. Indica, Chem.*, 2002, **28**, 131.

53. E. Tas, M. Aslanoglu, M. Ulusoy and H. Temel, *J. Coord. Chem.*, 2004, **57**, 677.

54. S. H. Rahaman, H. Chowdhury, D. Bose, R. Ghosh, C. Hung and B. K. Ghosh, *Polyhedron*, 2005, **24**, 1755.

55. A. Reiss, A. Kriza, S. Florea, T. Caproiu and N. Stanica, *Rev. Roum. Chim.*, 2005, **50**, 445.

56. A. Pui, C. Dobrota and J. Mahy, *J. Coord. Chem.*, 2007, **60**, 581.

57. A. Pui and J. Mahy, *Polyhedron*, 2007, **26**, 3143.

58. A. Pui, C. Policar and J. Mahy, *Inorg. Chim. Acta*, 2007, **360**, 2139.

59. I. Demir, M. Bayrakci, K. Mutlu and A. I. Pekacar, *Acta Chim. Slov.*, 2008, **55**, 120.

60. W. Dong, J. Duan, L. Chai, G. Liu and H. Wu, *J. Coord. Chem.*, 2008, **61**, 1306.

61. M. Fuentealba, M. T. Garland, D. Carrillo, C. Manzur, J. Hamon and J. Saillard, *Dalton Trans.*, 2008, 77.

62. A. Sousa-Pedrares, N. Camina, J. Romero, M. L. Duran, J. A. Garcia-Vazquez and A. Sousa, *Polyhedron*, 2008, **27**, 3391.

References begin on page 52

63. T. Tsumaki, *Bull. Chem. Soc. Jpn.*, 1938, **13**, 252.

64. E. C. Niederhoffer, J. H. Timmons and A. E. Martell, *Chem. Rev.*, 1984, **84**, 137.

65. A. Pui, I. Berdan, I. Morgenstern-Badarau, A. Gref and M. Perree-Fauvet, *Inorg. Chim. Acta*, 2001, **320**, 167.

66. L. I. Simandi, T. M. Simandi, Z. May and G. Besenyei, *Coord. Chem. Rev.*, 2003, **245**, 85.

67. S. Forster, A. Rieker, K. Maruyama, K. Murata and A. Nishinaga, *J. Org. Chem.*, 1996, **61**, 3320.

68. T. Bambaoud and J. Prandi, *Chem. Commun.*, 1996, 1229.

69. K. Maruyama, T. Kusukawa, T. Mashino and A. Nishinaga, *J. Org. Chem.*, 1996, **61**, 3342.

70. M. M. Aly, *J. Coord. Chem.*, 1998, **43**, 89.

71. R. Cini, S. J. Moore and L. G. Marzilli, *Inorg. Chem.*, 1998, **37**, 6890.

72. L. G. Marzilli, M. F. Summers, N. Bresciani-Pahor, E. Zangrando, J. P. Charland and L. Randaccio, *J. Am. Chem. Soc.*, 1985, **107**, 6880.

73. S. Sen, P. Talukder, S. K. Dey, S. Mitra, G. Rosair, D. L. Hughes, P. A. Yap Glenn, G. Pilet, V. Gramlich and T. Matsushita, *Dalton Trans*, 2006, 1758.

74. B. Meunier, *Biomimetic Oxidations Catalysed by Transition Metals*, Imperial College Press, London, 2000.

75. V. G. Makhankova, O. Y. Vassilyeva, V. N. Kokozay, B. W. Skelton, L. Sorace and D. Gatteschi, *J. Chem. Soc., Dalton Trans.*, 2002, 4253.

References begin on page 52

76. A. C. Rizzi, C. D. Brondino, R. Calvo, R. Baggio, M. T. Garland and R. E. Rapp, *Inorg. Chem.*, 2003, **42**, 4409.

77. W. Zeng, J. Li, Z. Mao, Z. Hong and S. Qin, *Adv. Synth. Catal.*, 2004, **346**, 1385.

78. E. C. Niederhoffer, J. H. Timmons and A. E. Martell, *Chem. Rev.*, 1984, **84**, 137.

79. A. Gerli, K. S. Hagen and L. G. Marzilli, *Inorg. Chem.*, 1991, **30**, 4673.

80. J. Costamagna, J. Vargas, R. Latorre, A. Alvarado and G. Mena, *Coord. Chem. Rev.*, 1992, **119**, 67.

81. K. M. Carroll, J. Schwartz and D. M. Ho, *Inorg. Chem.*, 1994, **33**, 2707.

82. W. Leung, E. Y. Y. Chan, E. K. F. Chow, I. D. Williams and S. Peng, *J. Chem. Soc., Dalton Trans.*, 1996, 1229.

83. T. Fukuda and T. Katsuki, *Tetrahedron*, 1997, **53**, 7201.

84. R. Dreos, G. Nardin, L. Randaccio, P. Siega, G. Tauzher and V. Vrdoljak, *Inorg. Chim. Acta*, 2003, **349**, 239.

85. S. Wu and S. Lu, *J. Mol. Catal. A: Chem.*, 2003, **197**, 51.

86. W. Adam, C. R. Saha-Moeller and P. A. Ganeshpure, *Indian J. Chem., Sect. A: Inorg., Bio-inorg., Phys., Theor. Anal. Chem.*, 2004, **43A**, 56.

87. S. Chattopadhyay, M. G. B. Drew and A. Ghosh, *Eur. J. Inorg. Chem.*, 2008, 1693.

88. W. Hirahata, R. M. Thomas, E. B. Lobkovsky and G. W. Coates, *J. Am. Chem. Soc.*, 2008, **130**, 17658.

References begin on page 52

89. W. Dong, J. Duan, Y. Guan, J. Shi and C. Zhao, *Inorg. Chim. Acta,* 2009, **362**, 1129.

90. A. K. Maldhure and A. S. Aswar, *J. Indian Chem. Soc.,* 2009, **86**, 697.

91. L. Mechi, P. Siega, R. Dreos, E. Zangrando and L. Randaccio, *Eur. J. Inorg. Chem.,* 2009, , 2629.

92. J. Welby, L. N. Rusere, J. M. Tanski and L. A. Tyler, *Inorg. Chim. Acta,* 2009, **62**, 1405.

93. R. M. Haak, M. M. Belmonte, E. C. Escudero-Adan, J. Benet-Buchholz and A. W. Kleij, *Dalton Trans.,* 2010, **39**, 593.

94. J. Yoo, S. J. Na, H. C. Park, A. Cyriac and B. Y. Lee, *Dalton Trans.,* 2010, **39**, 2622.

95. R. A. Sheldon and J. K. Kochi, *Metal Catalyzed Oxidations of Organic Compounds*, Academic Press, New York, 1981.

96. N. S. Venkataramanan, G. Kuppuraj and S. Rajagopal, *Coord. Chem. Rev.,* 2005, **249**, 1249.

97. K. L. Peretti, H. Ajiro, C. T. Cohen, E. B. Lobkovsky and G. W. Coates, *J. Am. Chem. Soc.,* 2005, **127**, 11566.

98. H. Ajiro, K. L. Peretti, E. B. Lobkovsky and G. W. Coates, *Dalton Trans.,* 2009, 8828.

99. C. T. Cohen, T. Chu and G. W. Coates, *J. Am. Chem. Soc.,* 2005, **127**, 10869.

100. C. T. Cohen, C. M. Thomas, K. L. Peretti, E. B. Lobkovsky and G. W. Coates, *Dalton Trans.,* 2006, 237.

References begin on page 52

101. W. Ren, Z. Liu, Y. Wen, R. Zhang and X. Lu, *J. Am. Chem. Soc.*, 2009, **131**, 11509.

102. D. J. Darensbourg and A. I. Moncada, *Macromolecules,* 2009, **42**, 4063.

103. K. Ramesh, P. Sivaprasad and Y. P. Reddy, *Czech. J. Phys.*, 1990, **40**, 466.

104. Y. Nishida and S. Kida, *Bull. Chem. Soc. Jpn.*, 1972, **45**, 461.

105. M. J. Norgett, J. H. M. Thornley and L. M. Venanzi, *J. Chem. Soc. A,* 1967, 540.

106. M. Ciampolini and I. Bertini, *J. Chem. Soc. A,* 1968, 2241.

107. A. B. P. Lever, *Inorganic Electronic Spectroscopy*, Elsevier, New York, 1984.

108. H. Kaneyoshi and K. Matyjaszewski, *Macromolecules,* 2005, **38**, 8163.

109. A. Debuigne, J. Caille and R. Jerome, *Angew. Chem., Int. Ed.*, 2005, **44**, 1101.

110. R. Poli, *Angew. Chem., Int. Ed.*, 2006, **45**, 5058.

111. S. Maria, H. Kaneyoshi, K. Matyjaszewski and R. Poli, *Chem. Eur. J.*, 2007, **13**, 2480.

112. W. A. Braunecker and K. Matyjaszewski, *Prog. Polym. Sci.*, 2007, **32**, 93.

113. A. Debuigne, C. Michaux, C. Jerome, R. Jerome, R. Poli and C. Detrembleur, *Chem. Eur. J.*, 2008, **14**, 7623.

114. A. Debuigne, Y. Champouret, R. Jerome, R. Poli and C. Detrembleur, *Chem. Eur. J.*, 2008, **14**, 4046.

115. U. Baisch and R. Poli, *Polyhedron,* 2008, **27**, 2175.

References begin on page 52

116. A. Debuigne, R. Poli, C. Jerome, R. Jerome and C. Detrembleur, *Prog. Polym. Sci.*, 2009, **34**, 211.

117. B. B. Wayland, G. Poszmik, S. L. Mukerjee and M. Fryd, *J. Am. Chem. Soc.*, 1994, **116**, 7943.

118. L. D. Arvanitopoulos, M. P. Gruel and H. J. Harwood, *Polym. Prepr. (Am. Chem. Soc., Div. Polym. Chem.)*, 1994, **35**, 549.

119. H. Fischer, *J. Am. Chem. Soc.*, 1986, **108**, 3925.

120. G. Pattenden, *Chem. Soc. Rev.*, 1988, **17**, 361.

121. B. E. Daikh and R. G. Finke, *J. Am. Chem. Soc.*, 1992, **114**, 2938.

122. A. Studer, *Chem. Eur. J.*, 2001, **7**, 1159.

123. J. Iqbal, B. Bhatia and N. K. Nayyar, *Chem. Rev.*, 1994, **94**, 519.

124. B. P. Branchaud, M. S. Meier and Y. Choi, *Tetrahedron Lett.*, 1988, **29**, 167.

125. B. P. Branchaud and Y. L. Choi, *Tetrahedron Lett.*, 1988, **29**, 6037.

126. T. P. Davis, D. Kukulj, D. M. Haddleton and D. R. Maloney, *Trends Polym. Sci.*, 1995, **3**, 365.

127. A. Gridnev, *J. Polym. Sci., Part A: Polym. Chem.*, 2000, **38**, 1753.

128. A. A. Gridnev and S. D. Ittel, *Chem. Rev.*, 2001, **101**, 3611.

References begin on page 52

Chapter 2

Syntheses and Structures of Mono- and Trimetallic Amine-bis(phenolate) Cobalt(II) Complexes

2.1 Introduction

The use of chelating tetradentate amine-bis(phenolate) ligands has recently played an increasingly important role in transition-metal catalyst design and modelling of metalloenzyme active-sites. They have been predominantly used with high-valent early transition-metals where they have been employed as alternative auxiliary ligands to cyclopentadienyl-based systems. In combination with group 4 metals they display high activities towards olefin or cyclic ester polymerization.[1-11] Also, group 3 and lanthanide metal complexes of these ligands have been effective as catalysts or initiators for ring-opening-polymerization of lactide and ε-caprolactone.[12-22] By comparison, there has been limited use of amine-bis(phenolate) ligands with the mid-to-late first row transition-metals.[23-33] Some iron^{III} complexes of this class of ligand have been investigated as a result of their close relationship to phenol-containing ligands found in non-heme iron containing metalloenzymes.[34-43] Novel iron^{III} compounds bearing amine-bis(phenolate) ligands have been reported recently, which effectively catalyze the cross-coupling of aromatic Grignard reagents with alkyl halides possessing β-hydrogens.[44] In terms of cobalt chemistry, a small number of bimetallic amine-bis(phenolate) complexes containing bridging phenolate groups have been structurally characterized and their magnetism investigated.[45-48]

In addition to fundamental studies of their physical properties, cobalt coordination complexes also show interesting reactivity. For example, salen coordination compounds of Co^{II} and Co^{III} have been utilized as catalysts for coupling and copolymerization of carbon dioxide with epoxides,[49-54] and homopolymerization of epoxides.[55-57] Also, interesting stoichiometric oxidation

References begin on page 93

chemistry using Co^{II} salen complexes has been reported,[58] and Co^{II} phthalocyanine compounds are known to mediate catalytic aerobic oxidation of a range of organic substrates.[59,60]

This chapter describes the preparation, structure determination and properties of mono- and trimetallic cobalt complexes of the sterically hindered tetradentate tripodal ligands, $[O_2NN']^{BuBuNMe2}$ and $[O_2NN']^{AmAmNEt2}$ (Figure 2.1). These ligands contain two dialkyl-substituted phenol groups bearing either *tert*-butyl or *tert*-amyl (*tert*-pentyl) groups *ortho* to the hydroxyl group. They are prepared through a modified Mannich reaction between the respective disubstituted phenol, aqueous formaldehyde, and the respective *N,N*-dialkylethylenediamine. Improved yields are obtained when these reactions are performed in water.[61,62]

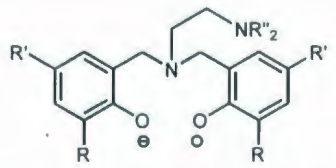

R = *t*-Bu, R' = R" = Me; $[O_2NN']^{BuMeNMe2}$
R = R' = *t*-Am, R" = Et; $[O_2NN']^{AmAmNEt2}$

Figure 2.1 Amine-bis(phenolate) ligands used in this study.

2.2 Results and Discussion

2.2.1 Syntheses and Structures of Monometallic Complexes

Reactions in a toluene/methanol mixture of approximately one equivalent of cobaltous acetate tetrahydrate with an equivalent of protio-ligand under basic conditions afforded dark purple mixtures. Upon removal of the solvent under vacuum and subsequent extraction of the products using toluene, a yellow-brown powder, (**2.1**) (Scheme 2.1), was isolated in good yield.

References begin on page 93

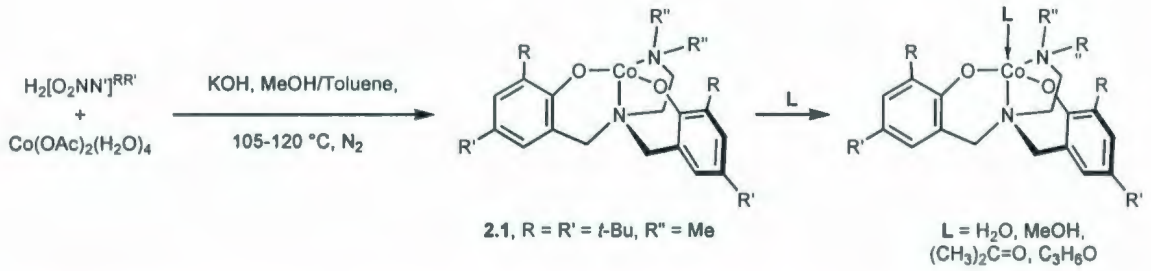

Scheme 2.1 Syntheses of monometallic amine-bis(phenolate) Co^{II} complexes.

Recrystallizations of the monometallic species **2.1** have been performed in a range of solvents. In the presence of donor solvents, trigonal bipyramidal Co^{II} complexes are obtained. The equatorial plane of each Co^{II} ion consists of two phenolate oxygens, O(1) and O(2), and a dimethylamino donor, N(2). The nitrogen donor in the backbone of the ligand, N(1), occupies an apical position with the remaining coordination site taken up by the oxygen atom, O(5), of the donor solvent. Complexes have been structurally characterized containing acetone **2.1**(CH_3COCH_3), methanol **2.1**(CH_3OH), and propylene oxide **2.1**(C_3H_6O) in this position. Their structures are shown in Figures 2.2 to 2.4 with bond lengths and angles given in Tables 2.1 to 2.3. Each structure contains two Co^{II} complexes in the asymmetric unit. A fourth complex of this class has also been structurally characterized and contains a 1:1 mixture of methanol and aquo solvent adducts. Bond lengths and angles for that version are similar to the methanol adduct and will not be discussed further. Crystallographic data and bond lengths and angles for the mixed aquo and methanol adduct, **2.1**(CH_3OH-H_2O), are available in the Appendices (Appendix 2.1, Tables A and B). The distorted trigonal bipyramidal coordination environments of the Co^{II} ions in **2.1**(CH_3COCH_3), **2.1**(CH_3OH) and **2.1**(C_3H_6O) posess τ values of 0.72 and 0.78, 0.66 and 0.80, and 0.74 and 0.77, respectively.[63] The significant differences in τ values between the two molecules of **2.1**(CH_3OH) are due to intermolecular hydrogen bonding between methanol solvent of crystallization and one molecule of **2.1**(CH_3OH). The protic nature of the coordinated methanol also leads to a degree of asymmetry in the Co-$O_{phenolate}$

References begin on page 93

bond distances in the two molecules of **2.1**(CH_3OH) in the structure. Each molecule contains a short Co-O bond (1.930(2) Å, 1.935(2) Å) and a longer Co-O bond (1.972(2) Å, 1.982(2) Å). In **2.1**(CH_3COCH_3) and **2.1**(C_3H_6O), this variation in Co-O bond distances is not observed and bond distances are in the range of 1.922(3) Å and 1.947(3) Å. A survey[64] of related Co^{II} structures shows that these Co-O bond distances are typical, as the mean value for these is 1.945 Å (standard deviation of 0.031 Å).[46,65-69] Furthermore, the tertiary amine N-Co bond distances are also similar to those previously reported (mean value of 2.144 Å, standard deviation of 0.053 Å).[46,66,70-74] However, the cavity-like nature of these ligands, as has been observed with a range of metals, means that an additional ligand in the apical position can be varied with some degree of control by simply changing the solvent of recrystallization. Also, the bond distance between the Co^{II} center and the apical donor appears to be related to the steric demands of this ligand, with the Co(1)-O(5) bond distance in **2.1**(C_3H_6O) being the longest of the three and the shortest being in **2.1**(CH_3OH). However, this variation may also result from the electronic differences among the three types of O-donor. Perhaps the most interesting of these three adducts is the propylene oxide complex, as Co^{III} complexes are known to catalyse reactions of epoxides and carbon dioxide. Although this complex contains Co^{II} rather than Co^{III}, this compound may potentially act as model for the higher oxidation state analog. Furthermore, there are relatively few Co^{II} phenolate complexes that also contain ethereal ligands in the coordination sphere. A tetrameric Co^{II} catecholate complex containing THF ligands within the Co coordination sphere exhibits Co-O_{ether} bond distances of between 2.089(12) Å and 2.225(12) Å.[75] The Co-O_{ether} bond distances in **2.1**(C_3H_6O) of 2.220(3) Å and 2.219(3) Å are comparable to the longer bond distances reported therein. Structurally characterized adducts of propylene oxide and other epoxides with a range of other metals have been reported.[76-80] In this context, the only M-phenolate complexes containing epoxides in the coordination sphere are Cd^{II} and Zn^{II} species.[78] In these complexes, M-O_{ether} bond distances are

References begin on page 93

between 2.301(5) Å and 2.357(2) Å for Cd complexes and an average for 2.108(3) Å for the Zn species. Therefore, the Co-O_{ether} bond distances in **2.1**(C_3H_6O) show good agreement with literature precedents.

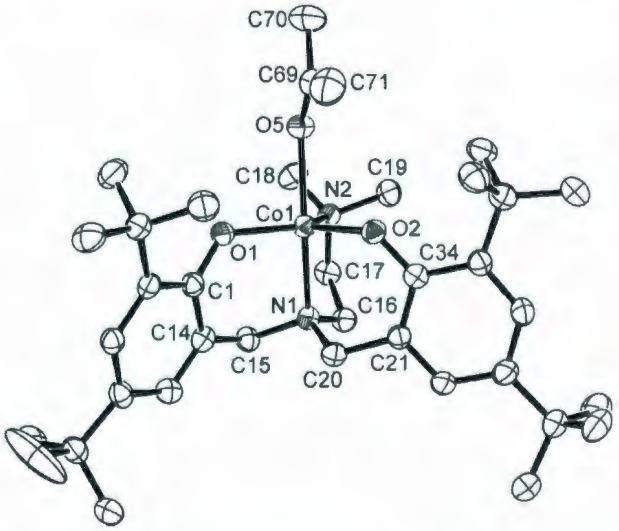

Figure 2.2 ORTEP diagram of the molecular structure of the acetone adduct of **2.1**(CH_3COCH_3) with 50% thermal ellipsoid probability. Only the molecule containing Co(1) is shown for clarity and solvent of crystallization omitted.

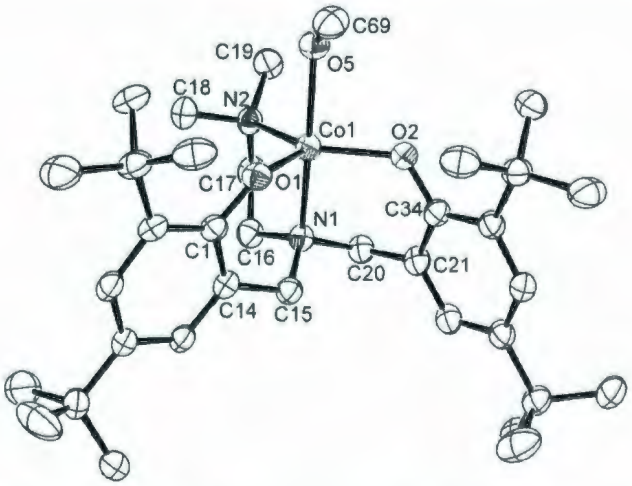

Figure 2.3 ORTEP diagram of the molecular structure of the methanol adduct of **2.1**(CH_3OH) with 50% thermal ellipsoid probability. Only the molecule containing Co(1) shown for clarity and the solvent of crystallization omitted.

References begin on page 93

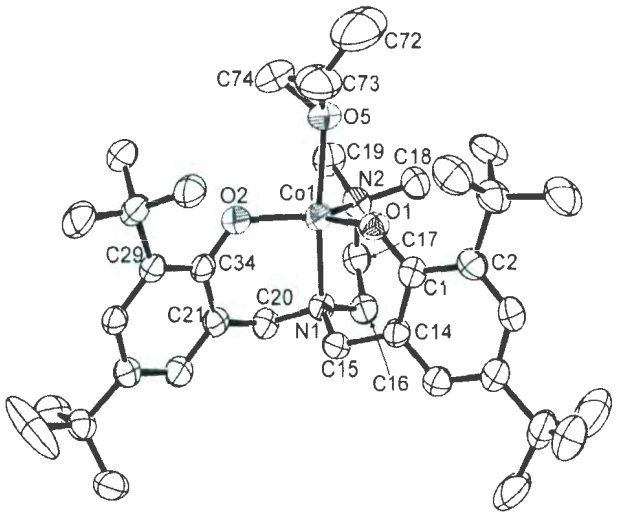

Figure 2.4 ORTEP diagram of the molecular structure of the propylene oxide adduct of **2.1**(C_3H_6O) with 50% thermal ellipsoid probability. Only the molecule containing Co(1) and (*R*)-isomer of propylene oxide are shown, and solvent of crystallization omitted.

References begin on page 93

Table 2.1 Selected Bond Lengths [Å] and Angles [°] for the acetone adduct of **2.1**(CH_3COCH_3)

Co(1)–O(1)	1.923(3)	N(1)–Co(1)–N(2)	82.79(11)
Co(1)–O(2)	1.937(3)	O(1)–Co(1)–O(5)	91.77(10)
Co(1)–N(1)	2.135(3)	O(2)–Co(1)–O(5)	93.62(10)
Co(1)–N(2)	2.150(3)	N(1)–Co(1)–O(5)	168.94(10)
Co(1)–O(5)	2.208(2)	N(2)–Co(1)–O(5)	86.49(11)
Co(2)–O(4)	1.929(3)	O(4)–Co(2)–O(3)	123.51(11)
Co(2)–O(3)	1.947(3)	O(4)–Co(2)–N(4)	116.22(12)
Co(2)–N(4)	2.140(3)	O(3)–Co(2)–N(4)	120.25(12)
Co(2)–N(3)	2.151(3)	O(4)–Co(2)–N(3)	91.91(10)
Co(2)–O(6)	2.159(3)	O(3)–Co(2)–N(3)	93.32(11)
O(1)–C(1)	1.331(4)	N(4)–Co(2)–N(3)	82.82(11)
O(2)–C(34)	1.332(4)	O(4)–Co(2)–O(6)	84.60(12)
O(3)–C(35)	1.339(4)	O(3)–Co(2)–O(6)	96.10(12)
O(4)–C(68)	1.333(4)	N(4)–Co(2)–O(6)	90.66(12)
O(5)–C(69)	1.207(4)	N(3)–Co(2)–O(6)	170.36(12)
O(6)–C(72)	1.191(5)	C(1)–O(1)–Co(1)	127.6(2)
O(7)–C(75)	1.195(10)	C(34)–O(2)–Co(1)	126.6(2)
O(8)–C(78)	1.217(6)	C(35)–O(3)–Co(2)	122.8(2)
N(1)–C(20)	1.479(4)	C(68)–O(4)–Co(2)	127.6(2)
N(1)–C(16)	1.482(4)	C(69)–O(5)–Co(1)	141.5(3)
N(1)–C(15)	1.491(4)	C(72)–O(6)–Co(2)	143.9(4)
N(2)–C(18)	1.472(5)	C(20)–N(1)–C(16)	112.9(3)
N(2)–C(19)	1.487(5)	C(20)–N(1)–C(15)	110.1(3)
N(2)–C(17)	1.492(4)	C(16)–N(1)–C(15)	109.5(3)
N(3)–C(50)	1.475(4)	C(20)–N(1)–Co(1)	108.82(19)
N(3)–C(49)	1.480(4)	C(16)–N(1)–Co(1)	106.40(19)
N(3)–C(54)	1.490(4)	C(15)–N(1)–Co(1)	109.0(2)

References begin on page 93

N(4)–C(52)	1.473(5)	C(18)–N(2)–Co(1)	114.6(2)
N(4)–C(53)	1.484(5)	C(19)–N(2)–Co(1)	106.3(2)
N(4)–C(51)	1.487(5)	C(17)–N(2)–Co(1)	108.1(2)
O(1)–Co(1)–O(2)	120.64(11)	C(50)–N(3)–Co(2)	107.7(2)
O(1)–Co(1)–N(1)	92.33(11)	C(49)–N(3)–Co(2)	109.4(2)
O(2)–Co(1)–N(1)	93.12(10)	C(54)–N(3)–Co(2)	111.96(19)
O(1)–Co(1)–N(2)	125.90(12)	C(52)–N(4)–Co(2)	113.4(2)
O(2)–Co(1)–N(2)	113.43(11)	C(53)–N(4)–Co(2)	107.8(2)
		C(51)–N(4)–Co(2)	107.3(2)

Table 2.2 Selected Bond Lengths [Å] and Angles [°] for the methanol adduct of **2.1**(CH_3OH)

Co(1)–O(1)	1.930(2)	O(4)–Co(2)–O(6)	90.97(9)
Co(1)–O(2)	1.972(2)	O(3)–Co(2)–O(6)	90.98(9)
Co(1)–N(1)	2.142(3)	N(4)–Co(2)–O(6)	91.88(9)
Co(1)–N(2)	2.153(3)	O(4)–Co(2)–N(3)	92.73(9)
Co(1)–O(5)	2.154(2)	O(3)–Co(2)–N(3)	90.57(9)
Co(2)–O(4)	1.935(2)	N(4)–Co(2)–N(3)	82.39(9)
Co(2)–O(3)	1.982(2)	O(6)–Co(2)–N(3)	174.06(9)
Co(2)–N(4)	2.142(2)	C(1)–O(1)–Co(1)	128.01(18)
Co(2)–O(6)	2.147(2)	C(34)–O(2)–Co(1)	124.89(19)
Co(2)–N(3)	2.176(2)	C(35)–O(3)–Co(2)	121.12(18)
O(1)–C(1)	1.333(3)	C(68)–O(4)–Co(2)	123.91(18)
O(2)–C(34)	1.351(4)	C(69)–O(5)–Co(1)	121.1(2)
O(1)–Co(1)–O(2)	117.11(9)	C(70)–O(6)–Co(2)	125.1(2)
O(1)–Co(1)–N(1)	92.89(9)	C(16)–N(1)–Co(1)	107.97(19)
O(2)–Co(1)–N(1)	90.77(9)	C(15)–N(1)–Co(1)	109.68(18)

References begin on page 93

O(1)–Co(1)–N(2)	112.44(9)	C(20)–N(1)–Co(1)	108.49(18)
O(2)–Co(1)–N(2)	130.18(9)	C(17)–N(2)–Co(1)	108.12(19)
N(1)–Co(1)–N(2)	81.83(10)	C(19)–N(2)–Co(1)	115.36(19)
O(1)–Co(1)–O(5)	95.18(9)	C(18)–N(2)–Co(1)	106.41(18)
O(2)–Co(1)–O(5)	90.91(9)	C(54)–N(3)–Co(2)	109.21(17)
N(1)–Co(1)–O(5)	169.93(9)	C(50)–N(3)–Co(2)	107.44(17)
N(2)–Co(1)–O(5)	89.50(9)	C(49)–N(3)–Co(2)	110.46(18)
O(4)–Co(2)–O(3)	126.29(9)	C(51)–N(4)–Co(2)	106.19(17)
O(4)–Co(2)–N(4)	113.03(9)	C(52)–N(4)–Co(2)	113.40(19)
O(3)–Co(2)–N(4)	120.53(9)	C(53)–N(4)–Co(2)	109.86(18)

Table 2.3 Selected Bond Lengths [Å] and Angles [°] for the propylene oxide adduct of **2.1**(C_3H_6O)

Co(1)–O(2)	1.922(3)	C(34)–O(2)–Co(1)	127.8(2)
Co(1)–O(1)	1.930(3)	C(35)–O(3)–Co(2)	123.2(2)
Co(1)–N(1)	2.123(3)	C(71)–O(4)–Co(2)	126.7(2)
Co(1)–N(2)	2.132(4)	C(74)–O(5)–C(73)	59.1(5)
Co(1)–O(5)	2.220(3)	C(74)–O(5)–Co(1)	123.7(3)
Co(2)–O(4)	1.925(3)	C(73)–O(5)–Co(1)	123.3(4)
Co(2)–O(3)	1.935(3)	C(77)–O(6)–C(78)	59.1(4)
Co(2)–N(4)	2.129(4)	C(77)–O(6)–Co(2)	130.1(3)
Co(2)–N(3)	2.143(3)	C(78)–O(6)–Co(2)	123.0(3)
Co(2)–O(6)	2.219(3)	C(80)–O(7)–C(81)	57.5(10)
O(1)–C(1)	1.314(5)	C(15)–N(1)–C(16)	112.5(3)
O(2)–C(34)	1.332(5)	C(15)–N(1)–C(20)	110.1(3)
O(3)–C(35)	1.341(4)	C(16)–N(1)–C(20)	110.4(3)
O(2)–Co(1)–O(1)	119.55(13)	C(15)–N(1)–Co(1)	108.2(2)
O(2)–Co(1)–N(1)	92.93(12)	C(16)–N(1)–Co(1)	106.3(2)

References begin on page 93

O(1)–Co(1)–N(1)	94.14(12)	C(20)–N(1)–Co(1)	109.2(2)
O(2)–Co(1)–N(2)	126.05(14)	C(19)–N(2)–C(17)	110.3(4)
O(1)–Co(1)–N(2)	114.40(14)	C(19)–N(2)–C(18)	108.2(4)
N(1)–Co(1)–N(2)	83.10(13)	C(17)–N(2)–C(18)	109.8(4)
O(2)–Co(1)–O(5)	93.72(12)	C(19)–N(2)–Co(1)	113.1(3)
O(1)–Co(1)–O(5)	88.38(13)	C(17)–N(2)–Co(1)	108.5(3)
N(1)–Co(1)–O(5)	170.58(13)	C(18)–N(2)–Co(1)	106.9(3)
N(2)–Co(1)–O(5)	87.58(14)	C(50)–N(3)–C(54)	110.2(3)
O(4)–Co(2)–O(3)	120.93(12)	C(50)–N(3)–C(49)	111.0(3)
O(4)–Co(2)–N(4)	115.94(13)	C(54)–N(3)–C(49)	108.1(3)
O(3)–Co(2)–N(4)	123.13(13)	C(50)–N(3)–Co(2)	107.3(2)
O(4)–Co(2)–N(3)	93.18(11)	C(54)–N(3)–Co(2)	111.5(2)
O(3)–Co(2)–N(3)	94.22(11)	C(49)–N(3)–Co(2)	108.8(2)
N(4)–Co(2)–N(3)	82.91(12)	C(52)–N(4)–C(51)	108.8(3)
O(4)–Co(2)–O(6)	90.10(12)	C(52)–N(4)–C(53)	108.3(3)
O(3)–Co(2)–O(6)	92.88(11)	C(51)–N(4)–C(53)	110.8(3)
N(4)–Co(2)–O(6)	86.42(12)	C(52)–N(4)–Co(2)	113.8(3)
N(3)–Co(2)–O(6)	169.23(12)	C(51)–N(4)–Co(2)	107.3(2)
C(1)–O(1)–Co(1)	125.7(2)	C(53)–N(4)–Co(2)	107.8(3)

References begin on page 93

2.2.2 Syntheses and Structures of Trimetallic Complexes

In the presence of excess cobaltous acetate during the synthetic procedure and in the absence of base, trimetallic complexes **2.2** – **2.4** were isolated that contain two $Co[O_2NN']^{RR'}$ fragments bridged with a $Co(OAc)_2(CH_3OH)_4$ unit (Scheme 2.2). The structures of these species are shown in Figures 2.5 and 2.6, respectively. Bond lengths and angles for **2.3** and **2.4** are given in Tables 2.4 and 2.5, respectively. It should be noted that the synthesis of **2.2** and crystal growth were performed by an undergraduate student, Candace Fowler, in the Kozak group. This chapter provides its further characterizations such as MALDI-TOF MS, VT-SQUID and electrochemistry.

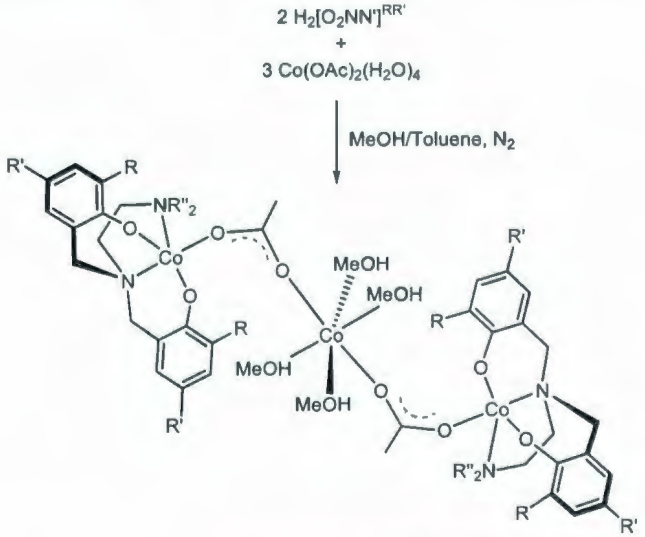

2.2, R = *t*-Bu, R' = Me, R" = Me
2.3, R = R' = *t*-Bu, R" = Me
2.4, R = R' = *t*-Am, R" = Et

Scheme 2.2 Syntheses of trimetallic amine-bis(phenolate) Co^{II} complexes.

The bridging cobalt unit contains a Co^{II} ion in a nearly perfect octahedral environment whereas the terminal cobalt amine-bis(phenolate) units for **2.3** and **2.4** possess distorted trigonal bipyramidal geometries, $\tau = 0.65$ and 0.75, respectively. The compounds are centrosymmetric and contain an inversion centre on Co(2). No differences are observed between the three structures in terms of $Co\text{-}O_{phenolate}$

References begin on page 93

(1.992(2) – 2.004(2) Å) and Co-N_{amine} (2.148(3) – 2.242(2) Å) bond distances. In comparison with the structures of **2.1**(solvent adducts), the Co-$O_{phenolate}$ bond distances are slightly longer than these monometallic species but the Co-N_{amine} distances are found to be similar. **2.3** and **2.4** are the first Co^{II} phenolate derivatives containing unsupported acetate bridges. Previous examples of Co^{II} trimetallic species contain either multiple acetate (or trifluoroacetate) bridges between the metal centres or have phenolate bridges in addition to the acetate bridges.[81-85] The bridging acetate O-Co bond distances in **2.3** and **2.4** (2.040(2) – 2.070(2) Å) are comparable with those in previously reported Co^{II} trimers.[81,83,85] The Co-$O_{methanol}$ interactions for the central cobalt in these complexes are also comparable with known Co-O bond distances for octahedral Co^{II} species.[86]

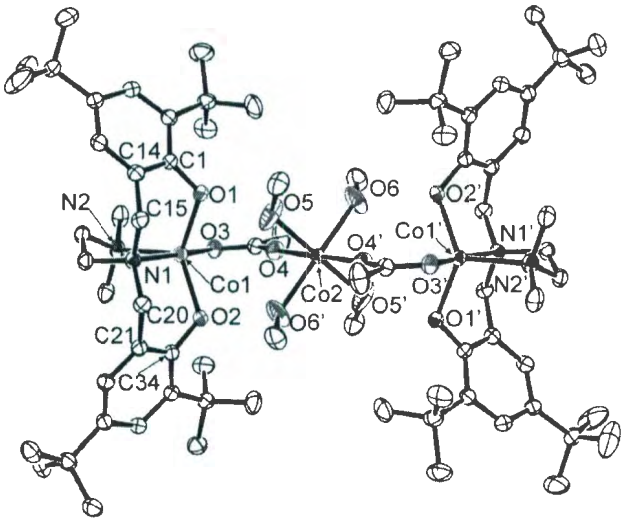

Figure 2.5 ORTEP diagram of the molecular structure of **2.3** with 50% thermal ellipsoid probability.

References begin on page 93

Table 2.4 Selected Bond Lengths [Å] and Angles [°] for **2.3**

Co(1)–O(2)	1.995(2)	O(4)–Co(2)–O(4)	179.996(1)
Co(1)–O(1)	2.004(2)	O(4)–Co(2)–O(5)	86.85(11)
Co(1)–O(3)	2.049(2)	O(6)–Co(2)–O(5)	90.58(18)
Co(1)–N(2)	2.148(3)	O(5)–Co(2)–O(5)	180.00(14)
Co(1)–N(1)	2.241(3)	C(1)–O(1)–Co(1)	121.08(18)
Co(2)–O(6)	2.061(3)	C(34)–O(2)–Co(1)	123.48(18)
Co(2)–O(4)	2.070(2)	C(35)–O(3)–Co(1)	112.42(19)
Co(2)–O(5)	2.076(3)	C(35)–O(4)–Co(2)	171.5(2)
O(1)–C(1)	1.347(3)	C(37)–O(5)–Co(2)	128.9(3)
O(2)–C(34)	1.346(3)	C(38)–O(6)–Co(2)	126.7(3)
O(2)–Co(1)–O(1)	133.91(9)	C(16)–N(1)–C(20)	109.8(2)
O(2)–Co(1)–O(3)	94.39(9)	C(16)–N(1)–C(15)	111.1(2)
O(1)–Co(1)–O(3)	94.51(9)	C(20)–N(1)–C(15)	107.1(2)
O(2)–Co(1)–N(2)	114.17(10)	C(16)–N(1)–Co(1)	108.18(18)
O(1)–Co(1)–N(2)	110.60(10)	C(20)–N(1)–Co(1)	110.67(18)
O(3)–Co(1)–N(2)	91.96(9)	C(15)–N(1)–Co(1)	109.94(17)
O(2)–Co(1)–N(1)	88.23(9)	C(18)–N(2)–C(19)	108.2(3)
O(1)–Co(1)–N(1)	88.53(9)	C(18)–N(2)–C(17)	109.1(2)
O(3)–Co(1)–N(1)	172.71(9)	C(19)–N(2)–C(17)	110.4(2)
N(2)–Co(1)–N(1)	80.77(9)	C(18)–N(2)–Co(1)	111.0(2)
O(6)–Co(2)–O(6)	180.0	C(19)–N(2)–Co(1)	109.70(19)
O(6)–Co(2)–O(4)	95.30(11)	C(17)–N(2)–Co(1)	108.39(18)

Symmetry transformation: $-x, y + ½, -z + ½$

References begin on page 93

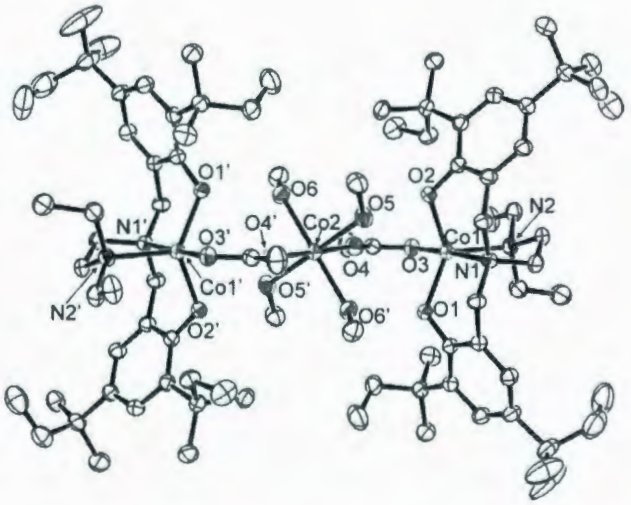

Figure 2.6 ORTEP diagram of the molecular structure of **2.4** with 50% thermal ellipsoid probability.

Table 2.5 Selected Bond Lengths [Å] and Angles [°] for **2.4**

Co(1)–O(1)	1.992(2)	O(5)–Co(2)–O(6)	90.36(9)
Co(1)–O(2)	1.999(2)	O(6)–Co(2)–O(6)	180.0
Co(1)–O(3)	2.040(2)	C(1)–O(1)–Co(1)	121.22(17)
Co(1)–N(2)	2.207(2)	C(40)–O(2)–Co(1)	123.63(17)
Co(1)–N(1)	2.242(2)	C(41)–O(3)–Co(1)	115.28(19)
Co(2)–O(4)	2.061(2)	C(41)–O(4)–Co(2)	170.3(2)
Co(2)–O(5)	2.079(2)	C(43)–O(5)–Co(2)	122.3(2)
Co(2)–O(6)	2.096(2)	C(44)–O(6)–Co(2)	125.80(19)
O(1)–Co(1)–O(2)	132.53(8)	C(18)–N(1)–C(24)	110.1(2)
O(1)–Co(1)–O(3)	93.80(8)	C(18)–N(1)–C(17)	111.2(2)
O(2)–Co(1)–O(3)	90.91(8)	C(24)–N(1)–C(17)	106.5(2)

References begin on page 93

O(1)–Co(1)–N(2)	109.27(9)	C(18)–N(1)–Co(1)	108.19(17)
O(2)–Co(1)–N(2)	116.77(9)	C(24)–N(1)–Co(1)	110.87(17)
O(3)–Co(1)–N(2)	97.91(9)	C(17)–N(1)–Co(1)	109.93(17)
O(1)–Co(1)–N(1)	88.71(8)	C(19)–N(2)–C(22)	111.6(2)
O(2)–Co(1)–N(1)	87.55(8)	C(19)–N(2)–C(20)	105.8(2)
O(3)–Co(1)–N(1)	177.48(9)	C(22)–N(2)–C(20)	112.0(2)
N(2)–Co(1)–N(1)	81.03(9)	C(19)–N(2)–Co(1)	106.29(17)
O(4)–Co(2)–O(4)	179.999(1)	C(22)–N(2)–Co(1)	105.56(17)
O(4)–Co(2)–O(5)	84.00(9)	C(20)–N(2)–Co(1)	115.47(18)
O(4)–Co(2)–O(6)	93.95(9)		

Symmetry transformation: $-x, y + ½, -z + ½$

2.2.3 UV-visible Spectroscopy

The colour of the compounds provides some qualitative information. Each of the novel compounds reported in this chapter contain five-coordinate Co^{II} ions (**2.1**(CH_3OH), **2.1**(CH_3COCH_3), **2.1**(C_3H_6O), **2.3** and **2.4**) and they are all dark pink/purple. Electronic absorption spectra of these complexes show multiple intense bands in the UV and visible regions. The absorption maxima observed in the UV region (below 300 nm) are caused by $\pi \rightarrow \pi^*$ transitions involving the phenolate units – absorptions in this region are also observed in the spectra of the unmetallated ligand precursors.[33] Intense bands are also observed in the region between 300 and 450 nm, which are assigned to charge transfer transitions from the p_π orbital (HOMO) of the phenolate oxygen to the *d* orbitals of Co^{II}. The broad charge transfer bands obscure the high-energy visible region where ligand field transitions would be expected, particularly in donor solvents such as methanol. For monomeric solvento complexes such as dark pink/purple **2.1**(CH_3COCH_3) in dichloromethane, the UV-vis spectrum (Figure 2.7) shows weaker bands ($\varepsilon < 200$ L mol^{-1} cm^{-1}) between 550 and 700 nm, which can be assigned to *d-d* transitions.[47,48,66] The trigonal bipyramidal coordination at Co in the solvento

References begin on page 93

complexes of **2.1** lowers the symmetry compared to a pure octahedral system, thereby easing the Laporte selection rule.

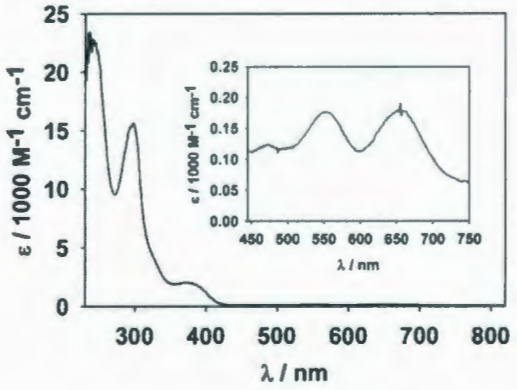

Figure 2.7 UV-vis spectrum of **2.1**(CH_3COCH_3) in CH_2Cl_2.

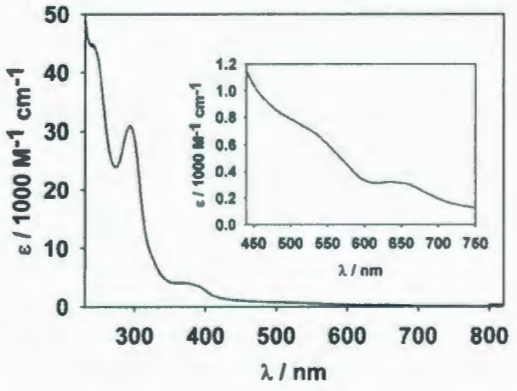

Figure 2.8 UV-vis spectrum of **2.3** in CH_2Cl_2.

It is difficult to unequivocally assign the observed bands to specific electronic transitions since high spin Co^{II} in a trigonal bipyramidal ligand field shows six spin-allowed electronic transitions starting from the $^4A_2'(F)$ ground state. However, assuming trigonal bipyramidal geometry around the cobalt ions in **2.1**(CH_3OH) and **2.1**(CH_3COCH_3), the bands in the visible region at *ca.* 15300 and 18000 cm^{-1} are assigned to $^4A_2'(F) \rightarrow {}^4E'(F)$ and $^4A_2'(F) \rightarrow {}^4E''(P)$ transitions, respectively.[48,87] The trimetallic complexes such as **2.3** (Figure 2.8) show poorly resolved *d-d* bands above 500 nm. It should be noted that the electronic absorption

References begin on page 93

spectra of **2.1**(CH_3OH) and **2.1**(CH_3COCH_3) in dicholoromethane are essentially identical. As these monometallic complexes possess high-spin Co^{II} ions, which are kinetically labile, it is therefore likely that the monodentate methanol and acetone ligands dissociate in solution, thereby resulting in similar electronic absorptions.

2.2.4 Magnetic Properties

The magnetic moments for complexes **2.1 – 2.3**, obtained either in solution (by Evans' NMR method) or as microcrystalline powder (by SQUID magnetometer), are given in Table 2.6. Average magnetic moments in the solid state were adjusted for diamagnetic contributions using Pascal's constants and where variable temperature data are presented, the data were fitted in the temperature ranges specified.

Table 2.6 Effective magnetic moments per Co center for complexes **2.1 – 2.3**

Complex	μ_{eff} at 300 K /μ_B	Complex	μ_{eff} at 300 K /μ_B
2.1(CH_3OH)	4.2[a], 4.5[b]	**2.2**	4.7[b]
2.1(CH_3COCH_3)	4.4[a]	**2.3**	4.7[b]
2.1(C_3H_6O)	4.2[a]		

[a] Measured in solution by Evans' method. [b] Measured in solid state.

The magnetic moments of the monometallic complexes were studied in solution by Evans' method and values are consistent with high spin Co^{II} ions (S = 3/2) in low symmetry environments: **2.1**(CH_3OH), 4.2 μ_B; **2.1**(CH_3COCH_3), 4.4 μ_B; **2.1**(C_3H_6O), 4.2 μ_B. These values are in the expected range for a high-spin Co^{II} d^7 ion exhibiting significant spin-orbit coupling. The temperature dependance of the effective magnetic moment, μ_{eff}, for a polycrystalline powder sample of complex **2.1**(CH_3OH) was examined (Appendix 2.2). This five-coordinate cobalt complex exhibits a magnetic moment of 4.5 μ_B at 300 K, consistent with a Co^{II} ion in a high-spin ground state.[88] This value is larger than the spin-only magnetic moment value of 3.9 μ_B for S = 3/2, indicating significant orbital contributions

References begin on page 93

from low energy excited states typical for high spin Co^{II}.[89] The data can be fit over the whole temperature range studied (2 – 300 K) to the Curie-Weiss law. The plot of χ_M^{-1} versus T reveals a line exhibiting a trend defined by $\chi_M^{-1} = 0.4003T + 1.8298$ ($R^2 = 0.9999$). This gives the Curie constant, C, of 2.50 cm^3 K mol^{-1} (resulting in a g-value of 2.3) and $\theta = -4.57$ K.

A polycrystalline sample of trimetallic **2.2** exhibits a magnetic moment of 8.0 μ_B per molecule (4.7 μ_B per Co), which is within the expected range for high spin ($S = 3/2$) Co^{II} ions exhibiting strong spin-orbit coupling.[89,90] Cooling the sample causes a steadily more rapid decrease in moment reaching 6.5 μ_B per molecule at 4 K (Figure 2.9).

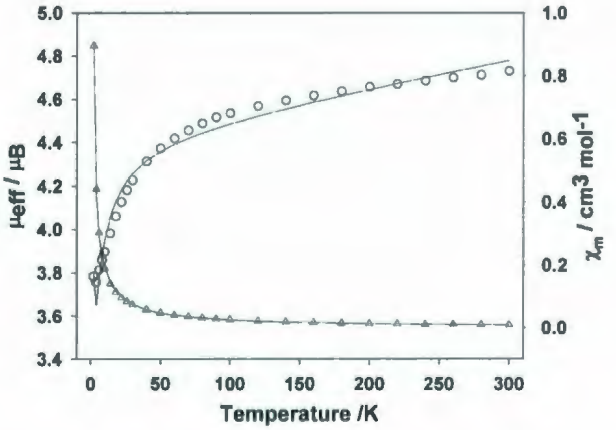

Figure 2.9 Magnetic moment (○) and susceptibility (Δ) versus temperature per Co atom for **2.2**. The solid lines represent the fit given in the text.

The shape of this curve is typical of polynuclear Co^{II} species, and is expected to include contributions from zero-field splitting of the Co^{II} and weak antiferromagnetic exchange within the chain. The data obey the Curie–Weiss law throughout the temperature range studied, with $g = 2.45$ and $\theta = -6.81$ K (Appendix 2.3). The magnetic data for **2.2** were modelled by the isotropic trimer model where $S = 3/2$.[91] The best fit obtained generated $g = 2.28$, an exceedingly weak antiferromagnetic exchange with $J = -0.07$ cm^{-1} and Weiss constant $\theta = -$

References begin on page 93

4.65. The presence of TIP was included to improve the fit, where TIP = 21.0×10^{-4} cm^3 mol^{-1}. For simplicity, ZFS was excluded from the model.

The related trimetallic complex, **2.3**, exhibits similar magnetic behaviour to **2.2**. Plots of χ_M and μ_{eff} versus T per Co atom are shown in Figure 2.10. A 300 K magnetic moment of 4.7 μ_B is similar to that observed for **2.2**. The moment decreases more rapidly as temperature is lowered and achieves a local minimum of 3.7 μ_B at 30 K before rising and falling to a low temperature limit of 2.4 μ_B at 2 K, consistent with significant zero-field splitting. Again, the absence of a maximum χ in the plot is indicative of very weak or no antiferromagnetic exchange between Co^{II} ions. It obeys the Curie-Weiss law giving g = 2.44 and θ = − 18.29 K (Appendix 2.4). Modelling these data was performed as for compound **2.2** resulting in the following parameters: g = 2.01, J = − 0.03 cm^{-1}, θ = − 5.25 K and TIP = 32.0×10^{-4} cm^3 mol^{-1}. The variation in g-values obtained using the two models is observed in the deviation of each model from the experimental data for both **2.2** and **2.3**.

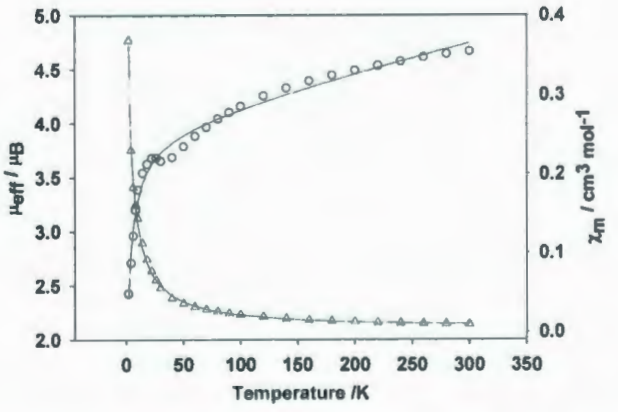

Figure 2.10 Magnetic moment (○) and susceptibility (Δ) versus temperature per Co atom for **2.3**. The solid lines represent the fit given in the text.

The Curie-Weiss model provided a superior fit to the μ_{eff} data at higher temperatures, whereas the isotropic linear trimer reproduces these data better at lower

References begin on page 93

temperatures. Interpretation of magnetic susceptibility data from polynuclear, high-spin Co^{II} species is complicated by the coexistence of weak superexchange ($|J| < 20$ cm^{-1}),[89] strong zero-field splitting (ZFS, $|D| > 20$ cm^{-1}), very large *g*-factor anisotropy[92] and that the parameters *J* and *D* are often of a similar magnitude.[93] The absence of a maximum in the susceptibility combined with strong spin-orbit coupling effects means a more elaborate treatment of the data is needed.[94]

2.2.5 Electrochemical Studies

Electrochemistry experiments were carried out using a three-compartment electrochemical cell, consisting of a platinum counter electrode, saturated calomel reference electrode (SCE) and a glassy carbon working electrode. Complexes **2.1**, **2.1**(CH_3OH), **2.2**, and **2.3**, along with the metal-free ligand precursor, $H_2[O_2NN']^{BuBuNMe2}$, were investigated by cyclic voltammetry (CV) in CH_2Cl_2 solutions containing 0.1 M $[(n\text{-}Bu)_4N]PF_6$ as electrolyte. Results are summarized in Table 2.7 and representative cyclic voltammograms of **2.1**(CH_3OH) and **2.3** are shown in Figures 2.11 and 2.12. Voltammograms of **2.1**, **2.2** and $H_2[O_2NN']^{BuBuNMe2}$ are given in Appendices (Appendix 2.5, 2.6, and 2.7, respectively). All experiments were performed at a scan rate of 100 mV s^{-1}. No redox events were observed at negative potential for any of the compounds investigated, therefore only events occuring at positive potentials are discussed.

Monometallic complexes **2.1** and **2.1**(CH_3OH) exhibit quasi-reversible oxidative responses (E_1^{Ox}) at + 0.62 and + 0.60 V, respectively. These signals may be attributed to ligand oxidation (phenolate/phenoxyl radical), however, metal-centered oxidation assigned to a Co^{II}/Co^{III} redox process has also been suggested for related cobalt(II) amino-phenolate complexes showing oxidation waves at similar potentials.[95] As mentioned in the UV-vis section, the high-spin Co^{II} ion is kinetically labile. it is therefore possible that the methanol molecule can dissociate when **2.1**(CH_3OH) is dissolved in CH_2Cl_2. The first electrochemical oxidation potentials (E_1^{Ox}) for **2.1** and **2.1**(CH_3OH) are very similar, thereby implying both

References begin on page 93

complexes may exhibit identical structures in solution.

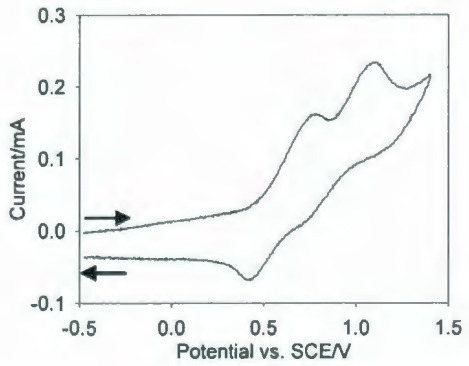

Figure 2.11 Cyclic voltammogram of **2.1**(CH_3OH) in CH_2Cl_2 (0.1M [(n-Bu)$_4$N]PF_6) at 20 °C and a scan rate of 100 mV s^{-1}.

Additional quasi-reversible oxidation waves (E_2^{Ox}) are observed at + 1.02 and + 0.91 V for **2.1** and **2.1**(CH_3OH), respectively, which are proposed to be ligand-centred redox processes. To further investigate whether the observed redox behaviour at the E_1^{Ox} potentials is indeed ligand centered, cyclic voltammetry was conducted on the unmetallated protioligand, $H_2[O_2NN']^{BuBuNMe2}$. The ligand exhibits a quasi-reversible oxidation wave at + 0.68 V. It also displays an irreversible reaction which gives an anodic wave at + 1.50 V. Therefore, in light of the similar E_1^{Ox} potentials for both the complexes and the unmetallated ligand, it is most likely that these oxidation processes are indeed ligand-based.

The trimetallic complexes also exhibit two oxidation waves. **2.2** shows quasi-reversible responses at + 0.85 and + 1.43 V, whereas **2.3** shows quasi-reversible events at + 0.71 and at + 1.34 V. These redox events occur at significantly different potentials to those observed for the monometallic complexes and the unmetallated ligand.

References begin on page 93

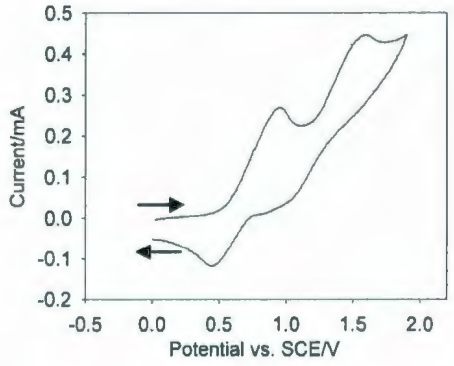

Figure 2.12 Cyclic voltammogram of **2.3** in CH_2Cl_2 (0.1M $[(n\text{-}Bu)_4N]PF_6$) at 20 °C and a scan rate of 100 mV s^{-1}.

It is possible that metal-centered (Co^{II}/Co^{III}) redox may be occuring at one of the Co^{II} ions in the trimetallic molecules, particularly since the central Co^{II} ion is coordinated to six ligands in monodentate fashion and ligand loss is therefore more facile than for the terminal, five-coordinate Co^{II} ions bearing the tetradentate ligands. As a result, geometric distortions caused by oxidation/spin-state changes at the metal centre may be more easily accommodated. Trimetallic complexes possessing linear Co^{II}-Co^{II}-Co^{II} and Co^{III}-Co^{II}-Co^{III} arrangements have been reported,[45] however, for those examples where cyclic voltammetry studies were performed, both metal- and ligand-based redox processes were proposed.

Table 2.7 Half wave potentials for oxidation of Co^{II} complexes and $H_2[O_2NN']^{BuBuNMe2}$

Compound	E_2^{ox}/V	E_1^{ox}/V
2.1	1.02[a]	0.62[a]
2.1(CH_3OH)	0.91[a,c]	0.60[a]
2.2	1.43[a,c]	0.85[a]
2.3	1.34[a]	0.71[a]
$H_2[O_2NN']^{BuBu}$	1.50[b]	0.68[a]

[a] Quasi-reversible reaction. [b] Irreversible reaction, anodic peak is given.

[c] Reduction waves possess a slight shoulder.

References begin on page 93

2.3 Conclusion

In summary, the syntheses and structures of new diamine-bis(phenolate) cobalt complexes, and their electronic, magnetic and electrochemical behaviour have been studied. Monometallic Co^{II} complexes are obtained in the presence of donor solvents, and they are in trigonal bipyramidal geometries. All of the monometallic species possess high-spin Co^{II} centers. It was also found that when the ratio of Co to ligand was greater than 1:1, trimetallic compounds were obtained. In these species, the two terminal cobalt ions are decorated by the diamine-bis(phenolate) ligands. These metals are bridged to the central metal centre by acetate ligands. The octahedral coordination sphere of the central ion is completed by four methanol ligands. The Co^{II} centers in these compounds are all high-spin and show only weak antiferromagnetic exchange when modelled as a linear isotropic trimer.

References begin on page 93

2.4 Experimental Section

2.4.1 General Considerations

Reactions were performed under an atmosphere of dry oxygen-free nitrogen by means of standard Schlenk techniques. However, some reactions (synthesis of **2.3** and **2.4**) were worked up in air. All solvents were purified using an MBraun Solvent Purification System, except methanol, which was distilled under nitrogen from CaH_2. Reagents were purchased either from Aldrich or Alfa Aesar and used without further purification. $H_2[O_2NN']^{BuMeNMe2}$, $H_2[O_2NN']^{BuBuNMe2}$ and $H_2[O_2NN']^{AmAmNEt2}$ were prepared by modification of the literature methods,[7,22,96,97] by using water instead of methanol as the reaction medium.[61,62] MALDI-TOF MS was performed using an Applied Biosystems Voyager DE-PRO equipped with a reflectron, delayed ion extraction and high performance nitrogen laser (337 nm). Anthracene was used as the matrix.[98,99] AP-CI and ESI MS experiments were performed using the detector of an Agilent 1100 series LC/MSD. NMR spectra were recorded on a Bruker AVANCE 500 MHz spectrometer. Variable temperature magnetic measurements were performed on powdered samples at 1000 G using a Quantum Design MPMS-5S SQUID Magnetometer. The data were corrected for background and for the diamagnetism of all atoms. UV-Vis spectra were recorded on an Ocean Optics USB4000+ fiber optic spectrophotometer. Infrared spectra were recorded as KBr pellets on a Bruker Tensor 27 FT-IR spectrometer. Cyclic voltammetry measurements were performed on a Model HA 301 Hokuto Deuko Potentiostat/Galvanostat. Elemental analyses were performed at Canadian Microanalytical Service, Ltd. Delta, BC, Canada or Guelph Chemical Laboratories, Guelph, ON, Canada.

2.4.2 Synthesis of Monometallic Complexes

Synthesis of 2.1. $H_2[O_2NN']^{BuBuNMe2}$ (2.00 g, 3.81 mmol), cobaltous acetate tetrahydrate (0.95 g, 3.81 mmol) and KOH (0.53 g, 9.45 mmol) were added under N_2 to a Schlenk flask fitted with a condenser. A dry, degassed mixture of

References begin on page 93

toluene (25 mL) and methanol (25 mL) was added to the solids. The resulting suspension was stirred and heated to reflux under N_2 for 18 h to afford a dark purple solution. The solvent was removed *in vacuo* and the residue was extracted with toluene (30 mL). The mixture was filtered using a frit and the solvent was removed under vacuum. Washing the residue with pentane (20 mL) afforded **2.1** as an orange powder (yield: 1.79 g, 3.01 mmol, ~79%). Crystals suitable for X-ray diffraction were obtained from a number of solvents by slow cooling.

Cooling of a methanol solution of **2.1** at –20 °C afforded pink crystals (yield: ~26%). The asymmetric unit in the solid state contained two Co^{II} species, $Co[O_2NN']^{BuBuNMe2}(H_2O)$ and $Co[O_2NN']^{BuBuNMe2}(CH_3OH)$, and three methanol solvent molecules of recrystallization. Cooling of a methanol solution of **2.1**, prepared using dry methanol, at –20 °C also afforded pink crystals. In the asymmetric unit, there were two five-coordinate $cobalt^{II}$-methanol adducts, [**2.1**(CH_3OH)], along with three methanol solvent molecules of recrystallization. Storage of a concentrated acetone solution of **2.1** at –20 °C afforded dark pink crystals (yield: ~45%). In the asymmetric unit, there were two five coordinate $cobalt^{II}$-acetone adducts along with two acetone solvent molecules of recrystallization, [**2.1**(CH_3COCH_3)]. Pink crystals of a propylene oxide adduct, [**2.1**(C_3H_6O)], were obtained by slow cooling of a concentrated propylene oxide solution of **2.1** at –35 °C (yield: ~51%). In the asymmetric unit, there were two five-coordinate cobalt(II)-propylene oxide adducts and one propylene oxide solvent molecule.

Characterization of 2.1. Anal. Calcd for $C_{34}H_{54}CoN_2O_2$; C, 70.20; H, 9.36; N, 4.82. Found: C, 69.95; H, 9.34; N, 4.77. MALDI-TOF MS (positive mode, anthracene) m/z = 581 ($[Co[O_2NN']^{BuBuNMe2}]^+$).

Characterization of 2.1(CH$_3$OH). Anal. Calcd for $C_{34}H_{54}CoN_2O_2(2CH_3OH)$; C, 66.95; H, 9.68; N, 4.34. Found: C, 67.11; H, 9.79; N, 4.49. IR (KBr, cm^{-1}): 668(w), 740(m), 779(m), 805(w), 830(m), 877(m), 912(w),

References begin on page 93

934(w), 997(w), 1036(w), 1087(w), 1108(m), 1132(w), 1165(m), 1202(w), 1237(s), 1271(s), 1302(s), 1361(m), 1412(m), 1437(s), 1465(s), 1602(w), 1770(w), 2859(w), 2900(w), 2950(m), 3368(br). UV-vis (CH_2Cl_2) λ_{max}, nm (ε): 241 (20020), 295 (15000), 373 (2000), 470 (145), 553 (154), 655 (154); μ_{eff} ($CDCl_3$, 298 K) = 4.2 μ_B. MALDI-TOF MS (positive mode, anthracene); *m/z* = 581 ($[Co[O_2NN']^{BuBuNMe2}]^+$).

Characterization of 2.1(CH_3COCH_3). Anal. Calcd for $C_{37}H_{60}CoN_2O_3$; C, 69.46; H, 9.45; N, 4.38. Found: C, 69.05; H, 9.38; N, 4.53. UV-vis (CH_2Cl_2) λ_{max}, nm (ε): 241 (22700), 297 (15600), 374 (2000), 472 (120), 553 (177), 655 (178); μ_{eff} ($CDCl_3$, 298 K) = 4.4 μ_B. MALDI-TOF MS (positive mode, anthracene); *m/z* = 581 ($[Co[O_2NN']^{BuBuNMe2}]^+$).

Characterization of 2.1(C_3H_6O). Anal. Calcd for $C_{37}H_{60}CoN_2O_3$; C, 69.46; H, 9.45; N, 4.38. Found: C, 69.98; H, 9.52; N, 4.43. IR (KBr, cm^{-1}): 740(m), 781(m), 806(w), 824(s), 878(m), 912(w), 939(w), 1021(w), 1044(w), 1111(w), 1166(w), 1202(w), 1250(m), 1279(s), 1304(s), 1369(m), 1412(m), 1440(s), 1467(vs), 1602(w), 2865(w), 2901(w), 2952(m), 3386(br). μ_{eff} ($CDCl_3$, 298 K) = 4.2 μ_B. AP-CI MS (positive mode, $CHCl_3$); *m/z* = 642 ($[Co[O_2NN']^{BuBuNMe2}(C_3H_6O)+2H]^+$); 605 ($[Co[O_2NN']^{BuBuNMe2}+Na]^+$); 582 ($[Co[O_2NN']^{BuBuNMe2}+H]^+$).

2.4.3 General Procedure for the Synthesis of Trimetallic Complexes, 2.2-2.4

$H_2[O_2NN']$ (4.40 mmol) and cobaltous acetate tetrahydrate (1.30 g, 5.22 mmol) were placed under N_2 in a Schlenk flask fitted with a condenser. A dry, degassed mixture of toluene (50 mL) and methanol (50 mL) was added to the mixture. The resulting suspension was stirred and heated to reflux under N_2 for 24 h to afford a pale pink solution and a pale purple solid. The solid was collected on a frit and dissolved in hot chloroform (25-50 mL) to give a purple solution. Room temperature methanol was added dropwise to the hot, saturated chloroform

References begin on page 93

solution until evidence of precipitation was seen. A few drops of chloroform were added to the purple solution to ensure complete dissolution of the solid. Crystals were obtained by cooling these solutions to –20 °C. Pink to purple crystals were isolated in yields of 1.53 g (70%) for **2.2**, 1.28 g (50%) for **2.3**, and 1.14 g (40%) for **2.4**.

Characterization of 2.2. Anal. Calcd for $C_{62}H_{100}Co_4N_3O_{12}$; C, 59.28; H, 8.02; N, 3.34. Found: C, 59.48; H, 8.05; N, 3.40. UV-vis (CH_2Cl_2) λ_{max}, nm (ε): 250 (43000), 300 (30000), 380 (3800), 535sh (700), 640 (300); μ_{eff} (solid, 300 K) = 4.73 μ_B (per Co). MALDI-TOF MS (positive mode, anthracene) *m/z* = 674 ($[Co[O_2NN']^{BuMeNMe2}Co(OAc)_2]^+$), *m/z* = 497 ($[Co[O_2NN']^{BuMeNMe2+}$).

Characterization of 2.3. Anal. Calcd for $C_{76}H_{130}Co_3N_4O_{12}$; C, 62.15; H, 8.92; N, 3.81. Found: C, 62.13; H, 8.35; N, 3.96. IR (KBr, cm^{-1}): 536(w), 586(w), 668(w), 740(w), 781(w), 806(w), 832(m), 878(m), 941(w), 1028(w), 1088(w), 1111(w), 1131(w), 1167(w), 1203(w), 1236(m), 1252(m), 1304(s), 1360(m), 1413(s), 1442(s), 1469(vs), 1576(vs), 2868(m), 2902(m), 2954(s), 3416(br). UV-vis (CH_2Cl_2) λ_{max}, nm (ε): 245 (44000), 295 (30800), 380 (4000), 528sh (700), 635 (320); μ_{eff} (solid, 300 K) = 4.67 μ_B (per Co). MALDI-TOF MS (positive mode, anthracene) *m/z* = 758 ($[Co[O_2NN']^{BuBuNMe2}Co(OAc)_2]^+$), *m/z* = 581 ($[Co[O_2NN']^{BuBuNMe2}]^+$).

Characterization of 2.4. Anal. Calcd for $C_{88}H_{154}Co_3N_4O_{12}$; C, 64.57; H, 9.48; N, 3.42. Found: C, 64.75; H, 9.70; N, 3.73. UV-vis (CH_2Cl_2) λ_{max}, nm (ε): 245 (44000), 295 (30000), 380 (4000), 528sh (700), 635 (320). MALDI-TOF MS (positive mode, anthracene) *m/z* = 783 ($[Co[O_2NN']^{AmAmNEt2}Co(OAc)]^+$), *m/z* = 665 ($[Co[O_2NN']^{AmAmNEt2}]^+$).

References begin on page 93

2.4.4 Crystal Structure Determination

Single crystals of suitable dimensions were used for data collection. Methods of crystal growth are outlined in the synthetic procedures above. Crystallographic and structure refinement data are given in Table 2.8.

All crystals were mounted on a diffraction loop. Measurements were made on a Rigaku Saturn CCD area detector with Mo-Kα radiation. Data were collected and processed using CrystalClear (Rigaku).[100] For **2.1**(CH_3COCH_3), **2.1**(CH_3OH) (excluding alcoholic protons, H(109, 113, 117, 121, 125, 129, 133), that were introduced in difference map positions), and **2.1**(C_3H_6O) hydrogen atoms were introduced in calculated positions with isotropic thermal parameters set twenty percent greater than those of their bonding partners. For **2.3**, H(61) and H(65) were introduced in their difference map positions and allowed to refine positionally, with fixed isotropic thermal parameters (1.2 times greater than their bonding partners at the time they were introduced) and all other hydrogen atoms were introduced in calculated positions with isotropic thermal parameters set twenty percent greater than those of their bonding partners. For **2.4**, alcoholic protons [H(73, 77)] were introduced in difference map positions while all other hydrogens were introduced in calculated positions with isotropic thermal parameters set twenty percent greater than those of their bonding partners. In all cases, hydrogen atoms were refined on the riding model. For **2.1**(CH_3COCH_3), **2.1**(CH_3OH), **2.1**(C_3H_6O), **2.5**, and **2.6** all non-hydrogen atoms were refined anisotropically. For **2.1**(CH_3COCH_3), **2.1**(C_3H_6O), **2.3**, and **2.4** the structures were solved by direct methods,[101] and for **2.1**(CH_3OH) by a Patterson orientation/translation search.[102] All of these structures were expanded using Fourier techniques.[103]

For **2.1**(CH_3COCH_3), **2.1**(CH_3OH) and **2.1**(C_3H_6O), two cobalt complexes are present in the asymmetric unit. For **2.1**(CH_3COCH_3), 1.5 acetone molecules are present as lattice solvent in the asymmetric unit with [C(75-77) and O(7)] at a half-occupancy and [C(78-80) and O(8)] at full-occupancy. For **2.1**(CH_3OH), the Z

References begin on page 93

value was set to four in order to give the formula per monomer, $[(C_{34}H_{54}O_2N_2)Co(CH_3OH)]$ $(CH_3OH)_{2.5}$, and 2.5 methanol molecules as lattice solvent. For **2.1**(C_3H_6O), the Z value was also set to four to give 0.25 propylene oxide (C_3H_6O) molecules as lattice solvent. Furthermore, for **2.1**(C_3H_6O), there are two disordered moieties in the model. The first is a disordered *t*-butyl group consisting of [C(59-61)] and [C(62-64)], refined with PART commands, each part at 50% occupancy. The corresponding protons could not be located in difference map positions and were omitted from the model. The second area of disorder consists of [C(72), H(100-102)] at 75% occupancy, and [C(75), H(103-105)] at 25% occupancy in a propylene oxide molecule, also refined with PART commands. The other three protons on this propylene oxide could not be located in difference map positions, and were omitted from the model. However, these protons are included in the formula unit for the structure. A fourth solvento adduct of **2.1** was also crystallographically characterized and contains both a methanol and water adduct in the crystallographic unit cell. Crystallographic data and bond lengths and angles for compound **2.1**$(CH_3OH\text{-}H_2O)$ are available in Appendices (Appendix 2.1, Tables A and B). For **2.3**, one full occupancy toluene molecule is also present as lattice solvent in the asymmetric unit. For **2.4**, the asymmetric unit contains half the Co^{II}_3 complex and so the Z value was set to two in order to give the formula per complex.

For all compounds, neutral atom scattering factors were taken from Cromer and Waber.[104] Anomalous dispersion effects were included in Fcalc;[105] the values for $\Delta f'$ and $\Delta f''$ were those of Creagh and McAuley.[106] The values for the mass attenuation coefficients are those of Creagh and Hubbell.[107] All calculations were performed using the CrystalStructure,[108,109] crystallographic software package except for refinement, which was performed using SHELXL-97.[101]

References begin on page 93

Table 2.8 Crystallographic and structure refinement data for compounds **2.1**, **2.3** and **2.4**

Compound	**2.1(CH_3COCH_3)**	**2.1(CH_3OH)**	**2.1(C_3H_6O)**	**2.3**	**2.4**
Chemical formula	$C_{39.25}H_{64.50}CoN_2O_{3.75}$	$C_{37.50}H_{68}Co\ N_2O_{5.50}$	$C_{37.75}H_{61.50}Co\ N_2O_{3.25}$	$C_{90}H_{146}Co_3\ N_4O_{12}$	$C_{88}H_{154}Co_3\ N_4O_{12}$
Formula weight	683.39	693.89	654.35	1652.96	1637.00
T/K	123(2)	123(2)	153(2)	123(2)	128(2)
Color, habit	Dark pink, irregular	Pink, irregular	Pink, irregular	Pink, prism	Light purple, prism
Crystal Dimensions/mm	0.20 × 0.19 × 0.18	0.24 × 0.14 × 0.09	0.26 × 0.23 × 0.21	0.18 × 0.17 × 0.17	0. 12 × 0.11 × 0.06
Crystal system	Orthorhombic	Triclinic	Orthorhombic	Monoclinic	Monoclinic
Space group	$Pna2_1$ (#33)	*P*-1 (#2)	$Pna2_1$ (#33)	$P2_1/c$ (#14)	$P2_1/c$ (#14)
a/Å	23.579(3)	14.902(2)	23.496(3)	11.027(3)	12.862(2)
b/Å	23.671(3)	15.3466(15)	23.319(3)	22.278(5)	22.109(3)
c/Å	14.476(2)	19.850(3)	14.4917(17)	20.267(5)	18.557(3)
α/°	90	74.869(10)	90	90	90
β/°	90	89.538(13)	90	113.692(6)	119.714(3)
γ/°	90	67.524(9)	90	90	90
V/Å^3	8079.7(20)	4028.0(10)	7940.3(16)	4559.3(20)	4583.0(12)
Z	8	4	8	2	2
D_c/g cm^{-3}	1.124	1.144	1.095	1.204	1.186
μ(MoKα)/cm^{-1}	4.62	4.67	4.66	5.98	5.94
F(000)	2968	1512	2840	1782	1774

References begin on page 93

θ Range for collection/°	2.72 to 26.50	2.71 to 26.50	2.72 to 26.50	2.72 to 27.50	2.69 to 26.50
Reflections collected	67575	35216	68663	42832	40123
Independent reflections	16357	16429	16419	10466	9487
Parameters/ restraints	848/1	831/0	848/1	500/0	485/0
R(int)	0.0623	0.0401	0.0492	0.0442	0.0472
R, *wR*2 (all)	0.0636, 0.1680	0.0810, 0.1776	0.0696, 0.1824	0.0795, 0.1996	0.0705, 0.1670
R, *wR*2 $[I > 2\sigma(I)]^a$	0.0601, 0.1632	0.0697, 0.1674	0.0667, 0.1792	0.0753, 0.1953	0.0651, 0.1623
GOF on F^2	1.068	1.094	1.101	1.076	1.116

^{a} $R = \Sigma\,(|F_o| - |F_c|)/\Sigma|F_o|$, $wR2 = [\Sigma(w(F_o^2 - F_c^2)^2)/\Sigma w(F_o^2)^2]^{1/2}$

References begin on page 93

2.5 References

1. A. Cohen, A. Yeori, J. Kopilov, I. Goldberg and M. Kol, *Chem. Commun.*, 2008, 2149.

2. S. Gendler, S. Groysman, Z. Goldschmidt, M. Shuster and M. Kol, *J. Polym. Sci. Part A: Polym. Chem.*, 2006, **44**, 1136.

3. S. Gendler, S. Segal, I. Goldberg, Z. Goldschmidt and M. Kol, *Inorg. Chem.*, 2006, **45**, 4783.

4. S. Groysman, E. Y. Tshuva, D. Reshef, S. Gendler, I. Goldberg, M. Kol, Z. Goldschmidt, M. Shuster and G. Lidor, *Isr. J. Chem.*, 2002, **42**, 373.

5. S. Groysman, I. Goldberg, M. Kol, E. Genizi and Z. Goldschmidt, *Organometallics*, 2003, **22**, 3013.

6. E. Y. Tshuva, S. Groysman, I. Goldberg, M. Kol and Z. Goldschmidt, *Organometallics*, 2002, **21**, 662.

7. E. Y. Tshuva, I. Goldberg, M. Kol and Z. Goldschmidt, *Organometallics*, 2001, **20**, 3017.

8. E. Y. Tshuva, M. Versano, I. Goldberg, M. Kol, H. Weitman and Z. Goldschmidt, *Inorg. Chem. Commun.*, 1999, **2**, 371.

9. A. Yeori, I. Goldberg and M. Kol, *Macromolecules*, 2007, **40**, 8521.

10. A. J. Chmura, M. G. Davidson, M. D. Jones, M. D. Lunn, M. F. Mahon, A. F. Johnson, P. Khunkamchoo, S. L. Roberts and S. S. F. Wong, *Macromolecules*, 2006, **39**, 7250.

11. S. Groysman, E. Sergeeva, I. Goldberg and M. Kol, *Inorg. Chem.*, 2005, **44**, 8188.

References begin on page 93

12. D. T. Dugah, B. W. Skelton and E. E. Delbridge, *Dalton Trans.*, 2009, 1436.

13. Z. Zhang, X. Xu, W. Li, Y. Yao, Y. Zhang, Q. Shen and Y. Luo, *Inorg. Chem.*, 2009, **48**, 5715.

14. H. E. Dyer, S. Huijser, A. D. Schwarz, C. Wang, R. Duchateau and P. Mountford, *Dalton Trans.*, 2008, 32.

15. C. E. Willans, M. A. Sinenkov, G. K. Fukin, K. Sheridan, J. M. Lynam, A. A. Trifonov and F. M. Kerton, *Dalton Trans.*, 2008, 3592.

16. E. E. Delbridge, D. T. Dugah, C. R. Nelson, B. W. Skelton and A. H. White, *Dalton Trans.*, 2007, 143.

17. H. Zhou, H. Guo, Y. Yao, L. Zhou, H. Sun, H. Sheng, Y. Zhang and Q. Shen, *Inorg. Chem.*, 2007, **46**, 958.

18. A. Amgoune, C. M. Thomas, T. Roisnel and J. F. Carpentier, *Chem. Eur. J.*, 2005, **12**, 169.

19. F. Bonnet, A. R. Cowley and P. Mountford, *Inorg. Chem.*, 2005, **44**, 9046.

20. C. L. Boyd, T. Toupance, B. R. Tyrrell, B. D. Ward, C. R. Wilson, A. R. Cowley and P. Mountford, *Organometallics*, 2005, **24**, 309.

21. C. Cai, A. Abderramane, C. W. Lehmann and J. Carpentier, *Chem. Commun.*, 2004, 330.

22. F. M. Kerton, A. C. Whitwood and C. E. Willans, *Dalton Trans.*, 2004, 2237.

23. S. Ito, S. Nishino, H. Itoh, S. Ohba and Y. Nishida, *Polyhedron*, 1998, **17**, 1637.

24. I. A. Koval, M. Huisman, A. F. Stassen, P. Gamez, M. Lutz, A. L. Spek and J. Reedijk, *Eur. J. Inorg. Chem.*, 2004, 591.

References begin on page 93

25. T. Nagataki and S. Itoh, *Chem. Lett.*, 2007, **36**, 748.

26. M. M. Olmstead, T. E. Patten and C. Troeltzsch, *Inorg. Chim. Acta,* 2004, **357**, 619.

27. A. Philibert, F. Thomas, C. Philouze, S. Hamman, E. Saint-Aman and J. L. Pierre, *Chem. Eur. J.*, 2003, **9**, 3803.

28. N. Reddig, D. Pursche, M. Kloskowski, C. Slinn, S. M. Baldeau and A. Rompel, *Eur. J. Inorg. Chem.*, 2004, 879.

29. N. Reddig, D. Pursche, B. Krebs and A. Rompel, *Inorg. Chim. Acta,* 2004, **357**, 2703.

30. N. Reddig, D. Pursche and A. Rompel, *Dalton Trans.*, 2004, 1474.

31. M. S. Shongwe, C. H. Kaschula, M. S. Adsetts, E. W. Ainscough, A. M. Brodie and M. J. Morris, *Inorg. Chem.*, 2005, **44**, 3070.

32. T. Weyhermuller, T. K. Paine, E. Bothe, E. Bill and P. Chaudhuri, *Inorg. Chim. Acta,* 2002, **337**, 344.

33. R. K. Dean, S. L. Granville, L. N. Dawe, A. Decken, K. M. Hattenhauer and C. M. Kozak, *Dalton Trans.*, 2010, **39**, 548.

34. P. Mialane, E. Anxolabehere-Mallart, G. Blondin, A. Nivorojkine, J. Guilhem, L. Tchertanova, M. Cesario, N. Ravi, E. Bominaar, J. J. Girerd and E. Munck, *Inorg. Chim. Acta,* 1997, **263**, 367.

35. R. Viswanathan, M. Palaniandavar, T. Balasubramanian and T. P. Muthiah, *Inorg. Chem.*, 1998, **37**, 2943.

36. M. Velusamy, M. Palaniandavar, R. S. Gopalan and G. U. Kulkarni, *Inorg. Chem.*, 2003, **42**, 8283.

References begin on page 93

37. M. Velusamy, R. Mayilmurugan and M. Palaniandavar, *Inorg. Chem.*, 2004, **43**, 6284.

38. M. Merkel, F. K. Muller and B. Krebs, *Inorg. Chim. Acta,* 2002, **337**, 308.

39. M. Lanznaster, H. P. Hratchian, M. J. Heeg, L. M. Hryhorczuk, B. R. McGarvey, H. B. Schlegel and C. N. Verani, *Inorg. Chem.*, 2006, **45**, 955.

40. K. Hasan, C. Fowler, P. Kwong, A. K. Crane, J. L. Collins and C. M. Kozak, *Dalton Trans.*, 2008, 2991.

41. J. Hwang, K. Govindaswamy and S. A. Koch, *Chem. Commun.*, 1998, 1667.

42. E. Safaei, T. Weyhermueller, E. Bothe, K. Wieghardt and P. Chaudhuri, *Eur. J. Inorg. Chem.*, 2007, 2334.

43. S. Sarkar, A. Mondal, J. Ribas, M. G. B. Drew, K. Pramanik and K. K. Rajak, *Eur. J. Inorg. Chem.*, 2004, 4633.

44. R. R. Chowdhury, A. K. Crane, C. Fowler, P. Kwong and C. M. Kozak, *Chem. Commun.*, 2008, 94.

45. S. Banerjee, J.-T. Chen, C.-Z. Lu, *Polyhedron,* 2007, **26**, 686.

46. E. Labisbal, L. Rodriguez, O. Souto, A. Sousa-Pedrares, J. A. Garcia-Vazquez, J. Romero, A. Sousa, M. Yanez, F. Orallo and J. A. Real, *Dalton Trans.*, 2009, 8644.

47. A. Mukherjee, F. Lloret and R. Mukherjee, *Inorg. Chem.*, 2008, **47**, 4471.

48. D. Schnieders, A. Hammerschmidt, M. Merkel, F. Schweppe and B. Krebs, *Z. Anorg. Allg. Chem.*, 2008, **634**, 2933.

References begin on page 93

49. W. Ren, Z. Liu, Y. Wen, R. Zhang and X. Lu, *J. Am. Chem. Soc.*, 2009, **131**, 11509.

50. D. J. Darensbourg and A. I. Moncada, *Macromolecules,* 2009, **42**, 4063.

51. C. T. Cohen and G. W. Coates, *J. Polym. Sci. Part A: Polym. Chem.*, 2006, **44**, 5182.

52. C. T. Cohen, C. M. Thomas, K. L. Peretti, E. B. Lobkovsky and G. W. Coates, *Dalton Trans.*, 2006, 237.

53. C. T. Cohen, T. Chu and G. W. Coates, *J. Am. Chem. Soc.*, 2005, **127**, 10869.

54. Z. Q. Qin, C. M. Thomas, S. Lee and G. W. Coates, *Angew. Chem. Int. Ed.*, 2003, **42**, 5484.

55. W. Hirahata, R. M. Thomas, E. B. Lobkovsky and G. W. Coates, *J. Am. Chem. Soc.*, 2008, **130**, 17658.

56. H. Ajiro, K. L. Peretti, E. B. Lobkovsky and G. W. Coates, *Dalton Trans.*, 2009, 8828.

57. K. L. Peretti, H. Ajiro, C. T. Cohen, E. B. Lobkovsky and G. W. Coates, *J. Am. Chem. Soc.*, 2005, **127**, 11566.

58. J. Muller, C. Wurtele, O. Walter and S. Schindler, *Angew. Chem. Int. Ed.*, 2007, **46**, 7775.

59. A. Shaabani, E. Farhangi and A. Rahmati, *Appl. Catal. A,* 2008, **338**, 14.

60. A. Shaabani, A. H. Rezayan, M. Heidary and A. Sarvary, *Catal. Commun.*, 2008, **10**, 129.

References begin on page 93

61. F. M. Kerton, S. Holloway, A. Power, R. G. Soper, K. Sheridan, J. M. Lynam, A. C. Whitwood and C. E. Willans, *Can. J. Chem.*, 2008, **86**, 435.

62. K. L. Collins, L. J. Corbett, S. M. Butt, G. Madhurambal and F. M. Kerton, *Green Chem. Lett. Rev.*, 2007, **1**, 31.

63. A. W. Addison, T. N. Rao, J. Reedijk, J. Vanrijn and G. C. Verschoor, *J. Chem. Soc. Dalton Trans.*, 1984, 1349.

64. I. J. Bruno, J. C. Cole, M. Kessler, J. Luo, W. D. S. Motherwell, L. H. Purkis, B. R. Smith, R. Taylor, R. I. Cooper, S. E. Harris and A. G. Orpen, *J. Chem. Inf. Comput. Sci.*, 2004, **44**, 2133.

65. S. L. Holt, R. Delasi and B. Post, *Inorg. Chem.*, 1971, **10**, 1498.

66. L. Rodriguez, E. Labisbal, A. Sousa-Pedrares, J. Garcia-Vazquez, J. Romero, M. L. Duran, J. A. Real and A. Sousa, *Inorg. Chem.*, 2006, **45**, 7903.

67. E. Solari, C. Floriani, D. Cunningham, T. Higgins and P. McArdle, *J. Chem. Soc., Dalton Trans.*, 1991, 3139.

68. A. R. F. Cox, V. C. Gibson, E. L. Marshall, A. J. P. White and D. Yeldon, *Dalton Trans.*, 2006, 5014.

69. M. Mikuriya, N. Nagao and K. Kundo, *Chem. Lett.*, 2000, 516.

70. L. Vaiana, C. Platas-Iglesias, D. Esteban-Gomez, F. Avecilla, J. M. Clemente-Juan, J. A. Real, A. de Blas and T. Rodriguez-Blas, *Dalton Trans.*, 2005, 2031.

71. K. Matsumoto, N. Sekine, K. Arimura, M. Ohba, H. Sakiyama and H. Okawa, *Bull. Chem. Soc. Jpn.*, 2004, **77**, 1343.

72. T. J. Mizoguchi, J. Kuzelka, B. Spingler, J. L. DuBois, R. M. Davydov, B. Hedman, K. O. Hodgson and S. J. Lippard, *Inorg. Chem.*, 2001, **40**, 4662.

References begin on page 93

73. A. Diebold, A. Elbouadili and K. S. Hagen, *Inorg. Chem.*, 2000, **39**, 3915.

74. K. S. Hagen, R. Lachicotte and A. Kitaygorodskiy, *J. Am. Chem. Soc.*, 1993, **115**, 12617.

75. M. M. Olmstead, P. P. Power and G. A. Sigel, *Inorg. Chem.*, 1988, **27**, 580.

76. D. J. Darensbourg, M. W. Holtcamp, B. Khandelwal, K. K. Klausmeyer and J. H. Reibenspies, *J. Am. Chem. Soc.*, 1995, **117**, 538.

77. H. V. R. Dias and Z. Y. Wang, *Inorg. Chem.*, 2000, **39**, 3724.

78. D. J. Darensbourg, J. R. Wildeson, S. J. Lewis and J. C. Yarbrough, *J. Am. Chem. Soc.*, 2002, **124**, 7075.

79. D. J. Darensbourg, D. R. Billodeaux and L. M. Perez, *Organometallics*, 2004, **23**, 5286.

80. P. Chen, M. H. Chisholm, J. C. Gallucci, X. Y. Zhang and Z. P. Zhou, *Inorg. Chem.*, 2005, **44**, 2588.

81. A. Gerli, K. S. Hagen and L. G. Marzilli, *Inorg. Chem.*, 1991, **30**, 4673.

82. V. Calvo-Perez, S. Ostrovsky, A. Vega, J. Pelikan, E. Spodine and W. Haase, *Inorg. Chem.*, 2006, **45**, 644.

83. D. Shi, Z. You, C. Xu, Q. Zhang and H. Zhu, *Inorg. Chem. Commun.*, 2007, **10**, 404.

84. Z. Tomkowicz, S. Ostrovsky, H. Mueller-Bunz, A. J. H. Eltmimi, M. Rams, D. A. Brown and W. Haase, *Inorg. Chem.*, 2008, **47**, 6956.

85. J. Welby, L. N. Rusere, J. M. Tanski and L. A. Tyler, *Inorg. Chim. Acta*, 2009, **362**, 1405.

References begin on page 93

86. G. Aromí, A. S. Batsanov, P. Christian, M. Helliwell, A. Parkin, S. Parsons, A. A. Smith, G. A. Timco and R. E. P. Winpenny, *Chem. Eur. J.*, 2003, **9**, 5142.

87. M. Ciampolini and I. Bertini, *J. Chem. Soc. (A),* 1968, 2241.

88. A. B. P. Lever, *Inorganic Electronic Spectroscopy*, Elsevier, Amsterdam, 1984.

89. O. Kahn, *Molecular Magnetism*, VCH, New York, 1993.

90. R. L. Carlin, *Magnetochemistry*, Springer-Verlag, Heidelberg, 1986.

91. T. Yi, C. Ho-Chol, S. Gao and S. Kitagawa, *Eur. J. Inorg. Chem.*, 2006, **7**, 1381.

92. R. Boca, *Coord. Chem. Rev.*, 2004, **248**, 757.

93. A. V. Palii, B. S. Tsukerblat, E. Coronado, J. M. Clemente-Juan and J. J. Borras-Almenar, *J. Chem. Phys.*, 2003, **118**, 5566.

94. F. Lloret, M. Julve, J. Cano, R. Ruiz-Garcia and E. Pardo, *Inorg. Chim. Acta,* 2008, **361**, 3432.

95. Y. Shimazaki, R. Kabe, S. Huth, F. Tani, Y. Naruta and O. Yamauchi, *Inorg. Chem.*, 2007, **46**, 6083.

96. E. Y. Tshuva, I. Goldberg, M. Kol, H. Weitman and Z. Goldschmidt, *Chem. Commun.*, 2000, 379.

97. Y. Sarazin, R. H. Howard, D. L. Hughes, S. M. Humphrey and M. Bochmann, *Dalton Trans.*, 2006, 340.

98. M. D. Eelman, J. M. Blacquiere, M. M. Moriarty and D. E. Fogg, *Angew. Chem. Int. Ed.*, 2008, **47**, 303.

99. N. Ikpo, S. M. Butt, K. L. Collins and F. M. Kerton, *Organometallics,* 2009, **28**, 837.

References begin on page 93

100. J. W. Pflugrath, *Acta Crystallogr., Sect. D: Biol. Crystallogr.*, 1999, **55**, 1718.

101. A. Altomare, G. Cascarano, C. Giacovazzo, A. Guagliardi, M. Burla, G. Polidori and M. Camalli, *J. Appl. Crystallogr.*, 1994, **27**, 435.

102. P. T. Beurskens, G. Admiraal, G. Beurskens, W. P. Bosman, S. Garcia-Granda, R. O. Gould, J. M. M. Smits, C. Smykalla, *'The DIRDIF program system'*, Technical Report of the Crystallography Laboratory, University of Nijmegen, Netherlands, 1992.

103. P. T. Beurskens, G. Admiraal, G. Beurskens, W. P. Bosman, R. de Gelder, R. Israel, J. M. M. Smits, *'DIRDIF99'*, University of Nijmegen, Netherlands, 1999.

104. D. T. Cromer, J. T. Waber, *"International Tables for X-ray Crystallography", Vol. IV,* The Kynoch Press: Birmingham, UK, 1974.

105. J. A. Ibers and W. C. Hamilton, *Acta Crystallogr.,* 1964, **17**, 781.

106. D. C. Creagh, W. J. McAuley, *"International Tables for Crystallography", Vol C,* ed. A.J.C. Wilson,, Kluwer Academic Publishers: Boston, 1992, 219.

107. D. C. Creagh, J. H. Hubbell, *"International Tables for Crystallography", Vol C,* ed. A.J.C. Wilson, Kluwer Academic Publishers: Boston, 1992, 200.

108. *CrystalStructure 3.7.0: Crystal Structure Analysis Package*, Rigaku and Rigaku/MSC, The Woodlands, Texas, 2000–2005.

109. D. J. Watkin, C. K. Prout, J. R. Carruthers, P. W. Betteridge, *CRYSTALS Issue 10*, Chemical Crystallography Laboratory: Oxford, UK, 1996.

References begin on page 93

Chapter 3

Synthesis and Characterizations of Monometallic Amine-bis(phenolate) Cobalt(III) Complexes

3.1 Introduction

A key route to the development of efficient cobalt catalysts for copolymerization reactions of CO_2 with epoxides is the preparation of Co^{II} complexes using suitable ligands followed by their oxidation to obtain Co^{III} analogues.[1-5] During the last decade, numerous Co^{III} salen complexes have been made which have shown activity in both homopolymerization of epoxides and copolymerization of CO_2 with epoxides. One route to such Co^{III} salen complexes is *via* aerobic or anaerobic oxidation of their respective Co^{II} precursors using various organic acids.[1-3,6,7] For example, Jacobsen and co-workers developed chiral Co^{III} salen complexes as effective catalysts for hydrolytic kinetic resolution (HKR) of epoxides. These Co^{III} species were prepared *via in situ* oxidation of Co^{II} analogues in the presence of air using organic acids such as benzoic acid or acetic acid.[8,9] Several of these were further modified through salt metathesis to incorporate halide ligands such as Cl^-.[10] A range of Co^{III} salen complexes have recently been reported by Coates and co-workers. These species were prepared through a similar procedure to that reported by Jacobsen and co-workers.[1-3] Most recently Lu and co-workers designed thermally stable Co^{III} complexes for mechanistic investigation of copolymerization reactions of CO_2 with epoxides. Two steps were applied to obtain these species. The first step is the oxidation reaction of the Co^{II} species using lithium chloride and oxygen bubbling through the mixture. The second step is salt metathesis which occurred with a variety of silver salts ($AgNO_3$, AgOAc, $AgBF_4$) to afford Co^{III} analogues.[4] It is therefore observed that the oxidation of Co^{II} salen complexes readily occurs in the presence of air using a variety of acids to afford Co^{III} analogues. Salt metathesis reactions by means of either sodium salts (NaX, X = Cl, Br, I) or silver salts have also been carried out to

References begin on page 112

replace the large anions with halide or small anionic ligands. The unsaturated salen ligand possibly plays an important role in easing the oxidizing ability of the Co^{II} ion.

All of the above described Co^{III} salen complexes were characterized by NMR spectroscopy (^{1}H and ^{13}C NMR), mass spectrometry, and elemental analysis.[1-4,8-10] Only a few were characterized by X-ray crystallography.[2] NMR spectroscopy is a very useful tool for characterization of low-spin diamagnetic species such as Co^{III} salen compounds. ^{1}H NMR spectra of such Co^{III} complexes contain well resolved peaks and can easily be assigned. In contrast, broad and shifted peaks are seen for Co^{II} salen compounds. It is therefore easy to determine the formation of such Co^{III} complexes. Mass spectrometry and elemental analysis are also valuable analytical tools to determine the formation of Co^{III} species and their purity.

Whilst aiming to develop efficient cobalt catalysts for both homopolymerization of epoxides and copolymerization of CO_2 with epoxides, the objective of this chapter is to investigate the oxidative synthesis of Co^{III} amine-bis(phenolate) complexes using various oxidants. This chapter therefore describes one successful oxidative synthesis of a Co^{III} species using $AgNO_3$ as the oxidant and several unsuccessful attempts for the preparation of Co^{III} amine-bis(phenolate) complexes. The preliminary characterizations of the Co^{III} species are also discussed in this chapter.

3.2 Results and Discussion

3.2.1 Syntheses of Monometallic Co^{III} Complexes

Monometallic four-coordinate Co^{II} species, **2.1** and one five-coordinate solvento complex, **2.1(CH_3COCH_3)** were mainly used for oxidation reactions. **2.1(CH_3OH)** was also examined on a few occassions. Silver salts such as silver triflate, silver hexafluorophosphate, silver tetrafluoroborate, and silver nitrate were initially chosen as oxidants. These salts have the ability to both oxidize the metal ion and can stabilize the desired Co^{III} complex by their bulky anions. However, oxidative syntheses of Co^{III} amine-bis(phenolate) complexes using silver triflate, silver

References begin on page 112

hexafluorophosphate and silver tetrafluoroborate were not promising. For instance, oxidation reactions in a dichloromethane solution of one equivalent of Co^{II} species [either **2.1** or **2.1(CH_3COCH_3)**] and approximately one equivalent of silver triflate under stirring at room temperature for 24 h in the presence of air afforded a dark brown solution and silver as a precipitate. Upon removal of the silver *via* filtration and the solvent under vacuum, a dark brown powder was isolated in moderate yield. ^1H NMR spectroscopy was chosen for preliminary characterization of all the oxidation products since it is expected the Co^{III} complexes to be diamagnetic and thereby should give easily assignable spectra. Unfortunately, ^1H NMR spectra of the dark powder obtained in each reaction contained no identifiable peaks. These spectra showed unresolved broad and few sharp resonances instead, which are likely due to the presence of unreacted paramagnetic Co^{II} complexes. Recrystallization of the dark brown powder by slow evaporation of dichloromethane solutions was also not successful. It is notable that while removing the silver precipitate, a small amount of green material was observed on the frit. However, the green solid was not soluble in any solvent and therefore failed to be characterized. An attempt to oxidize the monomeric species, **2.1(CH_3COCH_3)** using silver triflate under N_2 atmosphere also gave similar results to those described above in the presence of air.

The monometallic species, **2.1(CH_3COCH_3)** was then treated with other silver salts e.g., silver hexafluorophosphate and silver tetrafluoroborate. However, these oxidations were also unsuccessful. Reaction of a dichloromethane solution of one equivalent of **2.1(CH_3COCH_3)** with one equivalent of silver hexafluorophosphate under aerobic conditions yielded a grey black solution and silver as a precipitate after stirring at ambient temperature for 24 h. Upon removal of the silver precipitate and the solvent, a grey black powder was obtained in good yield. However, ^1H NMR in $CDCl_3$ did not confirm the formation of the desired Co^{III} species. A very small amount of green solid was also observed in these reactions, as observed with silver triflate, but again failed to be identified as it was not soluble in any solvent.

References begin on page 112

Several oxidation attempts were conducted following the previously reported literature procedures. In these reports, Co^{II} salen complexes were successfully oxidized into Co^{III} analogues by means of organic acids such as acetic acid, *p*-toluene-sulfonic acid monohydrate, trifluromethanesulfonic acid (triflic acid), etc. as oxidants.[1-3,11,12] However, no desired Co^{III} amine-bis(phenolate) complex was obtained using these oxidizing agents. The next attempt followed the method reported by Lu *et al.* for the successful synthesis of Co^{III} salen complexes.[4] The reaction was carried out by overnight stirring of a dry methanol solution of Co^{II} species, **2.1** with lithium chloride and oxygen bubbling through the reaction mixture. After removing the methanol under vacuum, a deep purple solid was obtained. Finally, the deep purple solid was dissolved in dichloromethane and a stoichiometric amount of silver nitrate was added to the reaction mixture. Stirring over 24 h open to air yielded a deep black solution and a grey precipitate of silver. However, the ^{1}H NMR spectrum of the deep black solid did not confirm the formation of a Co^{III} species.

Recently Welby *et al.* reported that a monometallic Co^{II} salen complex could be converted into a bimetallic Co^{III} salen complex after adding a drop of concentrated hydrochloric acid into a refluxed solution of monometallic Co^{II} species in dichloromethane.[13] To investigate this possibilty with monometallic Co^{II} amine-bis(phenolate) complexes, a few reactions were attempted following similar procedures. However, these attempts were also unsuccessful possibly due to reaction between the amine-bis(phenolate) ligand and HCl and thereby breaking apart the monometallic Co^{II} species in solution.

Finally, a successful oxidation of $Co^{II}[O_2NN']^{BuBuNMe2}$, **2.1** occured when silver nitrate was used as the oxidizing agent (Scheme 3.1). A dichloromethane solution of one equivalent of monometallic species **2.1** and approximately one equivalent of silver nitrate was stirred in the presence of air for 24 h to afford a dark brown solution and silver as a grey precipitate. Upon removal of the silver and the solvent, a dark brown powder of **3.1** was obtained in good yield.

References begin on page 112

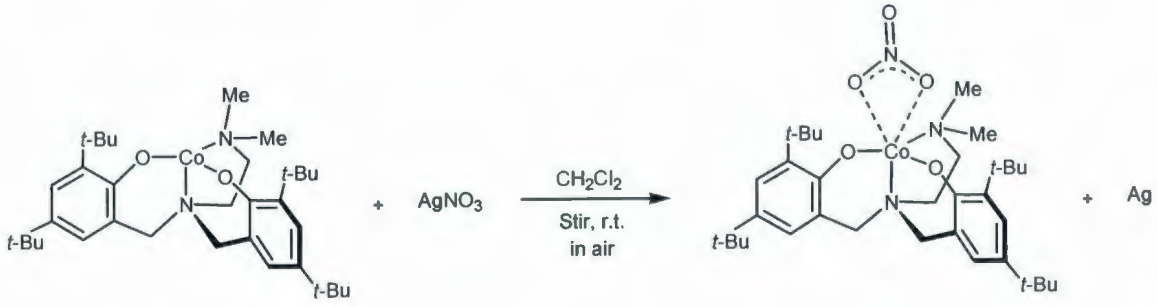

2.1 **3.1**

Scheme 3.1 Synthesis of a monometallic Co^{III} amine-bis(phenolate) complex **3.1**

3.2.2 Characterizations of Monometallic Co^{III} Complex 3.1

Preliminary characterization of this dark brown powder was achieved by ^1H NMR spectroscopy which clearly showed the formation of the Co^{III} species. Furthermore, elemental analysis and mass spectrometry also confirm the formation of **3.1**. The ^1H NMR spectrum of **3.1** is shown in Figure 3.1. All peaks are also assigned as shown in the Co^{III} complex, **3.1**. The ^1H NMR spectrum of the unmetallated ligand precursor, $H_2[O_2NN']^{BuBuNMe2}$ is also given in Appendix 3.1 for comparison to **3.1**.

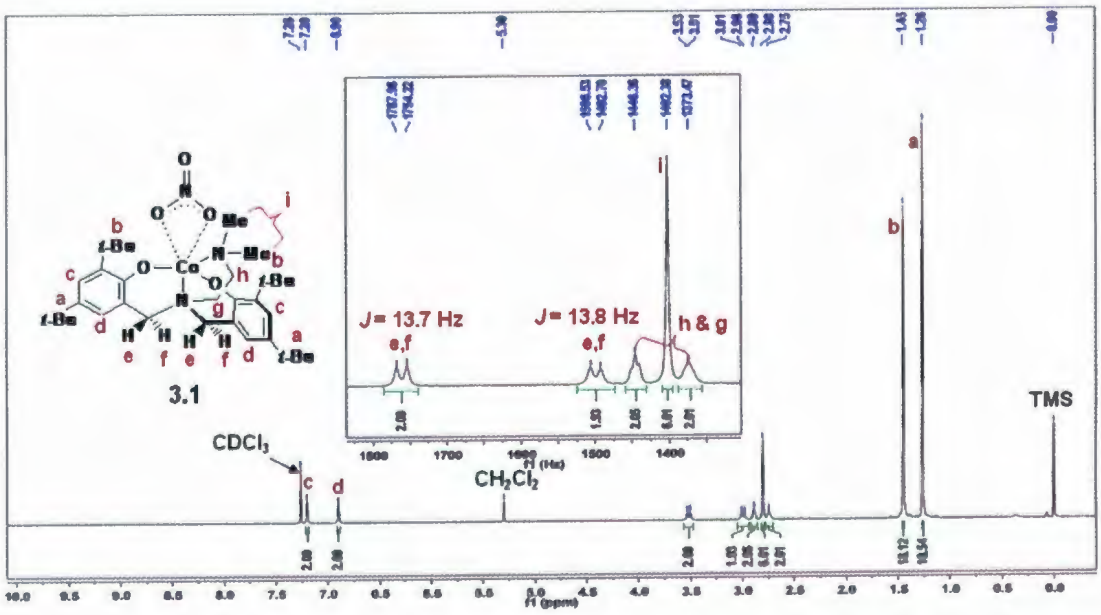

Figure 3.1 ^1H NMR (500 MHz) spectrum of $Co^{III}(NO_3)[O_2NN']^{BuBuNMe2}$, **3.1**.

References begin on page 112

It is observed from the spectrum of **3.1** that all peaks are sharp and assignable, supporting the formulation of **3.1** as $Co^{III}(NO_3)[O_2NN']^{BuBuNMe2}$. Two singlets in the downfield region are due to aromatic protons of two symmetric phenolate rings and no singlet is observed in this region where the amine-bis(phenolate) ligand-precursor gives a sharp singlet due to the phenolic protons (Appendix 3.1). Two doublets at δ 2.99 and 3.52 with equal intensity and identical coupling constants are assigned to the two methylene groups lying between the tertiary amine N-donor and the phenolate rings. These two doublets are not observed in the ^1H NMR spectrum of the ligand precursor and instead appear as singlets (Appendix 3.1). Therefore it is certain that the metal ion is coordinated to the ligand, which restricts the motion of these protons making them diastereotopic. One broad singlet at δ 2.75 and a triplet at δ 2.89 are due to four other methylene protons of the pendant arm of the ligand. Six protons of two chemically equivalent methyl groups give a sharp singlet at δ 2.80. Two singlets with high intensity in the upfield region are due to the *tert*-butyl protons in the ligand periphery. Furthermore, after integration the total number of protons was found to be accurate for the proposed Co^{III} amine-bis(phenolate) complex, **3.1**.

Recrystallization of the deep brown powder, **3.1** from dichloromethane has been attempted. However, either slow evaporation of a concentrated dichloromethane solution of **3.1** or slow diffusion of diethyl ether into the concentrated dichloromethane solution of **3.1** did not give any crystals of the compound. Although no suitable crystals of **3.1** were obtained, mass spectrometry (ESI MS) further suggests the formation of the Co^{III} species. Elemental analysis revealed that **3.1** is contaminated with a small amount (0.08 %) of $AgNO_3$.

References begin on page 112

3.3 Conclusion

One successful oxidative synthesis of a Co^{III} amine-bis(phenolate) complex and several unsuccessful attempts are discussed in this chapter. A wide range of oxidants have previously been used to afford Co^{III} species by other researchers but only $AgNO_3$ gave promising results here. The monometallic Co^{III} species, **3.1** was primarily characterized by ^1H NMR spectroscopy, mass spectrometry, and elemental analysis which suggest the formation of **3.1**. Detailed ^1H NMR assignment is also provided. One can conclude that unlike Co^{II} salen complexes, Co^{II} amine-bis(phenolate) compounds are not easily oxidized into the corresponding Co^{III} species. One reason is due to the ligand. Salen ligands are unsaturated and contain two imine N-donors that are π-acceptors whereas amine-bis(phenolate) ligands are saturated and do not contain any π-accepting donors. Therefore, due to the lack of π-accepting groups, and being saturated the electron-rich metal ion is harder to oxidize. Another reason may be due to the structural differences of the complex. The Co^{II} ion in salen compounds is in a square planar coordination environment but the Co^{II} ions in amine-bis(phenolate) complexes adopt either trigonal monopyramidal or trigonal bipyramidal geometries. Nevertheless, $AgNO_3$ gave promising results and proved the possiblity of oxidation of Co^{II} amine-bis(phenolate) complexes. For a better understanding, all of the oxidation reactions including the one successful synthesis of monometallic Co^{II} complex, various oxidizing agents, and reaction conditions are summarized in Table 3.1.

References begin on page 112

Table 3.1 Oxidation reactions for synthesizing Co^{III} amine-bis(phenolate) complexes using various oxidants

Monometallic Co^{II} complexes	Oxidants	Reaction condition and time	Product
2.1, $Co^{II}[O_2NN']^{BuBuNMe2}$	AgOTf	stir, r. t., in air CH_2Cl_2, 18 h	no
2.1, $Co^{II}[O_2NN']^{BuBuNMe2}$	AgOTf	stir, r. t., under N_2 CH_2Cl_2, 18 h	no
2.1, $Co^{II}[O_2NN']^{BuBuNMe2}$	TfOH	stir, r. t., in air CH_2Cl_2, 2 h	no
2.1, $Co^{II}[O_2NN']^{BuBuNMe2}$	$AgNO_3$	stir, r. t., in air CH_2Cl_2, 24 h	yes, **3.1** $Co^{III}(NO_3)[O_2NN']$
2.1, $Co^{II}[O_2NN']^{BuBuNMe2}$	$CH_3C_6H_4SO_3H.H_2O$	stir, r. t., in air CH_2Cl_2, 2 h	no
2.1, $Co^{II}[O_2NN']^{BuBuNMe2}$	CH_3COOH	stir, r. t., in air CH_2Cl_2, 18 h	no
2.1, $Co^{II}[O_2NN']^{BuBuNMe2}$	(i) LiCl (ii) $AgNO_3$	(i) bubbled through with air, CH_3OH, 24 h (ii) stir, r. t., CH_2Cl_2, 18h	no
2.1, $Co^{II}[O_2NN']^{BuBuNMe2}$	conc. HCl	reflux, toluene, 0.5 h	no
2.1(CH_3COCH_3)	AgOTf	stir, r. t., in air CH_2Cl_2, 18 h	no
2.1(CH_3COCH_3)	$AgPF_6$	stir, r. t., in air CH_2Cl_2, 18 h	no
2.1(CH_3COCH_3)	$AgBF_4$	stir, r. t., in air CH_2Cl_2, 18 h	no
2.1(CH_3OH)	$AgNO_3$	stir, r. t., in air CH_2Cl_2, 18 h	no

References begin on page 112

3.4 Experimental Section

3.4.1 General Considerations

All oxidation reactions were performed and worked up in air unless otherwise indicated. All solvents were purified using an MBraun Solvent Purification System, except methanol, which was distilled under nitrogen from CaH_2. Reagents were purchased either from Aldrich or Alfa Aesar and used without further purification. Since silver salts are light sensitive and hygroscopic, these were quickly added to the reaction vessel and light was avoided. After addition of the silver salts to the reaction mixtures, the round bottom flasks were wrapped with aluminum foil. NMR spectra were recorded on a Bruker AVANCE 500 MHz spectrometer. AP-CI and ESI MS experiments were performed using the detector of an Agilent 1100 series LC/MSD. Elemental analysis was performed at Guelph Chemical Laboratories, Guelph, ON, Canada.

3.4.2 General Procedure for the Synthesis of Monometallic Co^{III} Complexes

Monometallic Co^{II} species, **2.1**, **2.1**(CH_3COCH_3) and **2.1**(CH_3OH) were taken for oxidation reactions to produce respective Co^{III} species using a variety of oxidizing agents e.g., silver triflate, triflic acid, silver nitrate, silver hexafluorophosphate, silver tetrafluroborate, and *p*-toluenesulfonic acid monohydrate as outlined in Table 3.1. In all cases one equivalent of the above mentioned monometallic Co^{II} complex and approximately one equivalent of oxidant were placed in a round-bottom flask. Dichloromethane (20-30 mL) was added to the reaction mixture. In a few cases, however, dichloromethane was intially added to the round-bottom flask and stirred for dissolution of the Co^{II} species. Then the oxidizing agent was added to the reaction mixture. The resulting dark brown solution was stirred open to the air for 18-24 h. One oxidation reaction was also carried out under a dry nitrogen atmosphere using standard Schlenk techniques. Upon stirring under aerobic or anaerobic conditions, a black solution was obtained. However, silver salts gave grey precipitates of silver which confirms that the oxidation has occurred. The resulting mixture was filtered to remove the silver precipitate using a frit. The solvent was then removed *in vacuo* and

References begin on page 112

the resulting solid was dried to afford the desired product. The product was used for characterizations both with and without further purification.

Synthesis of 3.1. Monometallic species $Co^{II}[O_2NN']^{BuBuNMe2}$, **2.1** (0.52 g, 0.88 mmol) was added to a round-bottom flask. Dichloromethane (25 mL) was added and stirred until complete dissolution of the monometallic Co^{II} complex had been achieved. $AgNO_3$ (0.20 g, 0.96 mmol) was then added to the brown solution. The round-bottom flask was wrapped up with aluminum foil. The resulting mixture was stirred in air for 24 h to afford a dark brown solution and grey precipiate of silver. Using a frit the silver was removed by filtration. The solvent was then removed *in vacuo* which afforded a dark brown powder (yield: 0.51 g, 0.79 mmol, ~89%). The product was further dried under vacuum to remove any remaining solvent.

Characterization of 3.1. Anal. Calcd for $C_{34}H_{54}CoN_3O_5$ $(AgNO_3)_{0.08}$; C, 62.12; H, 8.28; N, 6.56. Found: C, 62.02; H, 8.53; N, 6.62. ^1H NMR ($CDCl_3$, 500 MHz): δ 1.26 (s, 18H), 1.45 (s, 18H), 2.75 (br s, 2H), 2.80 (s, 6H), 2.89 (t, 2H), 2.99 (d, ^2J = 13.8 Hz, 2H), 3.52 (d, ^2J = 13.7 Hz, 2H), 6.90 (s, 2H), 7.20 (s, 2H). ESI MS (negative mode, $CHCl_3$); *m/z* = 695 ($[Co[O_2NN']^{BuBuNMe2}(NO_3)+(AgNO_3)_{0.3}]^-$); 644 ($[Co[O_2NN']^{BuBuNMe2}(NO_3)]^-$).

References begin on page 112

3.5 References

1. C. T. Cohen, T. Chu and G. W. Coates, *J. Am. Chem. Soc.*, 2005, **127**, 10869.
2. C. T. Cohen, C. M. Thomas, K. L. Peretti, E. B. Lobkovsky and G. W. Coates, *Dalton Trans.*, 2006, 237.
3. C. T. Cohen and G. W. Coates, *J. Polym. Sci. Part A: Polym. Chem.*, 2006, **44**, 5182.
4. W. Ren, Z. Liu, Y. Wen, R. Zhang and X. Lu, *J. Am. Chem. Soc.*, 2009, **131**, 11509.
5. J. Yoo, S. J. Na, H. C. Park, A. Cyriac and B. Y. Lee, *Dalton Trans.*, 2010, **39**, 2622.
6. K. L. Peretti, H. Ajiro, C. T. Cohen, E. B. Lobkovsky and G. W. Coates, *J. Am.Chem. Soc.*, 2005, **127**, 11566.
7. H. Ajiro, K. L. Peretti, E. B. Lobkovsky and G. W. Coates, *Dalton Trans.*, 2009, 8828.
8. E. N. Jacobsen, F. Kakiuchi, R. G. Konsler, J. F. Larrow and M. Tokunaga, *Tetrahedron Lett.* 1997, **38**, 773.
9. M. Tokunaga, J. F. Larrow, F. Kakiuchi and E. N. Jacobsen, *Science,* 1997, **277**, 936.
10. L. P. C. Nielsen, C. P. Stevenson, D. G. Blackmond and E. N. Jacobsen, *J. Am. Chem. Soc.*, 2004, **126**, 1360.
11. R. N. Loy and E. N. Jacobsen, *J. Am. Chem. Soc.*, 2009, **131**, 2786.
12. X.-B. Lu, L. Shi, Y.-M. Wang, R. Zhang, Y.-J. Zhang and X.-J. Peng, *J. Am. Chem. Soc.*, 2006, **128**, 1664.

References begin on page 112

13. J. Welby, L. N. Rusere, J. M. Tanski and L. A. Tyler, *Inorg. Chim. Acta*, 2009, **362**, 1405.

References begin on page 112

Chapter 4

Conclusion and Future Work

4.1 Conclusion

The coordination chemistry of Co^{II} complexes has been studied widely since the 1890s and the birth of coordination chemistry.[1-3] Chapter 1 of this thesis provides an overview of Co^{II} coordination chemistry. Detailed discussion about various oxidation states, synthesis, and structures of previously reported Co^{II} complexes using a wide range of ligands is also provided in that Chapter. X-ray crystallographic analyses of previously reported Co^{II} complexes revealed the different structural parameters and geometries of the Co^{II} ions. Electronic structures of these Co^{II} species are also highlighted in Chapter 1. Furthermore, magnetism and redox chemistry unveiled interesting magnetic and electrochemical behaviours. In terms of applications, Co^{II} complexes are of paramount scientific interest owing to their numerous uses in many fields such as bioinorganic chemistry, polymer chemistry, and catalysis. Cobalt-mediated radical polymerization (CMRP), homopolymerization of epoxides, and copolymerization of carbon dioxide with epoxides are notable polymerization processes where both Co^{II} and Co^{III} coordination compounds have been used in recent years as effective catalysts.

Chapter 2 describes the syntheses and structures of new mono- and trimetallic Co^{II} amine-bis(phenolate) complexes. Their electronic, magnetic, and electrochemical behaviour have also been investigated. All monometallic species are five-coordinate complexes and the Co^{II} center adopts a distorted trigonal bipyramidal coordination environment. Amongst these species, the propylene oxide complex is the most interesting because it may act as a model for the higher oxidation analogue which could potentially be employed in alternating copolymerization reactions. Co^{III} complexes have widely been used as catalysts in this field. In the trimetallic species, a central Co^{II} ion is in an octahedral environment coordinated to four methanol ligands whereas the two terminal Co^{II} ions are in trigonal bipyramidal geometries and each metal ion is coordinated to an

References begin on page 120

amine-bis(phenolate) ligand. The terminal metal ions are bridged to the central metal ion by acetate ligands. Magnetic studies suggested that all of these species possess high-spin Co^{II} ions and in the trimetallic species very weak antiferromagnetic exchange occurs. Electrochemistry showed that the redox processes are most likely ligand based; however, a metal centered redox process is also possible. The results presented in Chapter 2 show that depending on the ratio of cobaltous acetate salt to amine-bis(phenolate) ligand under varying conditions, the synthesis of both mono- and multimetallic Co^{II} complexes is possible.

In Chapter 3, oxidation reactions of monometallic Co^{II} amine-bis(phenolate) complexes are described. Many oxidative reactions were attempted using a variety of oxidants to obtain Co^{III} amine-bis(phenolate) complexes. Although most of the reactions failed to yield Co^{III} species, silver nitrate gave promising results in oxidizing the monometallic Co^{II} species into the corresponding Co^{III} analogue.

4.2 Future work

Salen coordination compounds of Co^{II} and Co^{III} have been extensively utilized as efficient catalysts for both copolymerization of carbon dioxide with epoxides[4-9] and homopolymerization of epoxides.[10-12] Aiming to develop such catalysts for these processes, a series of monometallic Co^{II} amine-bis(phenolate) complexes were prepared and structurally characterized. The oxidative synthesis of a monometallic Co^{III} amine-bis(phenolate) complex and its preliminary characterizations were performed. Although only one Co^{III} species was obtained to date, the synthesis of many Co^{III} complexes could also be possible using a variety of oxidants under varying conditions. Therefore, the catalytic activity of these Co^{II} and Co^{III} complexes is worth investigating in future.

4.2.1 Scope of Copolymerization of Carbon Dioxide and Epoxides

Alternating copolymerization of carbon dioxide with epoxides to produce biodegradable polycarbonates has been a subject of much interest in the last decades.[4-9, 13-16] This process has some economical and environmental benefits such as (i) carbon

References begin on page 120

dioxide is readily available, inexpensive, non-toxic, non-flammable, and a biorenewable reagent,[5,7-9,15] (ii) polycarbonates have wide-scale uses in electronics, as optical media, and in the medical industry,[5] and eventually it is biodegradable, (iii) the byproduct of this transformation is a five-membered cyclic carbonate which is employed as a high boiling and flash point solvent in degreasing, paint stripping, and cleaning processes,[15] and (iv) commercially this is a more viable and 'green' route to polycarbonates because it restricts the use of hazardous bisphenol A and toxic phosgene gas.

The first metal-catalyzed alternating copolymerization of carbon dioxide and epoxides was achieved by Inoue and co-workers using $ZnEt_2/H_2O$ catalysts in the late 1960s.[17,18] Following this discovery, numerous catalysts systems (both homogeneous and heterogeneous) have been developed for this transformation. According to literature reports,[4-9,13-16] cobalt salen complexes, particularly Co^{III} salen compounds, are the most active catalysts to date. These catalysts exhibited excellent activity and selectivity in carbon dioxide/epoxides coupling even under mild conditions. In these studies, two types of epoxides: propylene and cyclohexene oxides were mostly used as monomers with carbon dioxide; however, recently Darensbourg and co-workers developed a Co^{II} salen complex which with an anion initiator e.g., Br^- acts as a very effective catalytic system for the coupling of oxetane and carbon dioxide.[5]

Coates and co-workers are also prominent in this field and have developed a wide range of homogeneous catalysts based on chiral Co^{III} salen complexes. These catalysts either alone[9] or with other co-catalysts e.g., $[Ph_4P]Cl$ or [PPN]Y ([PPN] = bis(triphenylphosphine)iminium; Y = Cl or $OBzF_5$) can catalyze efficiently the alternating copolymerization of carbon dioxide and epoxides (both propylene and cyclohexene oxides).[6-9] Most recently Lu and co-workers have designed a highly active and thermally stable single-site Co^{III} salen catalyst which can couple carbon dioxide/propylene oxide even at temperatures up to 100 °C and high epoxide/catalyst ratios, and/or low carbon dioxide pressures.[4] A few catalysts of this type are shown in Figure 4.1.

References begin on page 120

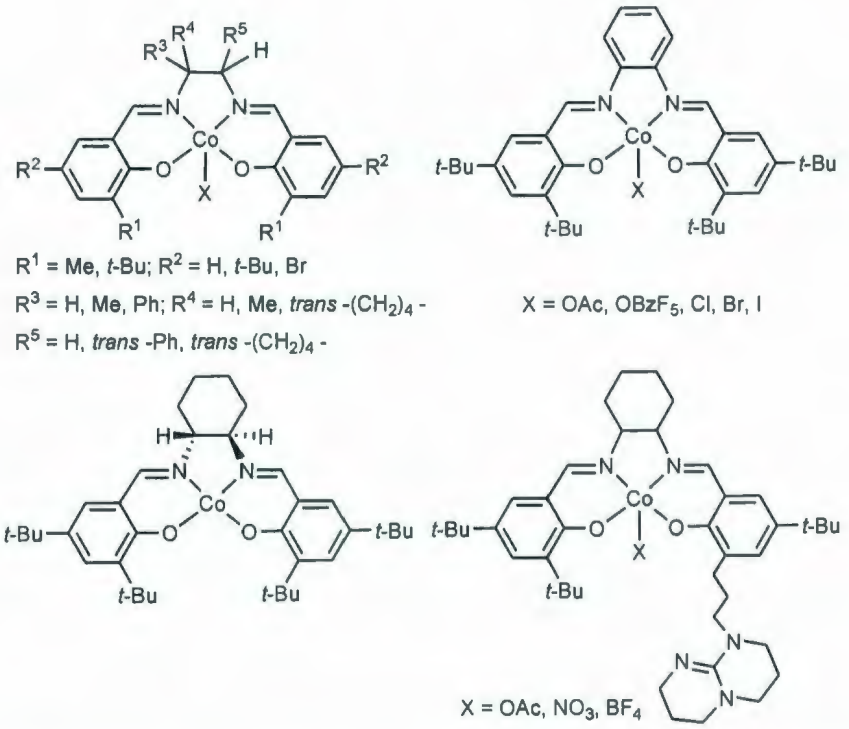

Figure 4.1 Cobalt salen complexes used as catalysts for copolymerization reactions.

Investigation of the mechanism of carbon dioxide/epoxide copolymerization revealed that it generally occurs in two steps: (1) ring opening of epoxide by a metal carbonate, followed by (2) carbon dioxide insertion into a metal alkoxide (Scheme 4.1).[9]

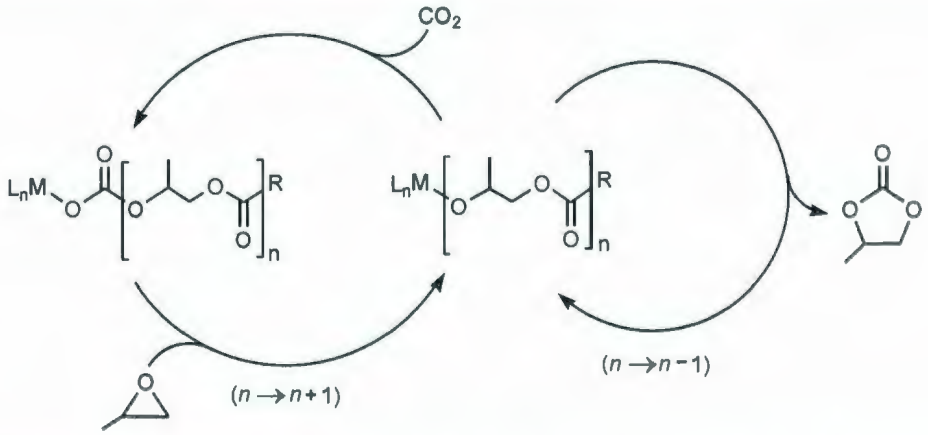

Scheme 4.1 Mechanism of carbon dioxide/epoxide copolymerization using discrete metal alkoxides (R = OR′) and carboxylates (R = alkyl, aryl).[9]

References begin on page 120

A common byproduct, cyclic carbonate, is likely formed when aliphatic epoxides such as propylene oxide or cyclohexene oxide are used. It is formed by a back-biting reaction from the propagating alkoxide.[9] However, some Co^{III} salen catalysts yield regioregular poly(propylene carbonate) without the generation of the byproduct, cyclic carbonate.[6] It is also demonstrated that variation of the salen ligand, reaction conditions, as well as organic based ionic or Lewis base cocatalysts have a profound effect on the rate of the copolymerization reaction and the selectivity for the copolymer over cyclic byproduct. Furthermore, the stereochemistry of the monomer and the cobalt catalysts used in this process are also significant in maintaining the catalytic activity and a controlled microstructure for the copolymer.[6-8]

4.2.2 Scope of Homopolymerization of Epoxides

Homopolymerization of epoxides, particularly propylene oxide polymerization, is another interesting process. Commercially a huge amount of propylene oxide (about 60 % annually) is used to generate polypropylene oxide. However, almost all of these commercially available polypropylene oxides are *atactic* which are readily synthesized by polymerizing propylene oxide in the presence of strongly basic initiators.[10] In 2005, Coates and co-workers developed a benchmark catalyst based on an achiral cobalt salen complex which displayed the highest activity and greatest stereoselectivity to date for generating regioregular, highly *isotactic* polypropylene oxide (Scheme 4.2).[10]

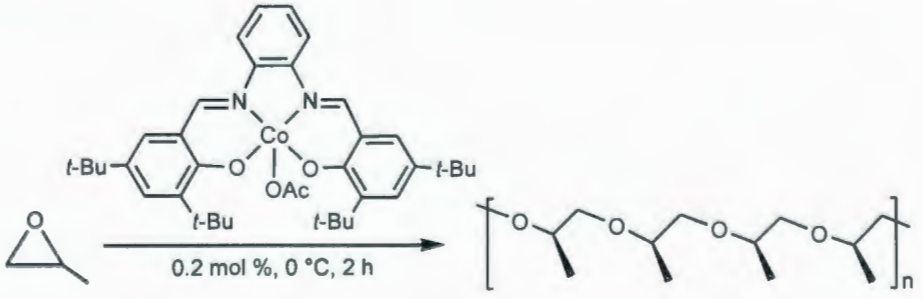

Scheme 4.2 Isospecific polymerization of propylene oxide by a Co^{III} salen catalyst.[10,11]

References begin on page 120

In a course of mechanistic investigations of this homopolymerization reaction, the Coates group recently discovered that the isospecific polymerization of propylene oxides occurs at the surface of undissolved, crystalline Co^{III} salen species.[11]

Recently Coates and co-workers reported a highly selective polymerization catalyst, chiral bimetallic Co^{III} salen complex (Figure 4.3), for the kinetic resolution of epoxides.[12] The group designed this bimetallic species by introducing a chiral binaphthol linker into the salen ligand which helps holding the two metal centers in an optimal distance apart and allows some flexibility by rotation about the C_{Nap}-C_{Nap} bond.[12] This is the first enantioselective catalyst discovered to date which in the presence of [PPN][OAc] ([PPN] = bis(triphenylphosphine)iminium) exhibited high activity and selectivity for polymerizing not only the racemic propylene oxide but also a wide range of terminal epoxides (alkyl, aryl, alkoxy, methyl, fluoroalkyl substituents) to give highly *isotactic* polyethers in quantitative yield.[12]

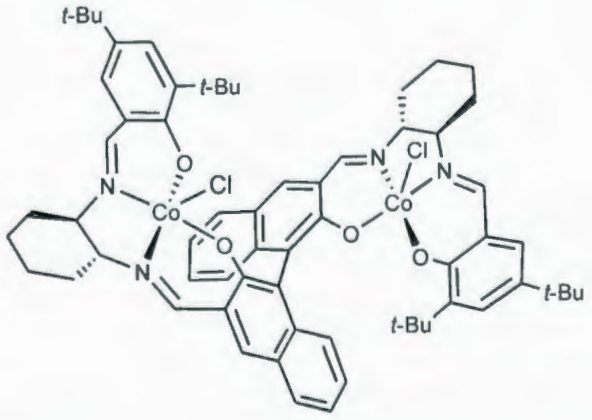

Figure 4.2 Chiral bimetallic Co^{III} salen complex acts as an enantioselective epoxide polymerization catalyst.[12]

Therefore, the important discussions presented above for both the copolymerization and the homopolymerization of epoxides will allow future investigations of the catalytic activities of the new cobalt complexes described in this thesis (Chapter 2 and 3) to be performed.

References begin on page 120

4.3 References

1. F. A. Cotton, G. Wilkinson, C. A. Murillo and M. Bochmann, *Advanced Inorganic Chemistry*, John Wiley & Sons Inc., New York, 1999.

2. P. V. Bernhardt and G. A. Lawrance, *in "Comprehensive Coordination Chemistry II"*, Elsevier Pergamon, Amsterdam, 2004, vol. 6, 1-122.

3. A. G. Blackman, *Cobalt: Inorganic & Coordination Chemistry in "Encyclopedia of Inorganic Chemistry" online resource*, John Wiley & Sons Inc., Hoboken, NJ, 2006, 1-25.

4. W. Ren, Z. Liu, Y. Wen, R. Zhang and X. Lu, *J. Am. Chem. Soc.*, 2009, **131**, 11509.

5. D. J. Darensbourg and A. I. Moncada, *Macromolecules*, 2009, **42**, 4063.

6. C. T. Cohen and G. W. Coates, *J. Polym. Sci., Part A: Polym. Chem.*, 2006, **44**, 5182.

7. C. T. Cohen, C. M. Thomas, K. L. Peretti, E. B. Lobkovsky and G. W. Coates, *Dalton Trans.*, 2006, 237.

8. C. T. Cohen, T. Chu and G. W. Coates, *J. Am. Chem. Soc.*, 2005, **127**, 10869.

9. Z. Qin, C. M. Thomas, S. Lee and G. W. Coates, *Angew. Chem., Int. Ed.*, 2003, **42**, 5484.

10. K. L. Peretti, H. Ajiro, C. T. Cohen, E. B. Lobkovsky and G. W. Coates, *J. Am. Chem. Soc.*, 2005, **127**, 11566.

11. H. Ajiro, K. L. Peretti, E. B. Lobkovsky and G. W. Coates, *Dalton Trans.*, 2009, 8828.

References begin on page 120

12. W. Hirahata, R. M. Thomas, E. B. Lobkovsky and G. W. Coates, *J. Am. Chem. Soc.*, 2008, **130**, 17658.

13. J. Yoo, S. J. Na, H. C. Park, A. Cyriac and B. Y. Lee, *Dalton Trans.*, 2010, **39**, 2622.

14. S. J. Na, S. S, A. Cyriac, B. E. Kim, J. Yoo, Y. K. Kang, S. J. Han, C. Lee and B. Y. Lee, *Inorg. Chem.*, 2009, **48**, 10455.

15. D. J. Darensbourg, *Chem. Rev.*, 2007, **107**, 2388.

16. E. K. Noh, S. J. Na, S. Kim and B. Y. Lee, *J. Am. Chem. Soc.*, 2007, **129**, 8082.

17. S. Inoue, H. Koinuma and T. Tsuruta, *J. Polym. Sci. B*, 1969, **7**, 287.

18. S. Inoue, H. Koinuma and T. Tsuruta, *Macromol. Chem.*, 1969, **130**, 210.

References begin on page 120

Appendices

Crystallographic data, magnetic moment plots, cyclic voltammograms, and ^{1}H NMR spectrum

Appendix 2.1

Table A 2.1 Crystallographic and structure refinement data for compound **2.1**(CH_3OH-H_2O)

Compound	**2.1**(CH_3OH-H_2O)
Chemical formula	$C_{72}H_{126}Co_2N_4O_9$
Formula weight	1309.68
T/K	123(2)
Color, habit	Pink, irregular
Crystal dimensions/mm	0.15 × 0.13 × 0.09
Crystal system	Triclinic
Space group	P-1 (#2)
a/Å	12.764(6)
b/Å	13.592(6)
c/Å	22.443(10)
α/°	96.005(9)
β/°	102.272(6)
γ/°	95.489(11)
V/Å^3	3756(3)
Z	2
D_c/g cm^{-3}	1.158
μ(MoKα)/cm^{-1}	4.95
F(000)	1424
θ Range for collection/°	2.56 to 26.50
Reflections collected	33698
Independent reflections	14811
Parameters/ restraints	785/0
R(int)	0.0500
R, *wR*2 (all)	0.1191, 0.3009
R, *wR*2 [$I > 2\sigma(I)$][a]	0.1031, 0.2781
GOF on F^2	1.082

[a] $R = \Sigma (|F_o| - |F_c|)/\Sigma|F_o|$, $wR2 = [\Sigma(w(F_o^2 - F_c^2)^2)/\Sigma w(F_o^2)^2]^{1/2}$

Table B 2.1 Selected Bond Lengths [Å] and Angles [°] for componud **2.1**(CH_3OH-H_2O)

Co(1)–O(1)	1.968(3)	O(4)–Co(2)–O(6)	89.80(14)
Co(1)–O(2)	1.932(3)	O(3)–Co(2)–O(6)	93.38(14)
Co(1)–N(1)	2.136(4)	N(4)–Co(2)–O(6)	89.80(14)
Co(1)–N(2)	2.131(4)	O(4)–Co(2)–N(3)	91.75(15)
Co(1)–O(5)	2.163(4)	O(3)–Co(2)–N(3)	92.69(14)
Co(2)–O(4)	1.961(3)	N(4)–Co(2)–N(3)	82.39(16)
Co(2)–O(3)	1.928(3)	O(6)–Co(2)–N(3)	171.70(14)
Co(2)–N(4)	2.129(4)	C(1)–O(1)–Co(1)	121.7(3)
Co(2)–O(6)	2.165(4)	C(34)–O(2)–Co(1)	127.0(3)
Co(2)–N(3)	2.147(4)	C(35)–O(3)–Co(2)	127.4(3)
O(1)–C(1)	1.349(5)	C(68)–O(4)–Co(2)	121.8(3)
O(2)–C(34)	1.345(5)	C(69)–O(6)–Co(2)	123.0(3)
O(1)–Co(1)–O(2)	126.43(14)	C(15)–N(1)–Co(1)	109.7(3)
O(1)–Co(1)–N(1)	91.78(14)	C(16)–N(1)–Co(1)	106.2(3)
O(2)–Co(1)–N(1)	93.02(14)	C(20)–N(1)–Co(1)	109.0(3)
O(1)–Co(1)–N(2)	119.62(15)	C(18)–N(2)–Co(1)	112.0(3)
O(2)–Co(1)–N(2)	113.94(16)	C(19)–N(2)–Co(1)	108.7(3)
N(1)–Co(1)–N(2)	83.47(15)	C(17)–N(2)–Co(1)	107.2(3)
O(1)–Co(1)–O(5)	90.91(13)	C(54)–N(3)–Co(2)	109.2 (3)
O(2)–Co(1)–O(5)	82.44(14)	C(50)–N(3)–Co(2)	108.1(3)
N(1)–Co(1)–O(5)	175.47(15)	C(49)–N(3)–Co(2)	109.8(3)
N(2)–Co(1)–O(5)	98.35(15)	C(51)–N(4)–Co(2)	108.2(3)
O(4)–Co(2)–O(3)	122.26(14)	C(52)–N(4)–Co(2)	106.9(3)
O(4)–Co(2)–N(4)	123.15(15)	C(53)–N(4)–Co(2)	115.4(3)
O(3)–Co(2)–N(4)	114.50(15)		

Appendix 2.2

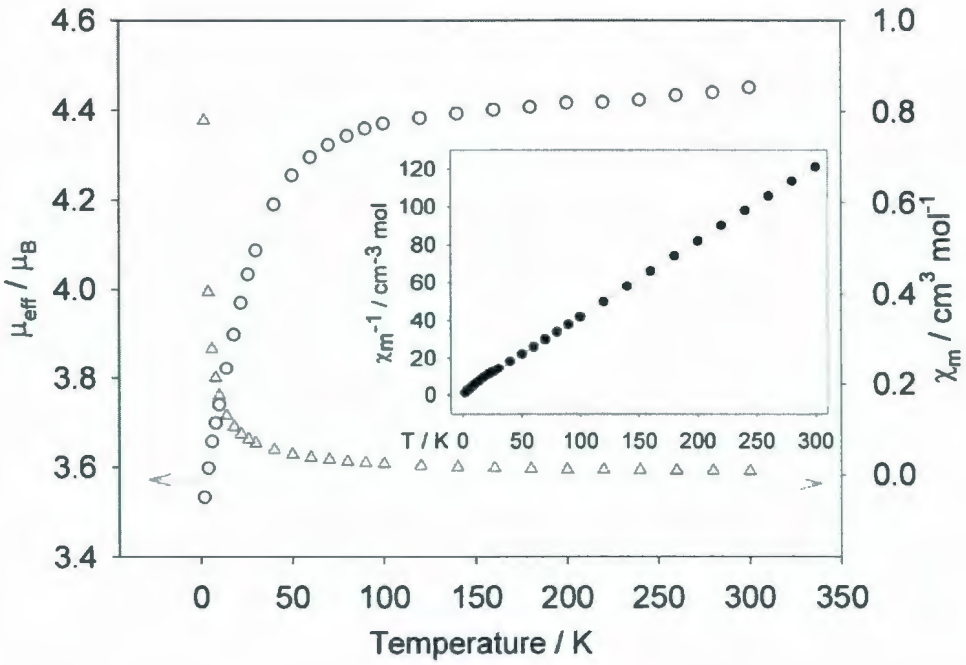

Figure A 2.2 Magnetic moment (○), susceptibility (Δ) and inverse susceptibility (inset) versus temperature data for **2.1**(CH_3OH). The solid line represents the best fit for the Curie-Weiss model, $\chi M = C/(T - \theta)$, where $\chi M\text{-}1 = 0.4003T + 1.8298$ ($R^2 = 0.9999$) giving a Curie constant, C, of 2.50 emu/mol (resulting in a g-value of 2.3) and $\theta = -4.57$ K.

Appendix 2.3

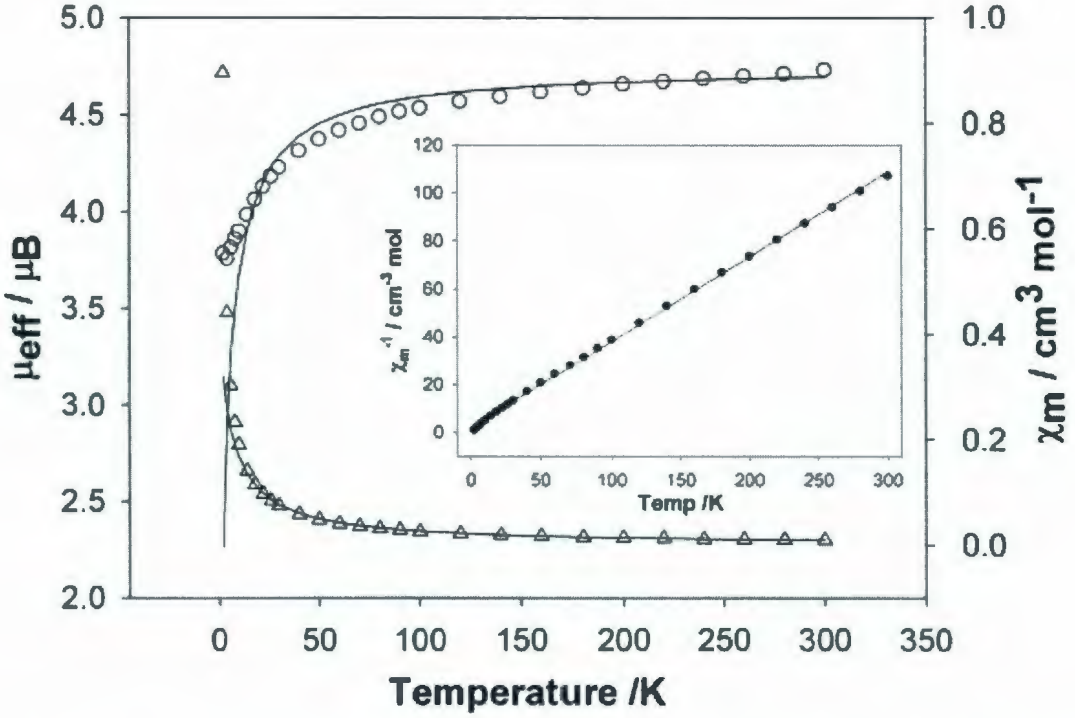

Figure B 2.3 Magnetic moment (○), susceptibility (Δ) and inverse susceptibility (inset) versus temperature data per Co atom for **2.2**. The solid line represents the best fit for the Curie-Weiss model, $\chi M = C/(T - \theta)$, where $\chi M\text{-}1 = 0.355T + 2.4174$ ($R^2 = 0.9993$) giving a Curie constant, C, of 2.82 emu/mol (resulting in a g-value of 2.45) and $\theta = -6.81$ K.

Appendix 2.4

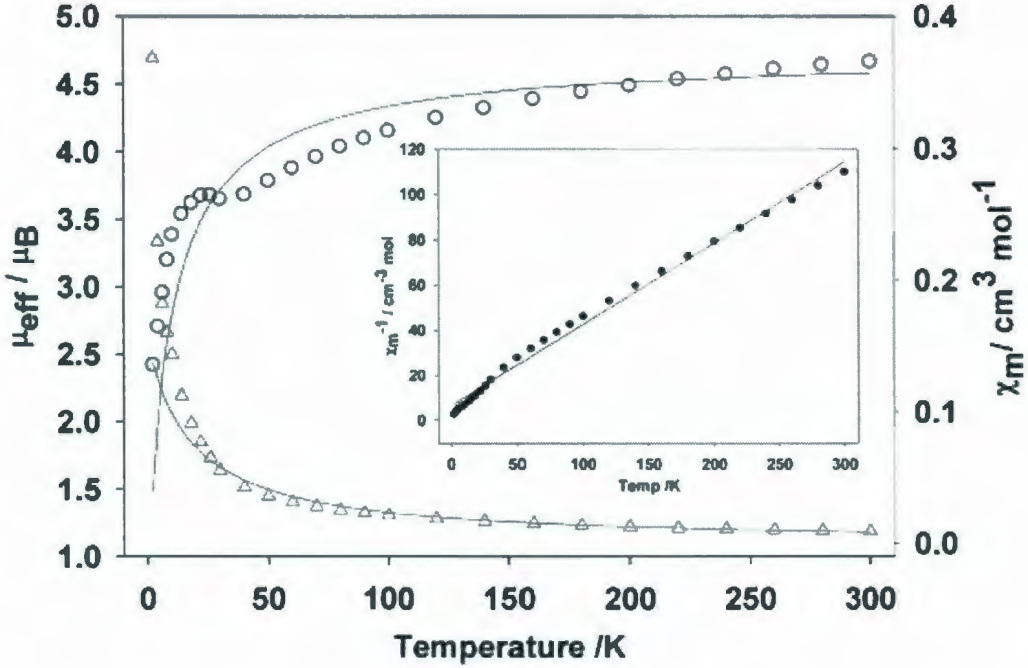

Figure C 2.4 Magnetic moment (○), susceptibility (Δ) and inverse susceptibility (inset) versus temperature data per Co atom for **2.3**. The solid line represents the best fit for the Curie-Weiss model, $\chi M = C/(T - \theta)$, where $\chi M\text{-}1 = 0.3595T + 6.5754$ ($R^2 = 0.9925$) giving a Curie constant, *C*, of 2.78 emu/mol (resulting in a *g*-value of 2.44) and $\theta = -18.29$ K.

Appendix 2.5

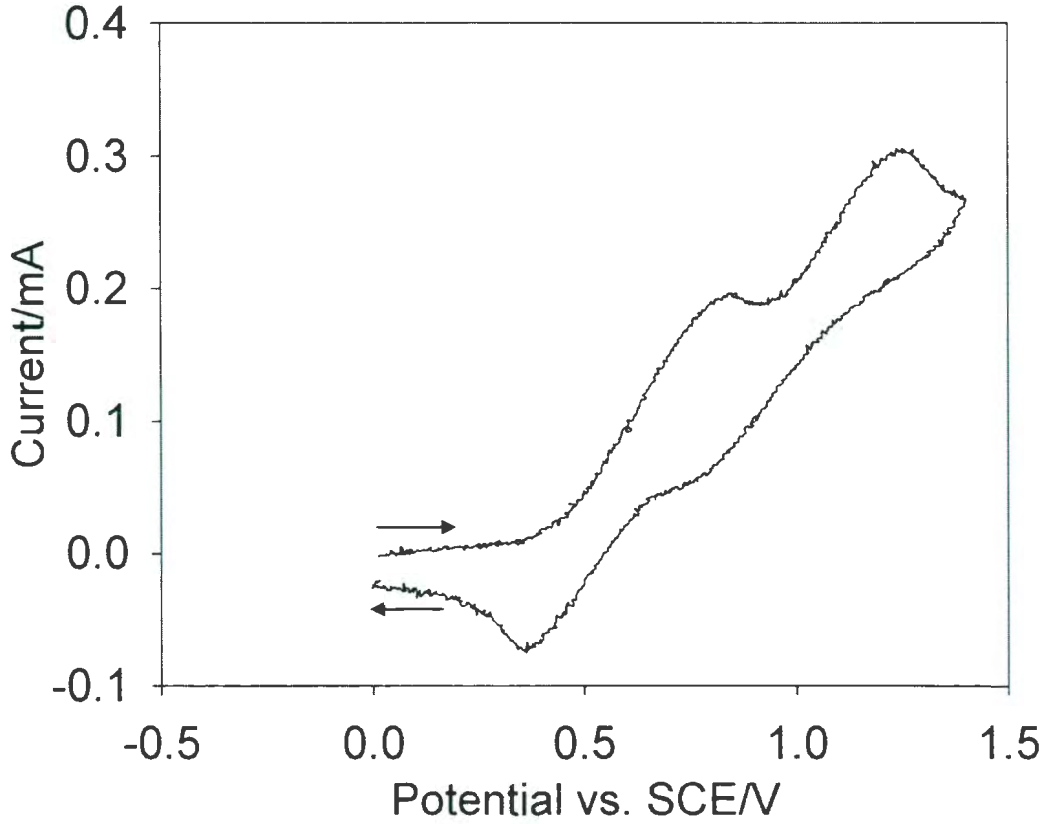

Figure D 2.5 Cyclic voltammogram of **2.1** in CH_2Cl_2 (0.1M $[(n\text{-}Bu)_4N]PF_6$) at 20 °C and a scan rate of 100mV s^{-1}.

Appendix 2.6

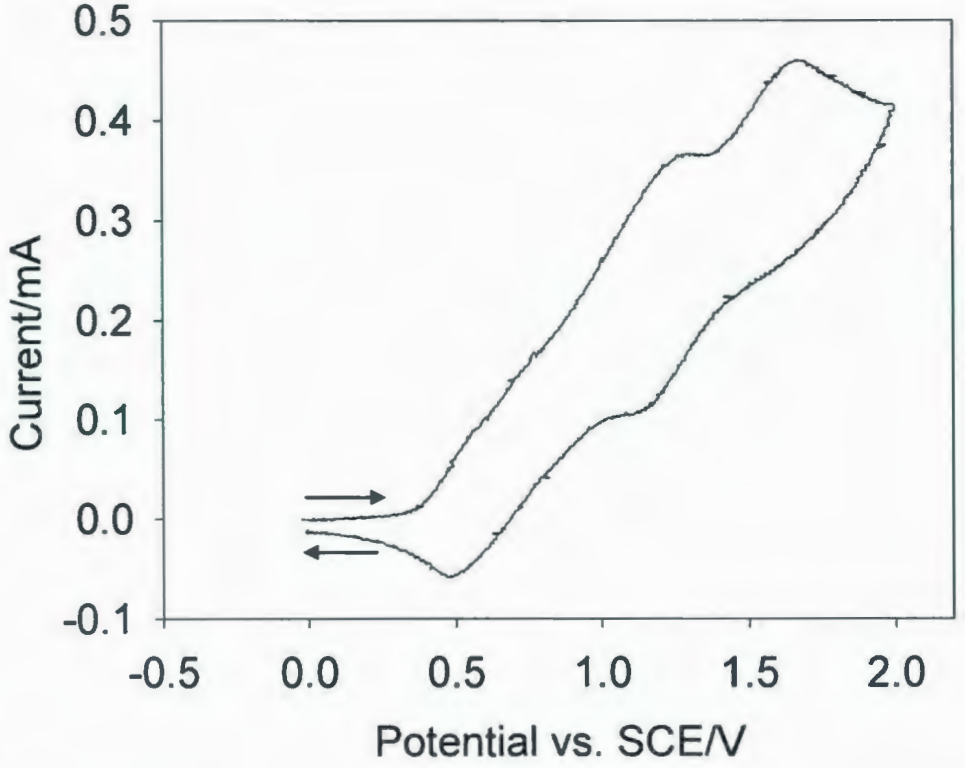

Figure E 2.6 Cyclic voltammogram of **2.2** in CH_2Cl_2 (0.1M $[(n\text{-}Bu)_4N]PF_6$) at 20 °C and a scan rate of 100mV s^{-1}.

Appendix 2.7

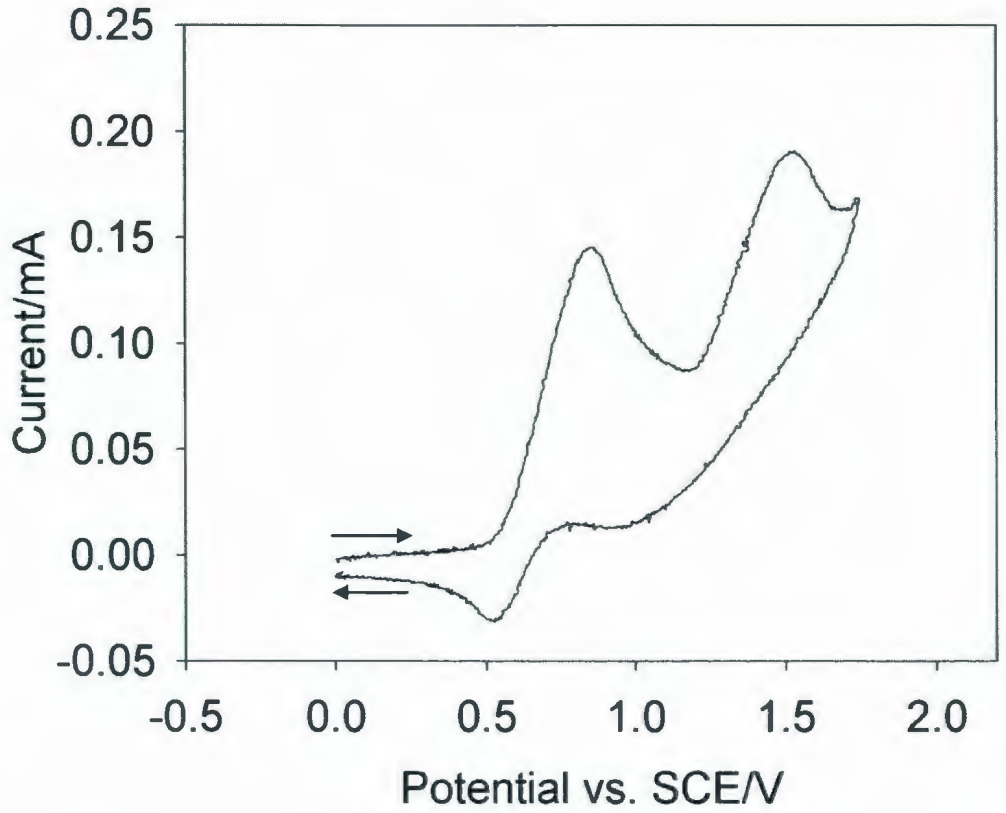

Figure F 2.7 Cyclic voltammogram of $H_2[O_2NN']^{BuBuNMe2}$ in CH_2Cl_2 (0.1M $[(nBu)_4N]PF_6$) at 20 °C and a scan rate of 100mV s^{-1}.

Appendix 3.1

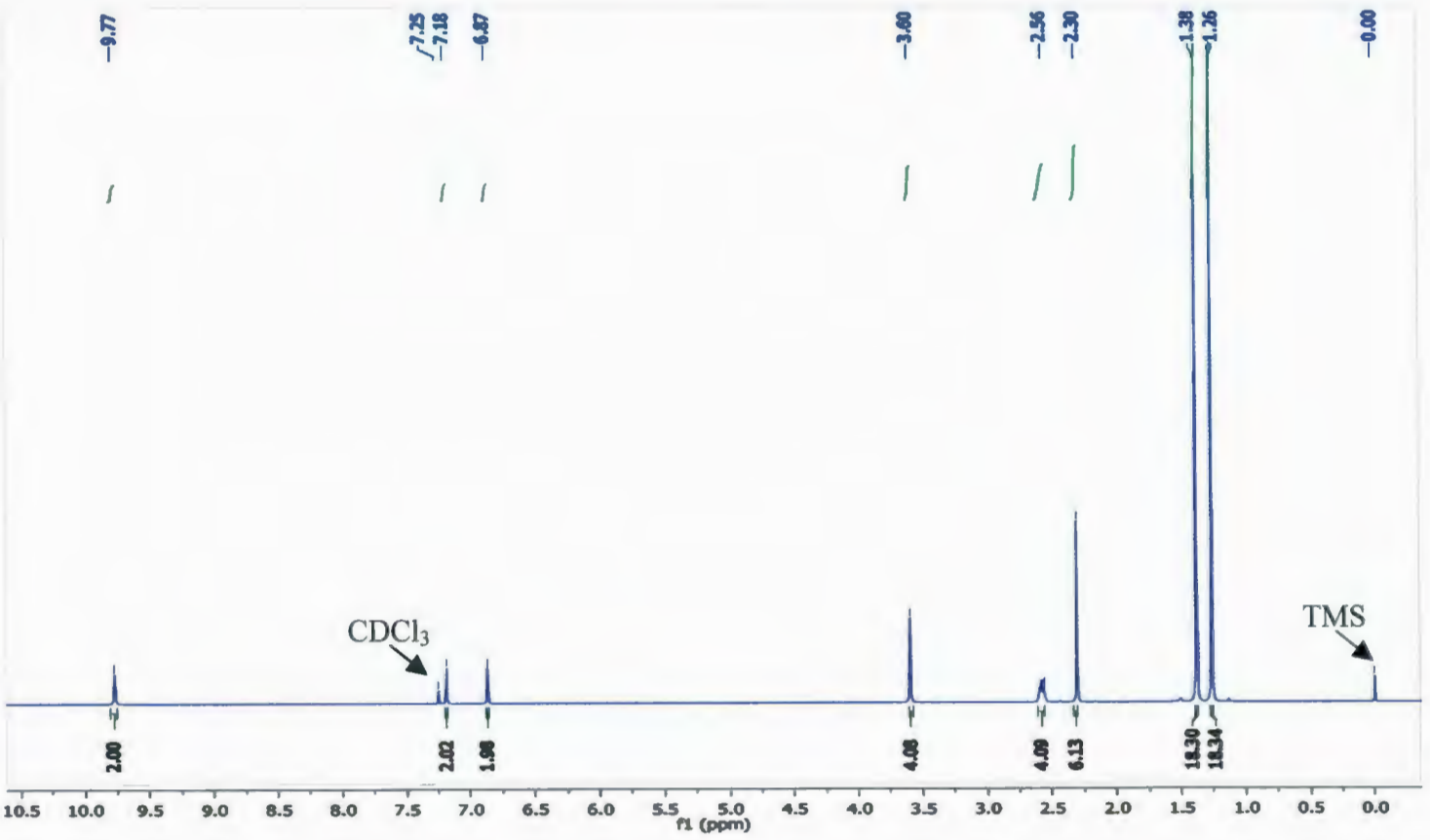

Figure G 3.1 ^{1}H NMR (500 MHz) spectrum of $H_2[O_2NN']^{BuBuNMe2}$ in $CDCl_3$.